Alicia Wong

Citrullination of LL-37 as a mechanism that selectively controls immunostimulatory potential of DNA

Doctoral thesis

Prepared under supervision of **Joanna Kozieł, D.Sc.**

Department of Microbiology
Faculty of Biochemistry, Biophysics & Biotechnology
Jagiellonian University

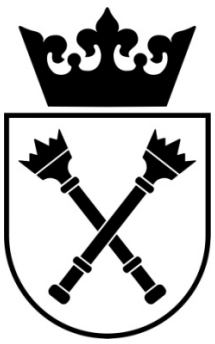

Kraków 2019

Acknowledgement

"No one person can take credit for the success of a motion picture. It's strictly a team effort." – Walt Disney –

Firstly, I would like to express my sincere thanks to **Prof. Jan Potempa, Ph.D.** for the continuous support and precious opportunities to experience a world-class scientific research.

My sincere gratitude to my advisor, **Joanna Kozieł, D.Sc.** for her patience, motivation, and her great efforts in guiding me throughout the time of research and writing of this thesis. Thank you for widen my research from various perspectives, good company and sound advice. Could not ask for more a better advisor and mentor in both PhD study and personal life.

I am grateful to my fellow labmates from the cell culture lab, especially **Danuta Bryzek, Ph.D.** and **Ewelina Dobosz** for their kind assistance and wise advice in the lab. My room-mates (you-know-who-you-are), for the insightful comments and encouragement.

Heartfelt thanks to **Hon Wei Min, Ph.D.** and **Kok Yik Lim**, **Ph.D.** for helping me get through the difficult times, and for all the emotional support, entertainment and caring they provided. And **my family members, Jay & Colette**: for supporting me and providing a loving environment for me.

Last but not least, to everyone in the microbiology department and MCB, it was great sharing laboratory with all of you during all these years.

Thank you!

Project Funding

The research presented in this doctoral dissertation has been financed by a few sources as below:
(a) **RAPID** (Rheumatoid Arthritis and Periodontal Inflammatory Disease) project implemented in 2012 - 2016, financed by the MC-ITN – Networks for Initial Training (ITN), on the basis of the contract for the implementation of the project No. FP7-PEOPLE-2011-ITN, which was led by Prof. Jan Potempa, Ph.D.
(b) **TRIGGER** (King of Hearts, Joints and Lungs; Periodontal Pathogens as Etiologic Factor in RA, CVD and COPD and Their Impact on Treatment Strategies) project implemented in 2013 - 2017, financed by the CP-FP – Small or medium-scale focused research project, on the basis of the contract for the implementation of the project No. FP7-HEALTH-2012-261460, which was led by Prof. Jan Potempa, Ph.D.
(c) **SONATA BIS** project entitled "The reins of NETs – identification of mechanisms controlling the inflammatory potential of NETs", ongoing project (2016 – 2022), financed by the National Science Center, on the basis of the contract for the implementation of the project No. UMO-2016/22/E/NZ6/00336, led by Joanna Kozieł, D.Sc.

Permission obtained for copyrighted material

Some of the research presented in this doctoral dissertation have been published in 2018 in the Journal of Immunology [*A Novel Biological Role for Peptidyl-Arginine Deiminases: Citrullination of Cathelicidin LL-37 Controls the Immunostimulatory Potential of Cell-Free DNA*. Wong A, Bryzek D, Dobosz E, Scavenius C, Svoboda P, Rapala-Kozik M, Lesner A, Frydrych I, Enghild J, Mydel P, Pohl J, Thompson PR, Potempa J, Koziel J.; J Immunol 2018; 200(7):2327-2340 (DOI:10.4049/jimmunol.1701391)].

The director of publications has given a written consent (received on May 9, 2018) to employ the published results in this dissertation.

Table of Contents

1. Abbreviations

Abs	antibodies
ADP	adenosine diphosphate
AMC ab	anti-modified citrulline antibody
AMPs	antimicrobial peptides
APCs	antigen-presenting cells
ApoA-1	apolipoprotein A1
APS	ammonium persulfate
BCA	bicinchoninic acid
BSA	bovine serum albumin
Bt-DNA	biotinylated CpG
CDCs	classical dendritic cells
cDNA	complementary DNA
Cl-A	chloroamidine
CpG	cytosine-phosphate-guanine oligodeoxynucleotides
CRAMP	cathelin-related antimicrobial peptide
DC	dendritic cells
DNA	deoxyribose nucleic acids
ECL	enhanced chemiluminescence
EDTA	ethylenediaminetetraacetic acid
EF2	elongation factor 2
ELISA	enzyme linked immunosorbent assay
FACS	fluorescence-activated cell sorter
FBS	fetal bovine serum
hCAP18	human cathelicidin
HDPs	host defence peptides
HEPES	hydroxyethyl piperazineethane sufonic acid
HNE	neutrophil elastase
HRP	horseradish peroxidase
i.d.	inner diameter
ICs	immune complexes
IFN	interferon
IgG	immunoglobulin G
IL	interleukin
IRAK	interleukin-1 receptor associated kinase
IRFs	interferon regulatory factors
K1, K2, K3	carbamylated forms of LL-37
LPS	lipopolysaccharide
LSM	lymphocyte separation medium
MAPK	mitogen-activated protein kinases
MHC	major histocompatibility complex
MIC	minimum inhibitory concentration
MOI	multiplicity of infection
MPO	myeloperoxidase
MS	mass spectrometry
MxA	myxovirus resistance protein A
MyD88	myeloid differentiation primary response 88
NETs	neutrophil extracellular traps
NF-κB	nuclear factor kappa B

P2X7	purinoceptor 7
PADs	peptidylarginine deiminases
PAMPs	pathogen-associated molecular pattern molecules
PBMCs	peripheral blood mononuclear cells
PBS	phosphate buffered saline
PCR	polymerase chain reaction
PD	periodontitis
pDCs	plasmacytoid dendritic cells
PMA	phorbol 12-myristate 13-acetate
PRRs	pattern recognition receptors
PTMs	post-translational modifications
PVDF	polyvinylidene difluoride
RA	rheumatoid arthritis
RAW264.7	murine macrophage cell line
RgpA	arginine specific gingipain
Rh-PG	rhodamine-phenylglyoxal
RIA buffer	radioimmunoassay buffer
RNA	ribonucleic acids
ROS	reactive oxygen species
RU	response units
SDS	sodium dodecyl sulphate
SLE	systemic lupus erythematosus
sLL-37	scrambled LL-37
SPR	surface plasmon resonance
TBS	tris-buffered saline
TBS-MLK	skimmed milk in TBS
TEMED	N,N,N',N'-tetramethylethylenediamine
TFA	trifluoroacetic acid
TLR	toll like receptor
TMB	3,3',5,5'-tetramethylbenzidine
TNF-α	tumor necrosis factor alpha
TRAF	TNF receptor associated factor

2. Streszczenie

LL-37, jedyna ludzka katelicydyna, jest amfipatycznym, kationowym peptydem bakteriobójczym, który zawiera 37 reszt aminokwasowych. Dojrzały peptyd uwalniany jest z 18 kDa białka prekursorowego (katelicydyny) przez proteazę-3 w neutrofilach lub przez proteazy serynowe z rodziny kallikrein w keratynocytach. Oprócz zdolności bezpośredniego zabijania mikroorganizmów, LL-37 pełni funkcję immunomodulacyjną. Jedną z nich jest tworzenie kompleksów z ujemnie naładowanymi oligonukleotydami pochodzącymi zarówno z obumierających komórek gospodarza, jak i patogenów. Interakcja ta ułatwia rozpoznawanie DNA przez receptory wewnątrzkomórkowe, takie jak TLR-9 prowadząc do indukcji odpowiedzi immunologicznej. W ostatnim czasie udokumentowano, że zdolność peptydu LL-37 do pełnienia funkcji bakteriobójczych i immunomodulacyjnych zależy w dużym stopniu od jego modyfikacji potranslacyjnych, wśród których deiminacja odgrywa wyjątkową rolę. Struktura pierwszorzędowa LL-37 zawiera pięć reszt argininy (Arg), które są wydajnie cytrulinowane przez deiminazy peptydylo-argininowe (PADs), enzymy, które są zależnymi od wapnia hydrolazami katalizującymi konwersję dodatnio naładowanej argininy do neutralnej cytruliny. W związku z powyższym w niniejszej pracy skupiono się na roli deiminacji peptydu LL-37 w regulacji odpowiedzi zapalnej na kwasy nukleinowe. Uzyskane wyniki dowiodły, że cytrulinacja LL-37 katalizowana przez PAD2 ogranicza zależne od peptydu pochłanianie DNA przez fagocyty. Co ciekawe, karbamylacja peptydu (homocytrulinacja reszt lizyny) nie ma wpływu na jego interakcję z DNA, tak długo jak karbamylowany peptyd nie zostanie poddany działaniu PAD2. W badaniach zastosowano również syntetyczny peptyd LL-37 z resztami Arg zastąpionymi homoargininą (hArg-LL-37), która jest niewrażliwa na proces enzymatycznej deiminacji przez PADy. Dane te wykazały, że wiązanie peptydu LL-37 z DNA, a tym samym jego działanie immunoregulacyjne względem fagocytów nie zależy wyłącznie od ładunku dodatniego peptydu, ale od prawidłowego rozmieszczenia guanidynowych łańcuchów bocznych argininy w natywnej sekwencji peptydu. Aby zbadać, czy powyższe zjawisko odgrywa rolę w stanie zapalnym przeprowadzono badania z wykorzystaniem zewnątrzkomórkowych pułapek neutrofilowych (NETs, ang. *neutrophil extracellular traps*). Tworzenie tych struktur, zbudowanych z nici genomowego DNA udekorowanych białkami pochodzącymi z ziaren azurofilnych, w tym LL-37, zależy od aktywności PAD4. Szczegółowa analiza składu NETs i ich wpływu na profesjonalne fagocyty sugeruje, że katelicydyna/LL-37 jest cytrulinowana przez PAD4 podczas tworzenia pułapek neutrofilowych. Proces ten odgrywa istotną rolę w kontroli potencjału zapalnego NETs, zwłaszcza w regulacji odpowiedzi

immunologicznej na uwolnione z obumierających komórek DNA, które jest rozpoznawane przez receptor TLR9. Przebieg procesu cytrulinacji w warunkach *in vivo* potwierdzają wyniki analizy serologicznej surowic pochodzących od pacjentów cierpiących na przewlekłe choroby zapalne, takie jak: paradontozę i reumatoidalne zapalenie stawów, w których wykazano podwyższony poziom przeciwciał rozpoznających cytrulinowaną formę peptydu LL-37. Ostatecznie, dowiedziono, że cytrulinowana forma peptydu LL-37 zwiększa powstawanie NETs, co sugeruje mechanizm pozytywnego sprzężenia zwrotnego. Podsumowując, cytrulinacja peptydu LL-37 odgrywa kluczową rolę w jego immunomodulacyjnym działaniu przeciwdziałając utracie tolerancji gospodarza na własne cząsteczki, w tym DNA.

3. Abstract

LL-37, the only human cathelicidin, is an amphipathic, cationic antimicrobial peptide that contains 37 amino acids residues. The mature peptide is released from an 18-kDa precursor protein (cathelicidin) by protease-3 in neutrophils or by serine proteases of the kallikrein family in keratinocytes. Besides playing antimicrobial role, LL-37 exerts several immunomodulatory functions that regulate host responses to pathogens. Among them is formation of complexes with negatively charged oligonucleotides derived from both dying host cells and pathogens. Such interaction facilitates the recognition of DNA by intracellular receptors such as TLR9, thereby stimulating the immune response. It was recently documented that the ability of peptide to execute its bactericidal and immunomodulatory functions strongly depends on posttranslational modifications, among which enzymatic deimination (citrullination) of Arg residues plays a unique role. The primary structure of LL-37 contains five arginine (Arg) residues that are effectively citrullinated by peptidyl-arginine deiminases (PADs), enzymes that are calcium-dependent hydrolases catalyzing the conversion of positively charged arginine to neutral citrulline. Therefore, presented study focused on the role of LL-37 deimination in the regulation of the host immune response to nucleic acids. Presented data revealed that citrullination of LL-37 by PADs hindered peptide-dependent DNA uptake and sensing by pDCs. In contrast, carbamylation of the peptide (homocitrullination of lysine residues) had no effect on its interaction with DNA. This activity was abolished by citrullination of Arg residues in the peptide by PAD2. We implemented in the study the synthetic peptide LL-37 with Arg residues substituted by homoarginine (hArg-LL-37), which is insensitive to enzymatic deimination. Using such peptide, we observed that regardless of PAD2 treatment hArg-LL-37 preserved full biological activity. These data have showed that peptide binding to DNA and its immunoregulatory effects on myeloid cells do not depend entirely on the positive charge of LL-37 but on the proper distribution of guanidium side chains of Arg (or homo-Arg) in the native peptide sequence. To explore if above phenomenon plays a role in inflammatory conditions, we introduced in the study neutrophil extracellular traps (NETs). Formation of those structures, composed of genomic DNA and decorated with azurophilic proteins including LL-37, depends on PAD4 activity. Detailed analysis of NETs composition and their influence on myeloid cells suggest that cathelicidin/LL-37 is citrullinated by PADs during NETs formation. Such process makes a marked contribution to the inflammatory potential of NET structures especially in regulating the immunostimulatory response of cell-free DNA, which is mediated by TLR9. Such conclusion was additionally supported by an elevated antibody

response against citrullinated LL-37 in blood serum obtained from patients suffering from chronic inflammatory diseases (periodontitis, rheumatoid arthritis). Finally, obtained data revealed that citrullinated LL-37 itself enhances the generation of NETs formation suggesting the mechanism of positive feedback. Taken together, by preventing the breakdown of tolerance to self-molecules, citrullination of LL-37 plays a critical role in immunomodulation of the host response.

4. Introduction

4.1. Innate Immunity

The innate immune system is the first line of defence in vertebrates protecting against pathogens. Its action is characterized by a rapid and non-specific response to invaders. The cascade is initiated by the recognition of pathogen-associated molecular pattern molecules (PAMPs) via pattern recognition receptors (PRRs) expressed by the host cells. Among PAMPs are such microbial components, as lipopolysaccharides, flagellin, lipoproteins and nucleic acids [1]. PRRs can induce three major types of responses upon activation: (1) phagocytosis, (2) inflammation, and (3) maturation of antigen-presenting cells (e.g. macrophages and dendritic cells), which can lead to the activation of the adaptive immune system [2]. The process of receptor activation accompanies the release of inflammatory mediators, including: chemokines, cytokines and host defence peptides. Cytokines and chemokines play essential roles in coordinating and regulating immune responses, such as mediating cell activation and differentiation, modulating inflammation and altering signalling pathways. They are characterized as pleiotropic factors and can be generally categorized into two major types, pro- or anti-inflammatory cytokines. Chemokines are a specific group of cytokines, which influence cell trafficking and recruit immune cells, such as monocytes, neutrophils and lymphocytes to a specific location. The process of cytokines expression is strictly regulated, as its breakdown can lead to excessive or prolonged inflammatory response. Deregulation of cytokine network may result in detrimental effects as observed in rheumatoid arthritis (RA), chronic obstructive pulmonary disease (COPD), asthma, or systemic lupus erythematosus (SLE). Therefore, the innate immune system engages some other host molecules that are essential in the modulation of inflammatory response. Many studies have shown that among them is a family of molecules called host defence peptides [3].

4.2. Host Defence Peptides (HDPs)

Host defence peptides (HDPs), also known as antimicrobial peptides (AMPs) constitute important branch of innate immune system and has gained substantial attention over recent years. The rise in multidrug resistant bacteria by the end of 20th century has led HDPs to become an interesting alternative ‘drug’ to control bacterial infections [4]. These proteins kill bacteria, but also yeasts, fungi, viruses and even cancer cells. HDPs are usually cationic and

amphipathic, thus they exert direct microbicidal effect by binding and disrupting the microbes' membranes. Therefore, antimicrobial activity of those molecules was considered for many years as their primary function [5]. More recent studies have reported their immunomodulatory activities. HDPs interact with surface receptors, such as G protein-coupled receptors e.g. formyl peptide receptor 2 in leukocytes and Mas-related gene X2 (MrgX2) in mast cells [6]. Moreover, they translocate across the cell membrane in a manner similar to that of cell-penetrating peptides. Translocation is essential in altering the cellular activities and promotes immune responses. Upon translocation, HDPs bind to the intracellular receptors (such as GAPDH and sequestosome 1) stimulating multiple signal transduction pathways including p38, IRF and NF- κB [6]. The immunomodulatory properties of HDPs play significant role in the cooperation of innate immune system with adaptive immunity. HDPs serve as early links to effector cells of adaptive immunity and lead the recruitment of lymphocyte and DC-mediated T-cell modulation. For example, α-defensins are reported to attract T cells and C3d of the complement cascade that amplifies B-cell secretion of specific antibodies, whilst LL-37 attracts polymorphonuclear and CD4+ T cells [7][8]. What is important, as host molecules those peptides are tolerated by immune system. For these reasons, HDPs have made an attractive template in antimicrobial therapeutics development.

There are more than 2,600 HDPs that have been identified within a variety of species, including bacteria, insects, fungi, amphibians, humans etc. [3]. Although there are different classification schemes, HDPs are categorized into four large families: α, β, αβ and non-αβ [9]. Peptides in the α family consist α-helical structure as their major secondary structure, such as human cathelicidin LL-37, histatins, dermcidin and granulysin. Whilst human α-defensins, hepcidins, human secretory leucoprotease inhibitor (SLPI) are categorized in the β family, containing at least a pair of two β-strands in the structure. The αβ family contains both α and β secondary structures, such as the β-defensins and antimicrobial chemokines (CCL1, CXCL10 etc.). Peptides in non-αβ family contain neither α nor β structure, but consist of extended structures. Structural example for this family is still being studied [10].

Defensins and cathelicidin families constitute the major groups of antimicrobial peptides in mammals. They are secreted by epithelial cells and professional phagocytes, such as macrophages and neutrophils [4]. Defensins are categorized into α, β, and θ-defensins. They are non-glycosylated peptides with arginine as their major cationic residue and six conserved cysteine residues. Their β-sheet structure is stabilized by intramolecular disulfide bonds [11]. Cathelicidins have a distinctive feature of highly conserved cathelin domain (N-terminal

sequence) and a C-terminal antimicrobial domain. The cathelin-like domain is flanked by a signal peptide domain on the N-terminus, which directs the peptide to either storage or to the exterior of the cells, where the peptide plays a key role to rapid host defence [7]. Besides mammals, cathelicidin is also found in a variety of species such as amphibians, avian and fishes. Each species expresses different number of cathelicidins, however, in human and mice, only one cathelicidin was identified. The murine cathelicidin (CRAMP - cathelin-related antimicrobial peptide) shares 67% homology with human cathelicidin peptide. The human cathelicidin, known as hCAP18 is encoded by the *CAMP* gene located on the chromosome 3p21. It consists of 4 exons. The first 3 encode the preproregion (signalling and cathelin-like domain) and the forth one codes the active domain [12]. hCAP18 is characterized by an N-terminal signal peptide (30 amino acid residues), a highly conserved pro-sequence (103 amino acid residues), which is also known as the cathelin-like domain and a mature antimicrobial peptide called LL-37 (37 amino acid residues) (**Fig. 1**). hCAP18 with the molecular weight of 18 kDa exhibits no antimicrobial activity [13]. However, upon cleavage of the C-terminal end of hCAP18 the 4.5 kDa-matured peptide termed LL-37 is formed [14]. Among enzymes catalysing this process are serine proteases of the kallikrein family in keratinocytes and/or proteinase 3 in neutrophils.

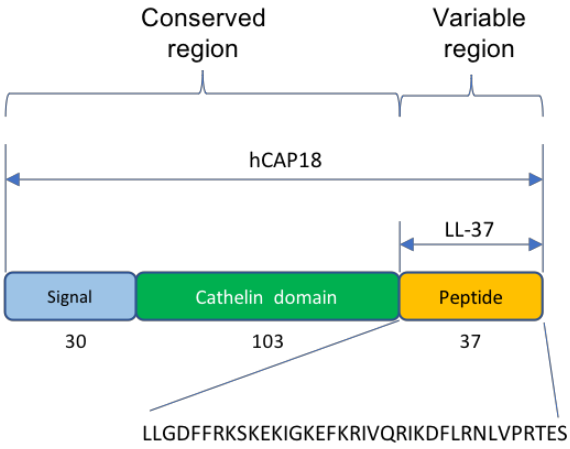

Fig. 1. Processing of human cathelicidin. The preprotein (hCAP18) consists of a conserved region (signal sequence and cathelin domain) and variable region, which codes for the mature antimicrobial peptide (LL-37). Active peptide (LL-37) is processed by several serine proteases, depends on the cell type/tissue [Adapted from Vandamme *et al.* [14]].

4.3. Peptide LL-37

LL-37 consists of 37 amino acid residues with Leu-Leu at the N-terminus (NH_2-LLGDFFRKSKEKIGKEFKRIVQRIKDFLRNLVPRTES-COOH), with the net positive charge of +6 at physiological pH [14]. The secondary structure of LL-37 depends on the environment as well as on peptide's concentration. LL-37 has a disordered conformation in aqueous solution but it is able to fold into an amphipathic α-helix in contacts with lipid membranes. Furthermore, some studies have demonstrated that a random disordered conformation of LL-37 at micromolar concentration in water transforms to α-helix conformation in the presence of physiological concentrations of certain salt ions, with the ion compositions similar as found in plasma and intracellular fluid. The α-helix conformation is anion-, pH-, lipid- and concentration-dependent. The circular dichroism (CD) spectrum of LL-37 has revealed the peptide adopted the characteristic of α-helical structure at the concentration of 10^{-3} M in the presence of 20 mM SO_4^{2-}, with pH values over 13 [15][16][17]. The α-helical structure is essential for the peptide's activities, such as anti-endotoxin, anti-microbial and anti-biofilm [18]. Furthermore, LL-37 is able to form aggregates in solution and lipid bilayers, enabling the peptide to be protected from proteolytic degradation [19].

LL-37 is constitutively expressed in almost all tissues and is also present in body fluids, such as plasma and bone marrow [7]. Sørensen and co-workers' studies have demonstrated that neutrophils are the main source of peptide. The concentration of pro-peptide found in secondary granules was estimated about 630 μg/10^9 cells [20]. The expression of LL-37 significantly increases at the site of infection, during inflammation and can be upregulated by a wide variety of stimuli, such as cytokines, growth factors, bacterial and fungal products [21].

4.3.1. Functions of LL-37

4.3.1.1. Antimicrobial role of LL-37

LL-37 exerts antimicrobial activity against a broad range of both Gram-positive and Gram-negative bacteria, which includes *Pseudomonas aeruginosa*, *Staphylococcus aureus* or *Escherichia coli*. The exact mechanism by which AMPs exert their antimicrobial properties is still unclear, however, the general accepted idea is that cationic peptide LL-37 interacts with the negatively charged phospholipids of bacterial cell wall. Such electrostatic interaction

provides the process of covering the surface of the bacterial membrane by peptide. The consequence is disruption of the membrane via a 'carpet-like' mechanism and pore formation [22]. The established minimum inhibitory concentration (MIC) of LL-37 against Gram-positive and Gram-negative bacteria range between 0.2 – 32 μM. Apart from that, LL-37 has strong anti-biofilm properties. This was shown in a study conducted by Overhage and co-workers on biofilms formed by *P. aeruginosa*. It was revealed that subinhibitory concentrations of the MIC (0.5 μg/ml) led to an approximately 40% decrease in *P. aeruginosa* biofilm mass [23]. Such observation was explained by the broad activity of LL-37 against biofilm development. Firstly, peptide significantly reduces the attachment of bacteria to the surface, causing a smaller number of bacteria involved in the initial steps of biofilm formation. Secondly, LL-37 also affects existing, pregrown *P. aeruginosa* biofilm by increasing the bacteria motility, limited their attachment to the surface and further biofilm growth. The conclusion comes from the observation of biofilm morphology, which is thin and flat without the mushroom-like structure [23]. And last but not least, LL-37 could affect the two major quorum-sensing system of bacteria, the Las and Rhl systems, by downregulating the key components, which are part of the respective regulons [23]. Besides *in vitro* studies, the antimicrobial role of LL-37 was confirmed using mice deficient in CRAMP. Mice deficient in CRAMP were more susceptible to pathogenic bacteria colonization and invasion when compared to wild-type animals, as reported by Chromek *et al.* [24]. It is proposed that as CRAMP is similar to LL-37 in structure, tissue distribution and antimicrobial activity, thus CRAMP knockout model would be useful to study the function of human cathelicidin. Strong clinical evidence showing antibacterial role of LL-37 comes from patients with Morbus Kostmann syndrome treated with G-CSF. These patients' neutrophils although in normal numbers lacks LL-37. In a consequence, those patients are more susceptible to develop oral infections [25]. LL-37 has also shown to exhibit antiviral activity against herpes simplex virus and vaccinia virus [26]. The peptide was also reported to inhibit the replication of HIV-1 in peripheral blood mononuclear cells, including the primary CD4+ T cells [27].

4.3.1.2. Immunomodulatory role of LL-37

Along with its antimicrobial properties, LL-37 plays an important role as a potent immunomodulator of the host immune response as presented in **Fig. 2**. LL-37 exerts both pro- and anti-inflammatory functions, depending on the microenvironment and cellular contexts

[28]. Upon stimulation by pro-inflammatory signals, LL-37 is able to direct macrophage differentiation to M1 phenotype characterized by proinflammatory signature, which involves the internalization of LL-37 by monocytes and activation of p38 mitogen-activated protein kinase (MAPK) signalling [29]. Peptide acting on the P2X7 receptor efficiently contributes to the inflammasome activation leading to the generation of IL-1β and IL-18 [30]. LL-37 also promotes type I IFN production providing protection, recognition and engulfment of both RNA and DNA into professional phagocytes leading to the activation of TLR7 and TLR9 respectively [31]. Besides that, LL-37 promotes NETosis as being integral component of NETs peptide is recognized by anti-LL-37 autoantibodies [32]. Another notable pro-inflammatory feature of LL-37 is its chemotactic activity. Peptide induces the migration of neutrophils and eosinophils by acting via the formyl peptide receptor 2 [28]. LL-37 also modulates the production of chemokines in keratinocytes by inducing the transcription of CXCL8 which acting in synergy with TNF-α [33].

Nevertheless, LL-37 plays an important anti-inflammatory role. The crucial one is neutralization of bacterial endotoxin and inhibition of TLR4 signalling in dendritic cells and macrophages [34]. LL-37 also exerts antagonistic role towards host inflammatory mediators, such as: IFN-γ, TNF-α, IL-4 and IL-12 [35]. The peptide has protective effects against invasion of pathogenic bacteria in intestine. Studies utilizing mice deficient in CRAMP have demonstrated such function for this peptide, such as providing protective effects against *Clostridium difficile* toxin-mediated colonic and ileal damage [36]. Altogether, the LL-37 peptide is a potent and pleiotropic host factor and its immunomodulation mechanism needs to be further elucidated.

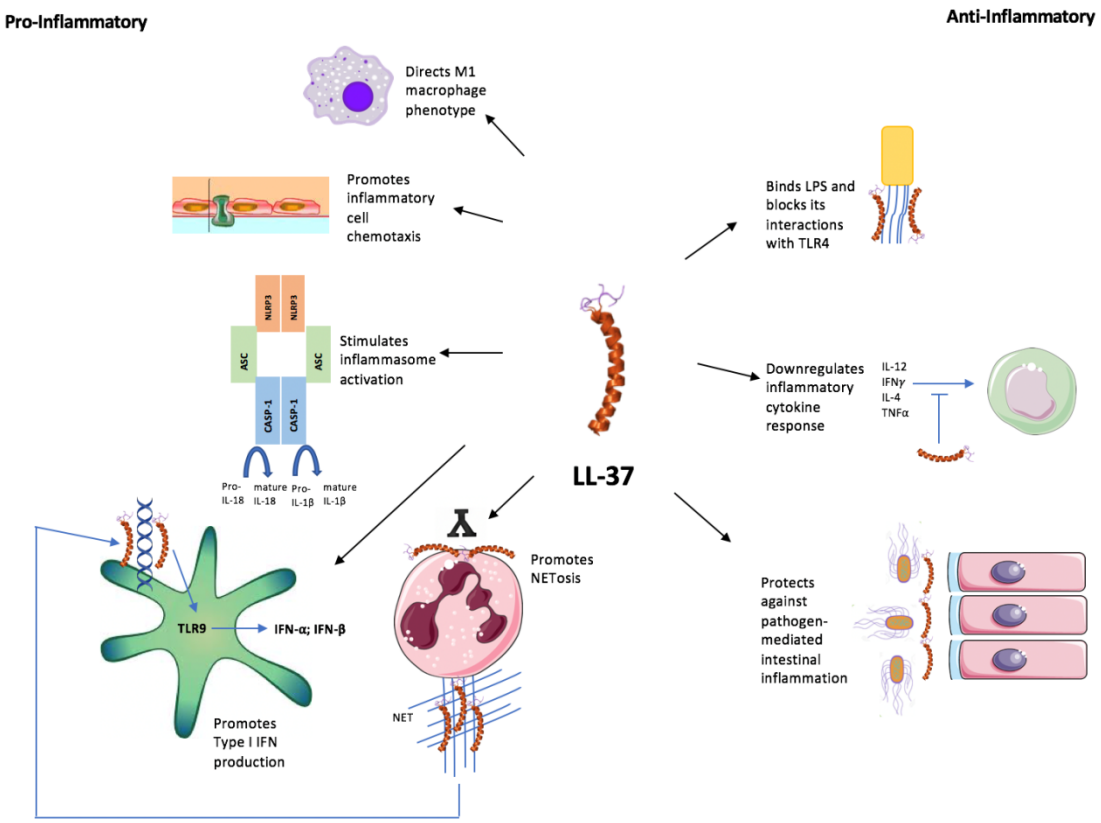

Fig. 2. Immunomodulatory role of LL-37. The figure was created with images adapted from Servier medical art by Servier [Adapted from Kahlenberg and Kaplan [28]].

4.3.1.3. The role of LL-37 in wound healing and angiogenesis

LL-37 is actively involved in tissue repair and wound healing, especially revascularization and cell growth. Increased expression of LL-37 was reported in human keratinocytes and in wounds. The peptide can be induced by wound-healing growth factors, such as transforming growth factor (TGF)-α and insulin-like growth factor 1 (IGF-1) [37]. The chemoattractant properties of the peptide, which enhance migration of epithelial and immune cells, increase synthesis of extracellular matrix proteoglycans and cellular proliferation that contributes to the wound healing process. Besides that, its anti-infective activities reduce microbial burden at the wound site [6]. LL-37 was also reported to promote IL-8 release and wound closure through the epidermal growth factor receptor (EGFR) and MAPK signalling pathway in human bronchial epithelial cells [38].

Moreover, the peptide has another interesting function, which is induction of angiogenesis by direct activation of endothelial cells, their increased proliferation and

formation of vessel-like structures [7]. Koczulla *et al*. have shown that LL-37 induces angiogenesis via a formyl peptide receptor-like 1 (FPRL1) protein expressed on endothelial cells. They have also observed decreased vascularization during wound repair in mice deficient in CRAMP, emphasizing the importance of cathelicidin in mediating cutaneous wound neovascularization *in vivo* [39].

4.3.2. Effects of LL-37 on disease pathogenesis

Although LL-37 plays protective and beneficial role in host defence, it also contributes to the development of autoimmune disorders and inflammatory diseases, such as atherosclerosis, psoriasis, systemic lupus erythematosus, and arthritis. The detrimental function of LL-37 was initially observed in atherosclerosis. Peptide efficiently binds to DNA forming complexes that promote type I IFN signatures and causing the development of atherosclerotic lesion. Moreover, enhanced transcription of LL-37 was found in human atherosclerotic aortas [40]. Harmful effect of the peptide was also documented in psoriasis, disease characterized by enhanced type I IFN production and skin inflammation. In those patients overexpression of LL-37 was documented. It was revealed that peptide binds to DNA thus induces accelerated activation of dendritic cells. Furthermore, the role of LL-37 in psoriasis development relays on its antiapoptotic influence on keratinocytes, causing the increased cellular proliferation [41]. Another serious inflammatory disease in which the role of LL-37 was documented is SLE. In sera of those patients LL-37-DNA complexes were detected. Moreover, the generation of autoantibodies against LL-37 promotes formation of immune complexes and further NETs induction. Such events accelerate inflammatory reaction [32][42][43]. The elevated expression of LL-37 was also documented in osteoclasts and granulocytes from patients suffer with RA, suggesting the role of LL-37 in development of joint disease. The mechanism of deleterious effect of LL-37 bases on induction of osteoblasts apoptosis causing the reduction of bone formation in arthritic joints [28]. Hoffman and co-workers have demonstrated the upregulation of CRAMP, the rat ortholog of LL-37 in granulocytes, macrophages in a pristine-induced arthritis model, suggesting the contribution of LL-37 in arthritis development, however, further studies are needed to clarify its role [44].

4.3.3. Post-translational modifications of LL-37

The interest in deciphering protein modifications and their impact on cellular microenvironment and disease pathophysiology was greatly enhanced in the past few decades. Post-translational modifications (PTMs) play a key role in multiple cellular processes, such as cell signalling, differentiation and regulation of gene expression. The result of PTMs that change properties of a protein, by adding or modifying chemical groups in a sequence of amino acids, has been reported to affect protein function via changes in protein structure and dynamics [45]. We focused on the major modifications of LL-37, which recently gained interest by the research community.

4.3.3.1. Proteolysis

Proteolysis of LL-37 is a common strategy used by pathogens that utilize proteases to confer resistance against the antimicrobial activities of peptide. An example is *Staphylococcus aureus*, which produces two major proteinases, metalloproteinase (aureolysin) and glutamylendopeptidase (V8 protease). Both enzymes cleave and inactivate LL-37, contributing to the resistance of the pathogen to the host innate immune system [46]. Furthermore, proteolysis of LL-37 has been reported to be associated with severe periodontal disease. *Treponema denticola*, *Porphyromonas gingivalis* and *Tannerella forsythia* are characterized by their high proteolytic and peptidolytic activities, which can degrade LL-37 *in vitro* [47]. For example, it was identified that a metalloprotease from *T. forsythia*, karilysin, can inactivate the bactericidal activity of LL-37 in a time- and concentration-dependent manner. This contributes to the development of chronic inflammatory response in periodontitis patients [48].

Apart from enzymatic degradation by bacteria, LL-37 can be proteolytically cleaved by protease β-tryptase released by human mast cells, causing the change in the function of the peptide, such as lacking the microbicidal and LPS-neutralizing activities [49]. Another proteolytic degradation of LL-37 was reported in cystic fibrosis bronchoalveolar lavage fluid by neutrophil elastase and cathepsin D. The truncated peptide fragments of LL-37 resulting from the proteolytic activity may alter the inflammatory and antimicrobial effect of the peptide, reducing the immunomodulatory properties compared with the intact LL-37 [50].

4.3.3.2. Carbamylation

Carbamylation, is a non-enzymatic post translational modification in which cyanate (OCN^-) reacts with the primary amino groups (NH_3^+) at the N-termini of proteins, and with the lysine residues in the polypeptide chain, generating α-carbamyl amino acids and homocitrulline respectively [51] (**Fig. 3**). Other amino acids such as arginine and cysteine contain side chains that can react with cyanate, however such binding is rarely reported apart from lysine. Cyanate is a reactive species which is always in equilibrium with urea in physiological conditions, however, that's not the case in uremic patients, with 150 nmol/L plasma concentrations of cyanate was reported, which is three times higher comparing to healthy individuals (50 nmol/L). High level of cyanate explains the intensity of carbamylation reaction in patients with renal dysfunction [52].

Carbamylation has attracted the attention as such modification can be enhanced in the context of chronic inflammatory diseases where myeloperoxidase (MPO) are found abundantly [53]. The concomitant release of LL-37 and MPO by activated neutrophils creates the perfect conditions for LL-37 carbamylation. When MPO acts on thiocyanate in the presence of hydrogen peroxide, cyanate is generated. Such reaction provides further carbamylation process. As thiocyanate can be brought by smoke, thus few studies have suggested a link between inflammation and smoking [53][54].

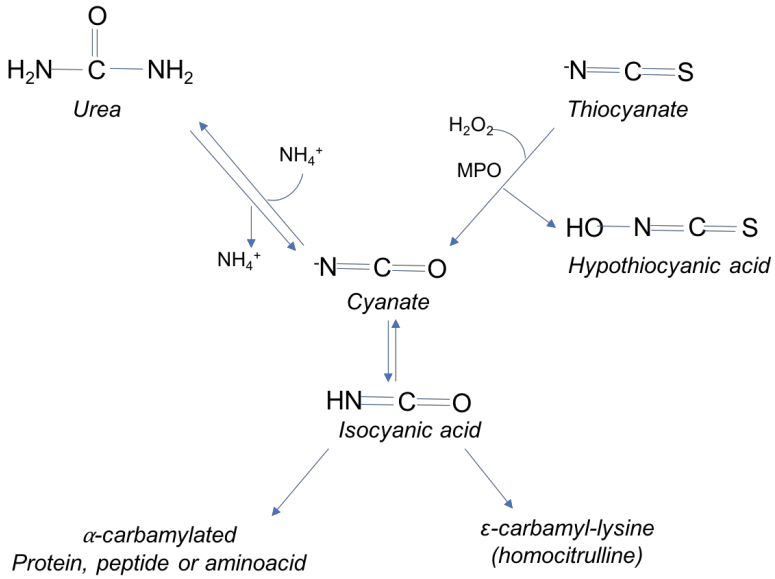

Fig. 3. The major biochemical pathways in carbamylation. Chemical modification that generates α-carbamylated proteins/peptides/amino acids and homocitrulline in the presence of cyanate [Adapted from Jaisson *et al.* [55]].

Mass spectrometry analysis has identified three possible common variants of carbamylated LL-37 by incubating LL-37 with 10 mM of potassium cyanate (KCNO), which is an equivalent to cyanate level detected in inflammatory milieu [51]. LL-37 bearing a carbamylated N-terminus (LL-37^{C1}) was the predominant form. The second most common single-modified peptide was LL-37 bearing homocitrulline residue at position 8 (LL-37^{C8}), while prolonged incubation of LL-37 with KCNO generates LL-37 bearing a double modification on Lys-12 and Lys-15 (LL-$37^{C12,C15}$). The posttranslational modification of Lys residues to neutral homocitrulline was reported to abrogate the biological function of LL-37, such as affecting the chemotactic capacity of LL-37, where neutrophils were less responsive to the carbamylated versions of LL-37 and showed lower directional accuracy. Carbamylated forms of LL-37 were also reported to have impaired ability to inhibit bacterial growth [51]. This is most likely due to the loss of two positive charges, which would have led to a significant impact on the secondary structure of the peptide and hence modified its physiochemical properties. It was also documented that the chemical conversion is dependent on time of exposure and OCN^- concentration [51]. Hence, administration of cathelicidin-derived peptides as therapeutic drugs should be considered carefully in the context of severe inflammation, where due to cyanate formation, lysine residues within LL-37 could undergo carbamylation leading to the inactivation of peptide.

4.3.3.3. Citrullination

Peptidyl arginine residues, such as present in LL-37, can undergo enzymatic deimination (often referred to as citrullination), which results in the conversion of arginine (Arg) to citrulline (Cit) (**Fig. 4**). Citrullination caused the reduction of overall net charge of a protein by the loss of a positive charge per citrulline residue. The conversion of ketimine groups ($=NH_2$) of the arginines to ketone groups (=O), results in the production of citrulline and is catalyzed by PAD enzymes (peptidylarginine deiminases, EC 3.5.3.15) [56]. These enzymes work by attacking the active site cysteine residue on the substrate guanidinium, resulting in the formation of a tetrahedral intermediate. A water molecule then acts as a nucleophile and attacks the tetrahedral adduct that ultimately forms an acyl-enzyme intermediate which is subsequently hydrolysed to form citrulline [57]. Calcium is a key regulator of PADs activity, but it remains uncertain how intracellular calcium levels can be raised to sufficiently high levels to activate these enzymes [58].

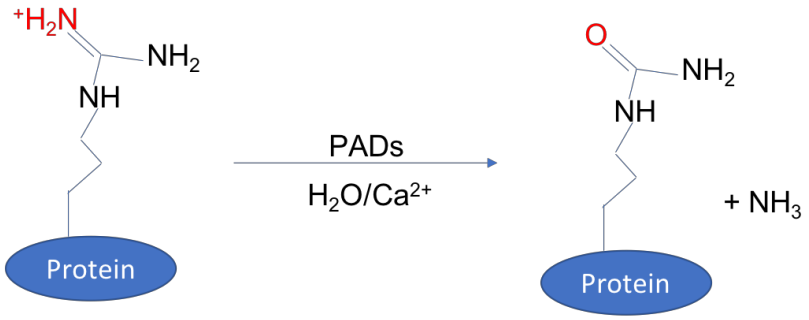

Fig. 4. Process of citrullination. Peptidylarginine deiminase (PAD) catalysed the hydrolytic conversion of peptidyl-arginine to non-standard residue peptidyl-citrulline [Adapted from Vossenaar *et al.* [59]].

Five isoenzymes of PAD have been identified (PAD1, 2, 3, 4, 6). They are differentially distributed in many tissue and cell types, as typical for epidermis and uterus is PAD1, for skeletal muscle, brain, inflammatory cells and secretory glands is PAD2, for hair follicles and keratinocytes is PAD3, for granulocytes is PAD4, while for oocytes and embryos is PAD6 [60]. PAD4 is the only isozyme that plays an essential role in histone deimination, however there's a growing number of reports suggesting that PAD2 may play equally important role. Under physiological functions, PADs activity is limited as the calcium concentration is at very low levels inside the cell (10^{-8} to 10^{-6} M). However, in the event of cell death (for example, apoptosis), intracellular concentration of calcium increases thus activating PADs [61]. Citrullination has variable effects based on target substrates for each PAD isozymes [57]. Major substrates for each isoform of PAD are summarized in **Table I**.

Isozyme	**Substrates**
PAD1	Keratin, filaggrin
PAD2	Myelin basic protein, vimentin, actin, histones
PAD3	Filaggrin, trichohyalin, vimentin, apoptosis-inducing factor
PAD4	Histones, nucleophosmin, nuclear lamin C
PAD6	Not known

Table I. List of major substrates modified by respective isozymes of the PAD family [Adapted from Witalison *et al.* [57]].

One of the earliest descriptions of physiological citrullination is the cornification of skin and the hardening of the hair follicle. Citrullination of filaggrin for example, provides

structural support in cells undergoing terminal epidermal differentiation. On the other hand, citrullination of filaggrin increases its susceptibility to proteolysis and allowing it to be cleaved into amino acids that make up natural moisturizing factor [62]. Apart from that, PADs can regulate gene expression at physiological concentrations of calcium and a lot of research has been performed on PAD4 in this context. Especially interesting is the role of the PAD4-mediated regulation of the p53 pathway, which is essential in responding to stresses that can disrupt the fidelity of DNA replication and cell division, although it is still unknown how PAD4 is recruits to the p21 (the transcriptional targets of p53) at the p53-binding sites on the promoter region and functioned at physiological calcium levels [63]. The PAD enzymes could deiminate several nuclear and cytoskeletal proteins such as vimentin, causing structural changes and results in the disintegration of secondary and tertiary protein structures [64]. On the other hand, PADs may have a role in the induction of apoptosis. Deimination of histones H2A, H3 and H4 could alter the chromatin organization and DNA susceptibility to fragmentation, leading to the induction of apoptosis through DNA damage signals [65]. As mentioned above citrullinated proteins play an important role in many cellular processes. It is crucial for the regulation of immune response, central nervous system, tissue structure generation and cytoskeletal stability. Dysregulation of citrullination can lead to serious abnormalities in immunological system. Rheumatoid arthritis, multiple sclerosis, psoriasis, Alzheimer's disease are inflammatory disorders, which aetiology is related with citrullination [61]. The modification has piqued the interest in the research community with reports showing the upregulation of PADs due to the presence of pro-inflammatory stimuli. Moreover, it was revealed that increased level of cell death that contributes to the calcium rich environment leads to PADs activation [66]. Thus, PADs regulation has gained the attraction as promising target against autoimmune and inflammatory diseases related to protein deimination [57].

Main isoforms of PADs enzymes involved in inflammation are PAD2 and PAD4. Both enzymes can efficiently citrullinate LL-37 as it was documented in recently published studies [67] [68]. All five Arg residues are citrullinated but at different time and efficiency (**Table II**) [67]. Moreover, citrullination of LL-37 depends on the form of PADs. PAD2 was reported to citrullinate all Arg residues, whilst exposition of LL-37 to PAD4 results in a generation of partially citrullinated peptide [68]. Predominantly generated forms of peptide are $Arg^{7}Cit$ (LL-37_{7}), $Arg^{7,29,34}Cit$ (LL-$37_{7,29,34}$), or $Arg^{7,19,23,29,34}Cit$ (LL-$37_{all\ cit}$).

PADs	PAD2		PAD4	
Citrullination of individual Arg residues in LL-37	**Cit-7**	**99.0%**	**Cit-7**	**93.0%**
	Cit-19	**15.0%**	**Cit-19**	**1.0%**
	Cit-23	**1.5%**	**Cit-23**	**0.8%**
	Cit-29	**49.0%**	**Cit-29**	**41.0%**
	Cit-34	**20.0%**	**Cit-34**	**50.0%**

Table II. Percentage of citrullination of individual Arg residues in LL-37 treated with either PAD2 or PAD4, quantitated by amino acid sequence analysis using automated Edman degradation [Table reproduced from Koziel *et al.* [67]].

The function of LL-37 largely depends on the cationic charge and the structure of the peptide, which is abrogated upon citrullination. Koziel *et al.* and Klisgård *et al.* have reported the loss of anti-inflammatory and bactericidal effects upon the citrullination of LL-37 [67][68]. Citrullinated LL-37 has reduced ability to quench the pro-inflammatory activity of LPS as documented *in vitro* using macrophages as model of immune cells. Moreover, citrullination abolishes the ability of LL-37 to prevent the mortality and morbidity associated with septic shock. Apart from that, citrullinated LL-37 is unable to downregulate cellular responses to other TLR ligands and host inflammatory mediators. Since the citrullination of LL-37 *in vivo* during inflammation, especially in sepsis patients, is highly possible, thus therapeutic strategy by administering LL-37 should be analysed in detail as it might contribute to severity of sepsis [67].

4.3.3.4. Other modifications

The presence of five arginine residues in LL-37 has enabled this peptide to be subjected for ADP-ribosylation. Picchianti and co-workers have shown that LL-37 can be ADP-ribosylated by ADP-ribosyltransferases (ART1), a surface-exposed enzyme expressed on the apical surface of human airway epithelial cells, at multiple arginine residues *in vitro* [69]. The attachment of one or more negatively charged ADP-ribose moieties to arginine residues result in a reduced cationicity of the peptide, which affects the ability of the peptide to interact with biological membranes or polyanionic molecules such as DNA, RNA or actin. This might be useful to develop new therapeutic compounds for cystic fibrosis and psoriasis patients, where the properties of LL-37 was affected due to the formation of DNA-LL-37 complexes [69].

LL-37 can be acetylated on the N-terminus and amidated on the C-terminus, which enables the peptide to have a marked reduction in proteolytic degradation by V8 and aureolysin in solution [70]. Hence, such stabilized peptides may improve antimicrobial properties which might due to the increase helicity by stabilizing the helix by hydrogen bonding to the NH group, results from the terminal acetylation and amidation [71].

4.4. Immune recognition of DNA

4.4.1. Distinguishing self from non-self DNA

The mammalian immune system can recognize nucleic acids, however the process is regulated by their specific sequences, modifications or structures. The mammalian immune system selectively responds to DNA sequence motifs containing unmethylated CpG dinucleotides commonly found in bacterial DNA. The cellular activation in response to bacterial DNA is mediated by TLR9 and leads to the activation of host cells manifested with increase expression of cytokines. CpG DNA preferentially activates B cells and dendritic cells (DCs), but robust cytokines secretion increases the activity of other subsets of immune cells, such as monocytes, NK cells, or T cells, which lack TLR9 expression. That mechanism confers protection of the host from different pathogens containing unmethylated CpG motifs, which are classified as one of the PAMPs [72].

The unmethylated CpG oligonucleotides can be categorized into 2 different classes with distinct structures, sequence motifs and the subset of activated host cells. CpG-A (prototype ODN 2216) has a weaker activity on B cells or macrophages but induces strong response of type I IFN in dendritic cells. This is a consequence of the presence of poly-G tails that enable the formation of aggregated structures. Such aggregates retained longer in the early endosomes, creating a platform for extended activation of the signal-transducing complex, consisting MyD88 and IRF7, which leads to robust type I IFN production. Thus, plasmacytoid dendritic cells (pDCs) seem to detect aggregated DNA structures in the early endosomes, which express markers such as the transferrin receptor (TfR) and early endosomal antigen 1 (EEA1). Prolonged exposition of CpG to TLR9 receptors located inside early endosomes induces a signalling pathway enhancing the activation and recruitment of a signal-transducing complex, such as MyD88, interleukin-1 receptor associated kinase 1 (IRAK1), interleukin-1 receptor associated kinase 4 (IRAK4) and TNF receptor-associated factor 6 (TRAF6). IRAK-TRAF6

complex provides the phosphorylation of IRF7 and subsequent activation of type I IFN gene expression [31] (**Fig. 5 – upper panel**).

On the other hand, CpG-B (prototype ODN2006) is a potent activator of B cells but only trigger pDCs to produce proinflammatory cytokines (TNF-α and IL-6) and minute amounts of type I IFN, as well as induces the upregulation of CD80, CD83 and CD86 molecules. As monomeric CpG-B lacks poly-G tails, thus it travels rapidly to late endosomes or lysosomes. Hence, it is thought that pDCs sense linear DNA structures in the late endosomes, which is marked by the presence of lysosomal-associated membrane protein 1 (LAMP-1). This activates a different set of signal mediators, where TGF-β activated kinase-1 (TAK1) triggers the activation of NF-κB, mitogen-activated protein kinases (MAPK) and IRF5, leading to TNF-α and IL-6 production and pDC maturation [31] (**Fig. 5 – lower panel**).

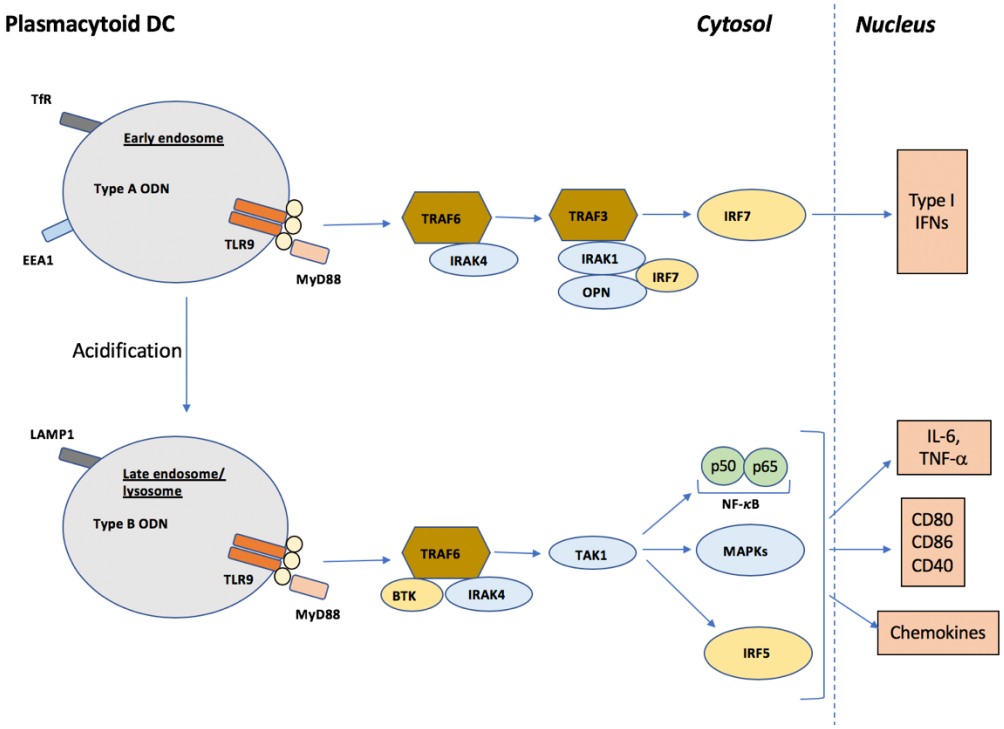

Fig. 5. Different CpG ODNs activates different signalling pathways. CpG-A ODNs tend to form aggregated structures, which are retained in early endosomes and cause a robust type I IFN-α response. CpG-B ODNs rapidly traffics to late endosomes or lysosomes and triggers the production of pro-inflammatory cytokines, TNF-α and IL-6 [Adapted from Gilliet *et al.* [31]].

Mammalian DNA is methylated and characterized with the lower frequency of CpG dinucleotides, thus it usually remains neutral for host immune system [73]. However, the

release of host (self) DNA into an extracellular environment is inevitable due to the process of cell death. The mechanism, which can protect the host against accelerated response to self-DNA, engages DNAses. Those enzymes deposited at high concentration in the extracellular environment should prevent against the development of the autoimmune response. The importance of DNase activity is reflected in SLE patients who fail to produce DNase in NETs degradation, as NETs is composed of nuclear DNA. The consequence is the formation of immune complexes comprising self-DNA and antibodies to DNA or nucleoproteins [31], which are proposed to break the host-tolerance.

4.4.2. The role of dendritic cells in DNA sensing

Dendritic cells are a specialized group of cells being capable to capture and process antigens, presenting them on major histocompatibility complex (MHC) molecules to be recognized by T cells [74]. The DCs family is divided into two subgroups, classical dendritic cells (CDCs) and plasmacytoid dendritic cells (pDCs). Classical dendritic cells are dedicated to antigen processing and different subsets of those cells are identified based on their localization and distinct functions [75]. CDCs are the most numerous DC subsets in lymphoid organs and can be cultured from the bone marrow or blood cells, such as blood monocytes (**Table III**). They have an enhanced ability to sense tissue injuries, capture and process and present antigens to T lymphocytes, inducing immunity to any foreign antigens that breach the tissue and enhance tolerance to self-antigens [76].

On the other hand, plasmacytoid dendritic cells (pDCs) are found mainly in the blood and lymphoid tissues, which acquire the morphology and functional properties of DCs only after activation. Plasmacytoid DCs constitute about 0.2 – 0.8% of all human peripheral blood cells and are reported to express low levels of MHC-II and co-stimulatory molecules (CD80, CD83 and CD86) [75]. In humans, the expression of TLR7 and TLR9 are restricted in pDCs and furthermore, the vertebrate immune system has established TLR9 and TLR7 to detect DNA and single stranded RNA respectively. Thus, these cells are unique as they produce an abundant amount of type I interferons upon the activation of TLR7 and TLR9 signalling pathways [77]. TLR9 can distinguish between the host (mammalian) and foreign nucleic acids [78], whilst TLR7 was identified as receptor for viral single-stranded RNA (ssRNA). Besides the secretion of type-I interferon, pDCs are also able to produce other inflammatory cytokines, mainly TNF-α, IL-6 and IL-12, serving as a bridge between the innate and adaptive immune response. Our

study focused on pDCs, as they constitutively express TLR9, remained inert to the exposure of some bacterial products such as lipopolysaccharide (LPS), flagellin, etc. [79].

Features	Classical dendritic cells (CDCs)	Plasmacytoid dendritic cells (pDCs)
Surface markers	CD11c high; CD11b high	CD11c low; CD11b negative
Expression of TLRs	TLRs 4, 5, 8	TLRs 7,9
Major cytokines produced	TNF-α, IL-6	type I interferons
Major functions	Induction of T cell responses against most antigens	Sense viral and bacterial pathogens and release high levels of type I interferons in response to infection

Table III. The major subpopulations of dendritic cells. Comparison between CDCs and pDCs [Adapted from Abbas et al. [75]].

4.4.3. The role of LL-37 in the recognition of nucleic acids

It was documented that LL-37 can bind nucleic acids with high affinity due to an electrostatic interaction between anionic phosphate groups of nucleic acids and cationic amino acids in the peptide. The consequence is nucleic acid packaging into aggregated and condensed structures [80]. DNA-LL-37 complexes with the net positive charges bind to anionic proteoglycans followed by lipid raft-mediated endocytosis [81]. The efficient binding of LL-37 with DNA promotes DNA translocation into the endocytic pathway of pDCs, breaking the safety mechanism for discrimination of pathogen derived DNA from self-DNA provided by the intracellular localization of TLR9. This allows the DNA-LL-37 complex to be retained in the early endosomes triggering TLR9 signalling and results in the production of type I IFNs, in a similar way to the anti-viral response. Described above interaction plays important role for bacterial DNA recognition. Hurtado and Peh have showed a significant reduction of time needed for pDCs to sense the presence of bacterial DNA via TLR9, which is beneficial especially when limiting quantities of bacterial DNA are present [82]. It was revealed that observed phenomenon plays also a crucial role in the initiation of autoimmune diseases, such as psoriasis or systemic lupus erythematosus etc. [32]. Ganguly *et al.* have also shown similar phenomenon for RNA, however in this case the mechanism is slightly different. Authors shown

that RNA-LL-37 complexes trigger TLR7 in pDCs and TLR8 in the classical myeloid DCs (CDCs) by interacting with heparan-sulfate-containing proteoglycans in the membranes of DCs [83].

The finding that LL-37 may contribute the delivery of bacterial DNA to the endosomal compartment of cells to stimulate TLR9 has opened up possibilities that other cationic peptides can share that function. For example, lactoferrin, an identified NET-associated protein [84] which is highly cationic and a major component of neutrophil secondary granules [85]. Britigan's studies have showed the cationic N-terminal component of lactoferrin was capable to bind a variety of biologically important negatively charged molecules, including unmethylated CpG motifs in bacterial DNA, on the basis of a charge-charge interactions [85].

4.5. Neutrophil extracellular traps (NETs)

Neutrophils are dominant population of white blood cells, playing bactericidal role and thus being classified as the first line of defence against intruders. They use three major strategies against microbes, as: phagocytosis, degranulation and generation of neutrophil extracellular traps (NETs). NETs are formed by activated neutrophils, which release into extracellular milieu DNA structure decorated with components of azurophilic granules. Such multidimensional structure can efficiently capture, neutralize and kill a variety of pathogens [86]. It is postulated that NETs form a physical barrier against microbial invasion and increase the effective concentration of antimicrobial effectors [86]. NETosis can be initiated by different stimuli, including chemical compounds, as phorbol 12-myristate 13-acetate (PMA), but also selected pathogens and their virulence factors [87].

The formation of NETs is a multistep process (**Fig. 6**), which results in generating large amounts of reactive oxygen species (ROS) upon the activation of the NADPH oxidase, which is the biochemical hallmark in NETosis [86]. Following stimulation, primary or azurophilic granules containing neutrophil elastase (HNE) and myeloperoxidase (MPO) are relocated into the nucleus. Morphological changes of the cells are the first observation for the event of NETosis. Neutrophils start to be flattened and gradually lose their lobes. In the nucleus, HNE degrades the linker histone H1 and the core histones, followed by chromatin decondensation and activation of PADs (particularly PAD4) which citrullinate histone. PADs are essential for NETs formation and their extrusion. It was documented that PAD4-deficient mice and cells treated with PAD4 inhibitors formed NETs at low yields. Moreover, PAD4-deficient mice are more susceptible to bacterial infections [88]. The loss of negative charge via citrullination

causes the uncoiling of heterochromatin, leading to the disintegration of nuclear and granular membranes, where the nucleoplasm and cytoplasm fused together. In this process, DNA is decorated with AMPs and proteins such as elastase and MPO, forming NETs complexes. Finally, the cytoplasmic membrane breaks and DNA is released in the form of thin filaments [89] (**Fig. 6**).

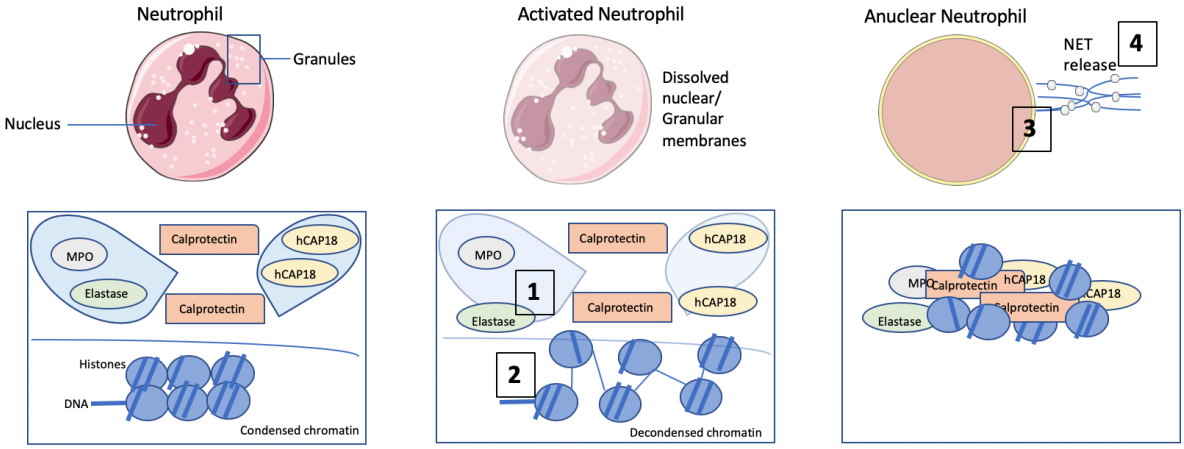

Fig. 6. Stages of NETs formation. The production of ROS followed by (1) the transportation of elastase and MPO to the cell core, (2) histone modification by PAD4, (3) the rupture of the cytoplasmic membrane and (4) the release of chromatin. The figure was created with images adapted from Servier medical art by Servier [Adapted from Sorensen and Borregaard [90]].

As NETs formation is considered beneficial during infectious process it can cause host cell damage too. It is postulated that large amount of neutrophil extracellular content being released upon septic or non-septic inflammation can lead to an autoimmune disorder. It was reported that NETs constitute a rich source of autoantigens. The reason for this is expression and activity of PAD, which catalyses the generation of a myriad of citrullinated proteins/peptides, which have significant effect on human health. Recent investigation has reported that about 84% of NETs components were identified as autoantigens in patients with autoimmune diseases (such as SLE, RA, vasculitis) [91]. Apart from playing an important role in modification of autoantigens, the generation of NETs may induce a potent activation of immune cells. The mechanism relies on formation of a complex between cationic molecules and DNA both derived from invaders or host. The consequence is accelerated stimulation of phagocytes or B cells [32].

4.5.1. Neutrophil extracellular traps (NETs) and LL-37

Neutrophil extracellular traps are decorated with bactericidal proteins such as LL-37, defensins, histones, elastase and MPO. The high levels of extracellular self-DNA complexed with LL-37 can activate TLR9 in pDCs, resulting in a robust release of interferon-α (**Fig. 7**), as reported by Lande *et al.* [32] in lupus patients. Self-DNA is unable to induce type I IFN production until it is combined with LL-37. Such interaction is responsible for the breach in the innate tolerance by converting self-DNA from being immunologically inert into a potent activator of host phagocytes. Generation of the complex with LL-37 allows for accelerated recognition and engulfment of DNA into endosomal compartments (**Fig. 7**). Moreover, such interaction efficiently protects the nucleic acids from extracellular degradation executed by circulating nucleases.

There is a mutual relationship between NETs formation and production of IFN-α. Neutrophil priming by type I IFN causes phagocytes to be more responsive to external stimuli, augmenting the NETs formation. The SLE is characterized by the chronic activation of pDCs and production of autoantibodies directed against nuclear self-antigens such as nucleic acids. Lupus patients develop autoantibodies to LL-37 and self-DNA, which bind NETs (containing DNA complexed with LL-37) to form immune complexes (ICs), which are efficiently taken up by pDCs via the Fc receptor for IgG (FcγRIIA) and thereafter translocated to TLR9-containing endosomal compartments (**Fig. 7**) [31]. The chronic activation of plasmacytoid dendritic cells by these immune complexes is known to be the early trigger for autoimmunity in patients with SLE or psoriasis [92]. Moreover, the findings of Lande *et al.* and Garcia-Romo *et al.* has led to the prediction on the generation of anti-LL-37 autoantibodies that activate neutrophils and subsequently trigger the event of NETosis that releases the complexes containing DNA and antimicrobial peptide (LL-37), providing the feedback mechanism between NETs and secretion of type I IFN. This has indicated that the accelerated formation of LL-37-DNA complexes in NETs plays a role of potent stimulators of pDCs [32][42].

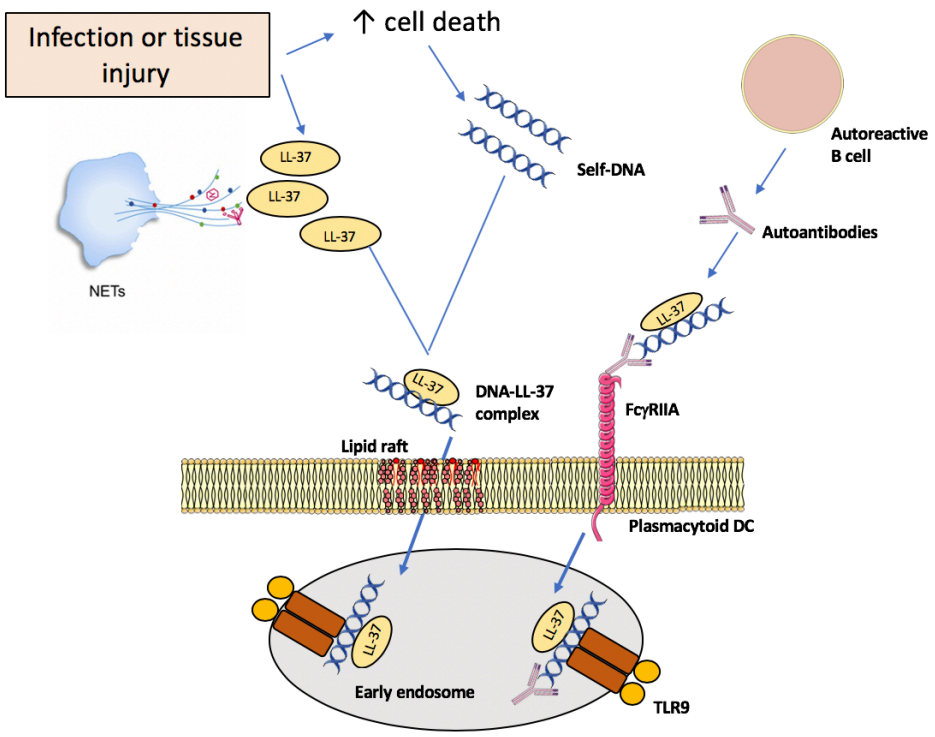

Fig. 7. The model for breakdown of innate tolerance to self DNA. LL-37 facilitates the nucleic acid delivery across membrane and activates intracellular TLR9 and enhanced the production of interferon-α. In SLE, autoantibodies produced by autoreactive B cells bind to self-DNA-LL-37 complexes and translocate into TLR9-containing endosomes in pDCs through Fc receptor for IgG (FcγRIIA) [Adapted from Lande et al. [93]].

Apart from triggering type I IFNs production in pDCs, DNA-LL-37 complexes found in NETs can directly activate human memory B cells (mBC) in lupus patients. The high immunogenic DNA-LL-37 complexes trigger polyclonal B cell activation via TLR9 with IgG production. NETs in lupus patients also led to the activation of self-reaction B cells that produce antibodies against LL-37 which are potent inducers of NETosis, creating a feedback loop. Besides that, NETs can induce NET-specific mBC of lupus patients as there was an increased frequency of NET-specific B cells in these patients compared to healthy individuals [94].

Besides dendritic cells, the inflammatory potential of NETs has been documented towards macrophages. Kahlenberg *et al.* observed the activation of the NALP3 inflammasome by lupus NETs and NET associated LL-37 in LPS-primed macrophages. This stimulation likely

leads to a self-perpetuating cycle of enhanced IL-1β and IL-18 production that promotes inflammation and NETosis [30].

As described above LL-37 is a molecule that plays the important role in the regulation of DNA recognition by host cells. As a component of NETs, structure characterized with high activity of PAD, is highly possible that LL-37 undergoes deimination changing the function of the peptide. Therefore, studies presented in my thesis are focused on that topic.

5. Aims of this study

Post-translational modifications play an important role in the regulation of innate immunity. Several studies have reported their association with the development of inflammatory diseases, with the emphasis on citrullination process catalysed by peptidyl arginine deiminases [57][61]. The only human cathelicidin – peptide LL-37 consists five Arg residues, which are efficiently modified by PAD enzymes. As documented recently, deimination of LL-37 abolished the protective role of the peptide against endotoxin [67]. Therefore, presented study is focused on another immunological pathway effectively modulated by LL-37, which is formation of complexes with nucleic acids and subsequent activation of inflammatory response manifested by interferon type I pathway activation. Therefore, in the study we examined how citrullination of LL-37 affects the immunostimulatory potential of cell-free DNA.

The particular aims of this study were as follows:

1. To determine the efficiency and specificity of LL-37 deimination on the binding of nucleic acid.
2. To determine the role of LL-37 citrullination on sensitization of TLR9 positive cells to DNA.
3. To identify the presence of citrullinated LL-37 *in vivo.*
4. To study the effect of LL-37 citrullination on immunomodulatory potential of NETs.

6. Materials and Methods

6.1. Materials

6.1.1. Primary cells and cell lines

Name	Source
Macrophages, plasmacytoid dendritic cells, neutrophils	Blood from healthy human volunteers was obtained from Regional Blood Centre, Krakow, Poland. Description of the isolation methods is as per methods section 6.2.8. and 6.2.16.
RAW264.7 (murine macrophage cell line)	Obtained from ATCC (American Type Culture Collection)
HeLa cell line (epithelial cells from human cervix)	

6.1.2. Human probes

Name	Source
Inflamed sera and synovial fluid obtained from rheumatoid arthritis patients for the estimation of LL-37 half-life in biological fluids	Courtesy of Piotr Mydel, Ph.D., MD.
Sera from periodontitis, RA patients or patients with both diseases (periodontitis and RA) and control donors (patients without RA and periodontitis) for identification of antibodies against LL-37 and citrullinated LL-37	Courtesy of Prof. Sigrun Eick, Ph.D., D.D.S.

6.1.3. Reagents for cell cultures

Reagents	Source
Autologous plasma	Isolated from human peripheral blood from healthy donor
BD IMAG^{TM} buffer	BD Biosciences
Black 96-well microplates	Thermo Fisher Scientific
Dulbecco's Phosphate Buffered Saline (DPBS - without calcium and magnesium)	
Gentamicin (50 mg/mL)	
Gibco DMEM (with High Glucose, ι-Glutamine, HEPES) With/without Phenol Red	

Gibco RPMI-1640 with L-glutamine	
Heat Inactivated Fetal Bovine Serum (FBS)	
BD IMag^{TM} Human Dendritic Cell Enrichment Set	BD Biosciences
Lymphocyte Separation Medium (LSM 1077)	PAA
Penicillin-Streptomycin Solution (10,000 units Penicillin, 10 mg Streptomycin/ml) (PEST)	Sigma Aldrich
Poly-D lysine	Sigma Aldrich
Polyvinyl alcohol (PVA)	POCh

6.1.4. Reagents for cell stimulation

Name	**Source**
CpG oligodeoxynucleotides (ODN 2216) (5' -ggGGGACGA:TCGTCgggggg- 3')	Hycult Biotech
Cytochalasin D	Sigma Aldrich
Different variants of carbamylated LL-37*	The peptides were synthesized by ProImmune as per Koro *et al.* [51].
FITC labelled CpG (ODN 2216) (5' -ggGGGACGA:TCGTCgggggFITC- 3')	InvivoGen
Lipopolysaccharide from *E. coli* O111:B4	Sigma Aldrich
Native LL-37, CRAMP, scrambled LL-37 (sLL-37), LL-37 with arginine residues substituted by homoarginine (hArg-LL-37), different variants of the citrullinated peptide*	The peptides were synthesized by Jan Pohl (Division of scientific resources, Centers for Disease Control and Prevention)
Phorbol 12-myristate 13-acetate (PMA)	Sigma Aldrich

***** *Sequences of the peptides is as per section 6.1.20*

6.1.5. Reagents for transduction of RAW264.7

Name	**Source**
Cignal Lentiviral particles containing NF-κB luciferase reporters	SA Biosciences
Luciferase reporter assay system	Promega
Puromycin	Gibco
SureEntry transduction reagent	Qiagen
Opaque 96-well plate	PerkinElmer

6.1.6. Bacteria

Name	Source
Staphylococcus aureus (Newman)	Collection of laboratory strains, Department of Microbiology, WBBiB, UJ

6.1.7. Reagents for bacteria cultures

Reagents	Source
Agar	BioShop
Tryptic Soy Broth (TSB)	Fluka

6.1.8. Reagents for *in vitro* citrullination of LL-37

Reagent	Source
Recombinant human PAD2 or PAD4	Modiquest

6.1.9. Reagents for genomic DNA isolation

Reagent	Source
Genomic mini kit	A & A Biotechnology
Nuclease-free water	Thermo Fisher Scientific

6.1.10. Reagents for PCR

Reagents	Source
dNTP mix	Thermo Scientific
Kit: PCR purification	A&A Biotechnology
Starters (sequences as per section 6.2.1.)	Genomed
Taq buffer KCl	Thermo Scientific
Taq DNA Polymerase	Thermo Scientific

6.1.11. Reagents for electrophoretic mobility shift assay (EMSA)

Reagents	Source
Agarose, Biotechnology Grade	Bioshop
Ethidium Bromide	Sigma Aldrich
GeneRuler^{TM} Low Range DNA Ladder	Thermo Fisher Scientific

6.1.12. Reagents for fluorescence measurement and immunocytochemistry

Reagents	Source
Alexa-Fluor-647 goat anti-mouse antibody	Jackson ImmunoResearch Laboratories
Fluorescence Mounting Medium	Dako
Hoechst 33342	Molecular Probes
Human Monoclonal Anti-LL-37/CAP18	Hycult Biotech
Paraformaldehyde	PoCh
QuantiT^{TM} PicoGreen® dsDNA Reagent	Life Technologies
Saponin	Sigma Aldrich

6.1.13. Reagents for measuring protein concentration

Reagents	Source
Bicinchoninic Acid Protein Assay Kit (BCA)	Thermo Fisher Scientific

6.1.14. Reagents for SDS-PAGE and Western blot

Reagents	Source
Acrylamide	BioShop
Ammonium Persulfate (APS)	BioShop
Anti-modified citrulline detection kit	EMD Millipore
Glycerol	Sigma Aldrich
Glycine	ICN Biomedicals
Methanol 99.9%	PoCh
N,N,N',N'-tetramethyletyleneidamine (TEMED)	Sigma Aldrich

N,N'-Methylenebisacrylamide	Sigma Aldrich
Ovalbumin	Sigma Aldrich
PageRuler™ Plus Prestained Protein Ladder	Thermo Fisher Scientific
Pierce™ ECL Western Blotting Substrate	Thermo Fisher Scientific
Pierce™ Lane Marker Reducing Sample Buffer	Thermo Fisher Scientific
Polyvinylidene difluoride (PVDF) membrane	Amersham
Sheep Anti-Mouse IgG, HRP conjugate	Sigma Aldrich
Skimmed Milk	Bioshop
Sodium Dodecyl Sulphate (SDS)	ICN Biomedicals
Tricine	BioShop
Tris	Bioshop

6.1.15. Reagents for ELISA

Reagents	**Source**
Human LL-37 ELISA kit	Hycult Biotech
OptEIA Human IL-6 ELISA kit	BD Biosciences
OptEIA Human IL-1β ELISA kit	
OptEIA Mouse TNF-α ELISA kit	
VeriKine Human IFN-α kit	PBL Interferon Source
TransAM® IRF7 ELISA kit	Active Motif
TransAM® NF-κB ELISA kit	Active Motif
Nunc-Immuno™ strip with Maxisorp™ surface	Thermo Fisher Scientific
Peroxidase-conjugated mouse anti-human IgG	Genscript
Sodium Bicarbonate	PoCh
Sodium Carbonate	PoCh
Sulphuric Acid	PoCh
TMB Substrate Reagent Set	BD Biosciences
Tween-20	BioShop

6.1.16. Reagents for RNA isolation and cDNA synthesis

Reagents	Source
Chloroform	PoCh
Ethanol	PoCh
Isopropanol	PoCh
High-Capacity cDNA Reverse Transcription Kit	Applied Biosystems
RNase-free water	BioShop
Starters (sequences as per section 6.2.28.)	Genomed
SYBR™ Green JumpStart™ Taq ReadyMix™	Sigma Aldrich
TRIzol Reagent	Sigma Aldrich

6.1.17. Other chemicals

Chemicals	Source
1,4-dithiothreitol (DTT)	Biomol
Acetate	PoCh
Acetic Acid 99%	POCh
Bovine Serum Albumin (BSA)	Bioshop
Calcium Chloride ($CaCl_2$)	PoCh
Dimethyl Sulfoxide (DMSO)	Sigma Aldrich
RNase-free DNase I	Promega
Ethylenediaminetetraacetic acid (EDTA)	Bioshop
Hydroxyethyl piperazineethane sulfonic acid (HEPES)	Sigma Aldrich
L-Citrulline	Sigma Aldrich
Na-deoxycholate	Sigma Aldrich
Na-HEPES	Sigma Aldrich
Nonyl phenoxypolythoxylethanol (NP-40)	Sigma Aldrich
Phenylmethylsulfonyl fluoride (PMSF)	Thermo Fisher Scientific
Sodium Chloride (NaCl)	POCh
Trichloroacetic Acid	Sigma Aldrich
Triton X-100	Bioshop

6.1.18. List of equipment

Equipment	Trade Name	Company
Bright Field Microscope	Hund Wilovert S 30	Helmut Hund GmbH
Cell separation magnet	BD IMAGNET™	BD Biosciences
Centrifuges	Heraeus Multifuge X1R Heraeus Fresco 21 microcentrifuge	Thermo Scientific
Electrophoresis apparatus	Mini-PROTEAN II	BioRad
Flow cytometer	BD FACSCalibur™	BD Biosciences
Immunofluorescence Microscope	Nikon Eclipse Ti	Nikon
Gel Imaging	Gel Doc™ EZ System	BioRad
Heat Block	ThermoBlock TB941U	JW Electronic
Incubator	HeraCell 150	Haraeus
Laminar flow hood	SafeFlow 1.2	BioAir Instruments
Microplate reader	FlexStation™ 3 Multi Mode microplate reader	Molecular Devices
NanoDrop	NanoDrop™ 1000	Thermo Scientific
pH meter	Lab 850	Global Water Instrumentation
Real-Time Thermal Cycler	CFX96 Touch™ Real-time PCR Detection System	BioRad
Spectrophotometer	Cecil CE 3021	Cecil Instruments
Thermocycler	Tprofessional TRIO thermocycler	Biometra

6.1.19. Buffers

Anode Buffer for SDS-PAGE: 200 mM Tris; pH 8.9

Blocking buffer for ELISA: 2% BSA in PBS

Blocking buffer for membrane: 3% BSA in TTBS

Buffer for gel SDS-PAGE (Schagger/Von Jagow): 3 M Tris, 0.3% SDS; pH 8.45

Cathode Buffer for SDS-PAGE: 100 mM Tris, 100 mM Tricine, 0.1% SDS; pH 8.25

EB Buffer for nuclear extractions: 0.35 M NaCl, 5 mM EDTA, 1 mM DTT, 10 mM Na-Hepes, 0.2 mM phenylmethylsulfonyl fluoride (PMSF)

Electrotransfer buffer for Western blot: 25 mM Tris, 192 mM Glycine, 20% Methanol

PAD assay buffer: 100 mM Tris-HCl, 5 mM $CaCl_2$, 5 mM DTT; pH 7.6

RIA buffer: 1% BSA, 350 mM NaCl, 10 mM Tris-HCl, 1% Triton X-100, 0.5% Na-deoxycholate, 0.1% SDS; pH 7.6

RSB buffer for nuclear extractions: 10 mM NaCl, 3 mM $MgCl_2$, 10 mM Tris (pH 7.5), 0.2 mM (PMSF)

TAE buffer for EMSA: 40 mM Tris, 20 mM Acetate, 1 mM EDTA

TBS: 1 M Tris, 3 M NaCl; pH 7.5

TE buffer: 10 mM Tris, 1 mM EDTA; pH 8.0

TTBS: 20 mM Tris, 500 mM NaCl, 0.05% Tween-20; pH 7.5

Washing buffer for ELISA: 0.05% Tween-20 in PBS

6.1.20. Sequences of the peptides used in this study

Peptide	Sequence
LL-37	LLGDFFRKSKEKIGKEFKRIVQRIKDFLRNLVPRTES
LL-37_{7}	LLGDFF(**Cit**)KSKEKIGKEFKRIVQRIKDFLRNLVPRTES
LL-$37_{7,29}$	LLGDFF(**Cit**)KSKEKIGKEFKRIVQRIKDFL(**Cit**)NLVPRTES
LL-$37_{7,29,34}$	LLGDFF(**Cit**)KSKEKIGKEFKRIVQRIKDFL(**Cit**)NLVP(**Cit**)TES
LL-$37_{\text{all cit.}}$	LLGDFF(**Cit**)KSKEKIGKEFK(**Cit**)IVQ(**Cit**)IKDFL(**Cit**)NLVP(**Cit**)TES
LL-37_{K1}	LLGDFFR(**ε-carb-K**)SKEKIGKEFKRIVQRIKDFLRNLVPRTES
LL-37_{K2}	LLGDFFRSKE(**ε-carb-K**)IG(**ε-carb-K**) EFKRIVQRIKDFLRNLVPRTES
LL-37_{K3}	LLGDFFRKSKEKIGKEFKRIVQRI(**ε-carb-K**)DFLRNLVPRTES
sLL-37	RSLEGTDRFPFVRLKNSRKLEFKDIKGIKREQFVKIL
hArg-LL-37	LLGDFF(**hR**)KSKEKIGKEFK(**hR**)IVQ(**hR**)IKDFL(**hR**)NLVP(**hR**)TES
CRAMP	GLLRKGGEKIGEKLKKIGQKIKNFFQKLVPQPEQ
$CRAMP_{cit.}$	GLL(**Cit**)KGGEKIGEKLKKIGQKIKNFFQKLVPQPEQ

Modified residues (Cit, ε-carb-K, and hR) are shown in bold.
ε-carb-K, lysine carbamylated on the ε-carb; cit, citrullinated arginine; hR, homoarginine (hArg)

6.2. Methods

Biochemical analysis

Concentrations mentioned in this section are the final concentrations of the respective compounds.

6.2.1. Amplification of bacterial DNA

Genomic DNA of *Tannerella forsythia*, which was used as a template for the PCR assay, was a kind gift from Danuta Mizgalska, Ph.D. Concentration of nucleic acids was quantified with NanoDrop before performing PCR. PCR was conducted using 20 µl reaction mixture, which consisted of 20 ng of template DNA, 2 µl of *Taq* buffer KCl, 1.5 µl of 2 mM mixed dNTPs, 0.5 µl *Taq* DNA Polymerase and 10 µM of forward (5'-

CTCGTAGTGTGCCTTCTTCCAC-3') and reverse (5'-GCCTGATCGGCATTCATTCGG-3') primers. PCR was performed with the following conditions: initial denaturation at 95°C for 3 minutes, followed by 35 cycles of denaturation at 95°C for 30 seconds, annealing at 53°C for 20 seconds, extension at 72°C for 30 sec and final extension at 72°C for 5 minutes. Then, the spin column-based PCR purification was performed as per the manufacturer's instructions. A 5:1 ratio of binding solution was added to the PCR product prior transferring the sample onto minicolumn, which consists silica membrane. Minicolumn attaching to the tube was centrifuged for 30 sec at 16,100 x g. The flow-through in the tube were discarded before attaching the minicolumn to the same tube. The DNA binds to the silica membrane and contaminants were washed away by following washing steps: 600 µl of wash solution was added to the minicolumn before the centrifugation at 16,100 x g for 30 seconds. The flow-through was discarded and this step was repeated twice before the final centrifugation at 16,100 x g for 2 minutes. The minicolumn was then placed into a new 1.5 ml eppendorf tube. Thirty µl of nuclease-free water was added to the silica membrane and DNA bound to the silica membrane was harvested by collecting the eluent after 1 minute of centrifugation at 16,100 x g. The pure DNA was quantified with NanoDrop to determine its concentration.

6.2.2. Isolation of HeLa genomic DNA

HeLa cells were grown in culture medium (DMEM supplemented with 10% FBS and 50 µg/ml PEST (penicillin/streptomycin) at 37°C in a humidified 5% CO_2 atmosphere. To isolate genomic DNA from HeLa cells, the culture was first trypsinized after washing the cells with PBS, and then centrifuged for 10 min at 4°C, 280 x g. The cell pellet was resuspended in fresh culture medium and number of cells were counted using Fuchs-Rosenthal haemocytometer as described in section 6.2.9.

Genomic DNA of the HeLa cell line was isolated using the Genomic Mini kit as according to the manufacturer's instructions. The genomic DNA was isolated from one million of cells, which were resuspended in 100 µl Tris buffer with 200 µl lysis buffer and 20 µl proteinase K, which were all provided in the kit. The sample was incubated for 20 min at 37°C, followed by 5 min at 70°C. Next, the sample was vortexed for 20 sec and centrifuged for 3 min at 13,200 x g at 4°C. Supernatant was collected and transferred to a microcolumn for genomic DNA purification, followed by centrifugation at 13,200 x g for 1 min at 4°C. Then 500 µl of the rinsing solution was added to the DNA bound to the column bed and centrifuged for 1 min

at 13,200 x g, 4°C. Subsequently, the microcolumn was moved to a new tube and 400 µl of rinse solution was added to the microcolumn. After 2 min of centrifugation at 13,200 x g, 4°C, the dried microcolumn was placed in a new 1.5 ml eppendorf tube and 200 µl of DNase-free water which was preheated to 75°C was added to the microcolumn. After 5 min incubation at room temperature, the sample was centrifuged for 1 min at 13,200 x g, 4°C. Finally, the microcolumn was removed and the purified genomic DNA contained in the eppendorf tube was stored at -20°C. The concentration of the isolated genomic DNA was measured using the Nano Drop 1000 device.

6.2.3. *In vitro* citrullination of LL-37

To determine the process of LL-37 citrullination, peptide was incubated with either recombinant human PAD2 or PAD4. The *in vitro* citrullination of native LL-37, CRAMP, scrambled LL-37 (sLL-37), hArg-LL-37 and carbamylated LL-37 (K1-K3) was performed according to the previously described protocol [67]. Briefly, peptides were diluted to a concentration of 1 mg/ml in PAD assay buffer and incubated with either recombinant human PAD2 or PAD4 at concentration of 23 U/mg, for different time points (0, 15, 30, 120 minutes or just 120 minutes for CRAMP, sLL-37, hArg-LL-37 and carbamylated LL-37) at 37°C. Citrullination was terminated by freezing.

6.2.4. Gel retardation assay

The interaction of LL-37 and DNA was evaluated with a gel retardation assay. Complexes of nucleic acid with the peptide were generated as described by Chuang *et al.* [95]. PCR product obtained from *T. forsythia* genomic DNA as described in 6.2.1. was mixed with either the synthetic native or modified forms of LL-37 or CRAMP at a 1:5 molar ratio (DNA:peptide) and incubated at room temperature for 10 minutes. The complex formation was determined with a gel retardation assay by running probes on 1.5 % agarose gel.

6.2.5. Spectra analysis

Another approach to evaluate the complex formation between DNA and LL-37 was based on the fluorescence of nucleic acid as described by Lande *et al.* [32]. Complexes were

generated as mentioned above (section 6.2.4.). The complexes were treated with diluted Quant-iT PicoGreen dye solution (1:200) according to manufacturer's instructions and the amount of unbound DNA was analyzed across a spectrum of wavelengths 500 nm - 600 nm after excitation at 480 nm.

6.2.6. Surface plasmon resonance (SPR)

Surface Plasmon Resonance used for more detailed and quantitative studies of interaction between DNA and LL-37 (native and different modified forms) was performed by Prof. Maria Rąpała-Kozik, Ph. D. from the Department of Comparative Biochemistry and Bioanalytics, FBBB, Jagiellonian University. Selected fragment of DNA (5' ggGGGACGA:TCGTCgggggg- 3'), biotinylated at the 5′ end of the antisense strand (Bt-DNA) was immobilized on the streptavidin (SA) sensor chip (GE Healthcare) with streptavidin covalently attached to the dextran. For the immobilization, the sensor surface was pre-treated according to the manufacturer's instruction and the solution of Bt-DNA (0.05 ng/µl) in 0.5 M NaCl was injected into the cell at a flow rate of 2 µl/min for 7 minutes. The chip surface was then washed with subsequent solutions of 0.5 M NaCl, 1 M NaCl and 0.1% SDS, for 3 minutes each at a flow rate of 20 µl/min to remove the non-specifically bound ligand. Further conditioning of the chip surface was performed with the running buffer (10 mM HEPES, 150 mM NaCl, pH 7.4 with 0.05% P20 surfactant) until a stable baseline signal was obtained. The amounts of coupled DNA correspond to 210 response units (RU). A flow cell without DNA was used as a reference. For the binding experiments a series of native and different variants of the modified LL-37 peptide samples were prepared by dilution of 100 µM peptide stock solution in running buffer. In some experiments, ApoA-1 was mixed with native and different variants of the modified LL-37 peptide samples ranging from 0 – 20 µM. The samples were injected over the sensor surface at 30 µl/min flow rate using 2 minutes interval for association and for dissociation process. The surface regeneration with 1 M NaCl for 30 seconds was performed after each sample injection. Mass transfer effects did not influence the LL-37 binding. The collected data were analysed using BIAevaluation software version 4.1 (Biacore).

6.2.7. DNase protection assay

Free DNA is susceptible to degradation by DNases. However, the electrostatic interaction of DNA and LL-37 has provided the possibility of protection of these condensed

particles against extracellular enzymatic degradation [83]. To verify the protection of DNA by its binding to peptide we applied the assay published by Lande *et al.* [32]. For that purpose, mixtures of isolated HeLa DNA with either LL-37 or LL-37_7 prepared as described above (section 6.2.4) were treated with 100 U/ml DNase A (A&A Biotechnology) for 60 min at 37°C, followed by inactivation of the enzyme by incubating the samples at 75°C for 10 minutes. The protection from extracellular degradation was analyzed as described in 6.2.18. with Quant-iT PicoGreen, upon excitation at 480 nm and emission at 520 nm.

***In vitro* studies**

6.2.8. Cell cultures

Peripheral blood mononuclear cells (PBMCs) were isolated from healthy human EDTA-treated blood, collected from Regional Blood Centre (Krakow, Poland), using density gradient centrifugation. Blood cells were first separated from plasma by centrifuging at 400 x g for 12 min at 20°C. Plasma was collected and centrifuged for 15 min, 3,000 x g at 20°C. Supernatant was collected and this was followed by incubation at 56°C for 30 minutes. The clean autologous plasma was obtained by another centrifugation at the same condition (3,000 x g/ 15 min/ 20°C). Whilst phosphate-buffered saline (PBS) was added to the blood and the diluted cell suspension was carefully layered over 15 ml of lymphocyte separation medium before centrifuging at 400 x g for 35 min at 20°C. Whitish buffy coats were collected into RPMI containing 1% Fetal Bovine Serum (FBS) and cell pellet was obtained by centrifuging at 350 x g for 12 min at 20°C. Then, cells were overlaid on FBS and centrifuged at 280 x g for 10 min at 20°C. After the final centrifugation, cells were resuspended in RPMI supplemented with 2 mM L-Glutamine, 10% of the autologous plasma and 50 μg/ml gentamicin. Three million PBMCs/well were seeded on 24-well plate and incubated overnight at 37°C in a humidified 5% CO_2 atmosphere. Non-adherent cells were removed next day by washing with PBS and fresh media (RPMI supplemented with 2 mM L-Glutamine, 10% of the autologous serum and 50 μg/ml gentamicin) were replaced for each well. Adherent monocytes differentiated within one week into monocyte-derived macrophages (hMDMs).

Isolated PBMCs were also used to obtain plasmacytoid dendritic cells (pDCs) with BD IMAG™ Cell Separation System (BD Biosciences). Firstly, clumps of cells from PBMCs were removed by passing the suspension through a 70 μm nylon cell strainer. The suspension was

centrifuged at 300 x g for 10 min at 4°C to remove the media and cells were resuspended in BD IMAG™ buffer (commercialized buffer containing bovine serum albumin, EDTA, and sodium azide in PBS - recommended for optimal cell separation) at the concentration of 5 x 10^7 cells/ml. Next, Human Dendritic Cell Enrichment Cocktail from BD IMag™ Human Dendritic Cell Enrichment Set was added to the cell suspension with the amount of 5 µl per 1 x 10^6 cells. After 15 min incubation at room temperature the labelled cells were washed with 10 times excess volume of BD IMAG™ buffer, followed by centrifugation at 300 x g for 7 min at 4°C. Cell pellet was resuspended with BD IMAG™ Streptavidin Particles Plus at the amount of 7.5 µl of particles per 1 x 10^6 cells and incubated for 30 min at room temperature. BD IMAG™ buffer was added up to the volume of 1 ml, the labelled cells were transferred to a 12 x 75 mm round bottom test tube and placed on the BD IMagnet™ for 7 minutes. Supernatant was collected into new sterile tube and 1 ml of BD IMAG™ buffer was added to resuspend the pellet carefully. Then, the tube was placed again on the BD IMagnet™ for 7 minutes. This process was repeated twice and to increase the purity of the cells, the tube containing collected supernatant was placed on the BD IMagnet™ for 10 min before centrifugation at 300 x g for 10 min at 4°C. Cell pellet was resuspended with RPMI containing 10% FBS and 50 µg/ml of gentamicin. Eighty thousand cells were seeded per well of 96 round-bottom plate followed by centrifugation at 300 x g for 10 min at 4°C before proceeding with the stimulation.

RAW264.7, a murine macrophage cell line, was maintained in DMEM supplemented with 10% FBS and 50 µg/ml PEST (penicillin/streptomycin) at 37°C in a humidified 5% CO_2 atmosphere. Cells were passaged, when they reached 60-75% of confluence on the flask by detaching them using a cell scraper. Then the cell suspension was collected and centrifuged at 280 x g for 10 min at 4°C. Obtained cell pellet was resuspended in fresh media and cells were seeded in the flask for further cultivation or in 96-well plate when used for experiments with the cell concentration of 0.2 x 10^6 cells/well.

6.2.9. Counting of cells and cell viability

Trypan blue exclusion method was used for cell count and to determine the cell viability. Trypan blue (180 µl) was added to 20 µl of cell suspension and next 20 µl of the mixture was transferred to Fuchs-Rosenthal haemocytometer, where the non-stained viable cells were calculated under the bright field microscope.

6.2.10. Cell stimulation with DNA – LL-37 complexes

Mixture of CpG (final concentration 3 μM) and different forms of modified LL-37 (final concentration 6.4 μM) was first incubated in PBS 10 min prior to cell stimulation. Plasmacytoid DCs were seeded at 0.8 x 10^5 cells/well in 200 μl of complete medium (RPMI 1640 medium supplemented with 10% FBS and 50 μg/ml gentamicin) and stimulated with CpG:peptide mixtures overnight or for 15 minutes, before their washing with PBS (3 times), followed by overnight incubation in fresh complete medium at 37°C in a humidified 5% CO_2 atmosphere. Supernatant was collected for further analysis with ELISA and cell morphology was visualized with bright-field microscopy. Murine macrophages RAW264.7 were seeded in a density 0.2 x 10^6 cells/well of 96–well plate. Next day adherent cells were washed with PBS, fresh medium was added followed by CpG:peptide mixtures stimulation as described above for pDCs.

6.2.11. Internalization of DNA upon interaction with LL-37

To study the uptake of DNA by phagocytes in the presence of LL-37 and its modified forms, flow cytometry analysis was applied. RAW264.7 (2 x 10^6 cells/well) or isolated plasmacytoid DCs (0.8 x 10^5 cells/well) was incubated with mixtures of FITC-labelled CpG (3 μM) and native/fully citrullinated LL-37 respectively (6.4 μM) for 15 min before washing the cells three times with PBS. The cell pellet was resuspended with cold PBS before FACS analysis. The uptake of the mixtures was determined by measuring the fluorescence intensity with flow cytometry (BD Biosciences). The mean fluorescence intensity and percentage of positive cells labelled with FITC-conjugated CpG were measured. In some experiments, cytochalasin D (5 μM), used to study the phagocytosis inhibition, was added for 30 min before the treatment of plasmacytoid DCs with complexes CpG-peptide.

6.2.12. Transduction of RAW264.7 cells and NF-κB activity measurement

To investigate the activation of NF-κB transcription factor following cell stimulation with CpG:peptide mixtures we used RAW264.7 cells expressing inducible reporter constructs for NF-κB and luciferase gene as an indicator of the signal transduction activity. Transduction of cells was performed with Cignal^{TM} Lenti NF-κB Reporter systems by SA Biosciences.

Selection of successfully transduced cells was based on their resistance to puromycin. RAW264.7 cells were seeded in 24-well plate with the concentration of 0.1 x 10^6 cells/well in DMEM supplemented with 10% FBS. Next day cells were infected with MOI 1:50 of Cignal^{TM} lentiviral particles in DMEM supplemented with 10% FBS. Eight μg/ml of SureENTRY^{TM} transduction reagent was added to enhance transduction efficiency. Transduction medium was removed after overnight incubation and 1 ml of fresh medium supplemented with 4 μg/ml of puromycin was added to each well. Next day, floating cells were discarded and adherent (transduced) cells were harvested by scraping in fresh medium before their transferring to cell culture flask. Transduced cells were incubated in DMEM supplemented with 10% FBS and 4 μg/ml of puromycin for 3 days and fresh culture media (DMEM/ 10% FBS/ 4 μg/ml of puromycin) were replaced until further use.

For analysis of NF-κB activity, transduced RAW264.7 cells were seeded on opaque 96-well plate (0.2 x 10^6 cells/well) and incubated overnight. Then, 20 μl of CpG:peptide mixtures (prepared as described in section 6.2.10) were added and incubate for 6 h. Activation of NF-κB was measured with luciferase assay system as per manufacturer's instructions. Cells were first lysed with 20 μl of cell culture lysis reagent provided in the kit followed by the addition of 100 μl luciferase assay reagent to each well. Luciferase activity was measured instantly with luminometer (FlexStation 3, Molecular Devices).

6.2.13. Enzyme linked immunosorbent assay (ELISA)

Commercialized sandwich ELISA (BD OptEIA™, US) kits were used to quantify cytokines (murine TNF-α, human IL-6, human IL-1β) secreted by phagocytes. Briefly, wells of Nunc-Immuno^{TM} strip with MaxiSorp^{TM} surface were coated with capture monoclonal antibody specific for murine TNF-α, human IL-6 and human IL-1β respectively. The plates were incubated overnight at 4°C and excess capture antibody was removed by washing three times with PBS containing 0.05% Tween-20 (washing buffer). Non-specific peptide binding was blocked by incubating each well with assay diluent (PBS supplemented with 10% FBS) for 2 hours, followed with three times washing. Samples and standards were prepared in assay diluent. Multiple dilutions with concentration suggested by the manufacturer were prepared. Standards and samples were incubated for 2 h and unbound cytokine was washed away with washing buffer for 5 times. Biotinylated anti-mouse TNF-α, human IL-6 and human IL-1β conjugated with avidin-horseradish peroxidase (HRP) was added to each well respectively and

incubated for 1 hour. After 7 washes, chromogenic substrate solution of tetra-methylbenzidine (TMB) was added and incubated in dark. Reaction was stopped adding 1 M H_2SO_4. The colour intensity of developed colour was proportional to the amount of cytokine present in the samples measured at 450 nm within 30 minutes, using the standard curve as a reference.

Type I IFN-α from cell supernatant was measured by ELISA using VeriKine Human IFN-α kit. Standards and samples were prepared with provided dilution buffer and added to each well, which was pre-coated with monoclonal antibody specific for human IFN-α. After 1 h of incubation at room temperature, wells were washed once with provided wash solution and diluted detection antibody was added to each well as according to manufacturer's instructions. Next, wells were washed three times with washing solution and incubated with diluted HRP solution (prepared as according to manufacturer's instructions) for 1 h at room temperature. After 4 times washing, TMB substrate solution was pipetted into each well and the plate was incubated in the dark for 15 min to allow the reaction development. Stop solution (1 M H_2SO_4) was added to each well and absorbance was measured at 450 nm within 5 minutes.

Specificity of antibody against native LL-37 towards modified forms of peptides was estimated using a commercial human LL-37 ELISA ready-to-use kit. Briefly, standards and samples (10 ng/ml native and differently modified forms of LL-37) were prepared in assay diluent and transferred into respective wells and incubated for 1 h at room temperature. Wells were washed with wash buffer provided by the kit for 4 times followed by the addition of diluted tracer to each well and incubated at room temperature for 1 hour. The wells were washed as mentioned before and working solution of streptavidin-peroxidase was added to each well and incubated 1 h at room temperature before the washing steps as previously. One hundred µl of TMB substrate were added to each well and incubated until the development of TMB reaction was observed. The reaction was stopped by adding stop solution and the plate was read at 450 nm within 30 minutes.

6.2.14. ELISA based measurement of NF-κB and IRF7 DNA binding activity

Activation of NF-κB in RAW264.7 cells and IRF7 in pDCs were analyzed using TransAM® DNA-binding ELISA. Cells were incubated for 15 min with CpG-LL-37 and mixture of CpG with modified forms of LL-37 (mixtures generation as per section 6.2.10.), then nuclear extracts were isolated according to following procedure. Briefly, cells were rinsed with PBS and scraped with a plate scraper in 0.5 ml of PBS. The samples were collected and

centrifuged at 400 x g for 5 min at 4°C. The resulting pellet was resuspended in 400 µl of RSB buffer and incubated 15 min on ice. Next, 25 µl of 10% NP-40 was added to the samples and after 30 sec, the samples were centrifuged at 500 x g for 1 min at 4°C. The nuclear fraction was extracted in 50 µl EB buffer and incubated on ice for 20 minutes. The suspension was centrifuged at 500 x g for 5 min at 4°C and supernatant was collected. The protein concentration was determined using BCA test. The activity of the NF-κB or IRF7 was measured using the commercialized available TransAm® NF-κB ELISA kit or TransAm® IRF7 ELISA kit respectively. Thirty µl of complete binding buffer provided by the kit and 20 µl of sample containing 10 µg of nuclear extracts was loaded in to a 96-well assay plate, coated with oligonucleotide representing a consensus-binding site for NF-κB (5'-GGGACTTTCC-3') or IRF7 (5′-GAAAGCAAAAA- GAGAAGTAGAAAGTAA-3′) respectively. The plates were incubated for 1 h at room temperature with mild agitation. Wells were washed 3 times with wash buffer and 100 µl of diluted anti-p50 or anti-IRF7 were added to respective wells and incubated for 1 h at room temperature without agitation. Wells were washed 3 times and 100 µl of diluted HRP-conjugated antibody were added and incubated at room temperature for 1 hour. Wells were washed 4 times before the addition of developing solution. Hundred µl of stop solution was added and the plates were read on a spectrophotometer within 5 min at 450 nm with the reference wavelength of 655 nm.

6.2.15. Measurement of protein concentration- BCA test

The total protein concentration was determined using the commercialized kit Pierce™ BCA protein assay. This assay was developed based on the reduction of Cu^{2+} to Cu^{1+} by protein in an alkaline medium with the highly sensitive and selective colorimetric detection of the cuprous cation (Cu^{1+}) by bicinchoninic acid., which is strongly influenced by four amino acid residues (cysteine, cystine, tyrosine and tryptophan) in the amino acid sequence of the protein. Total of 10 µl of samples or standards containing 2 µl of the protein lysates or standards (BSA) were added to each respective well. Next, 190 µl of a 1:50 ratio mixture of $CuSO_4$:BCA was added to all wells and the plate was incubated in the dark for 30 min at 37°C. The plate was measured at 562 nm using a spectrophotometer plate reader and the concentration of the test protein was determined using the standard curve of BSA.

NETs studies

6.2.16. Neutrophils isolation

Neutrophils were isolated from granulocyte-enriched fractions, which were harvested using a lymphocyte separation medium density gradient as described in 6.2.8. Briefly after 30 min incubation in 1% solution of polyvinyl alcohol, the upper phase that contains neutrophils were carefully collected into a new tube and centrifuged at 280 x g for 10 minutes, at room temperature. Supernatant was removed and the pellet was subjected to hypotonic lysis to remove contaminating RBCs. For that purpose, pellet was resuspended in 2 ml of sterile water, pipetted for 30 sec and 2 ml of 2x PBS was added. Then, cells were centrifuged at 280 x g for 10 min and the pellet containing purified neutrophils was resuspended in DMEM without phenol red.

6.2.17. Induction of NETs

24-well plate was treated with poly-D-lysine prior the seeding of 2 x 10^6 neutrophils/well. The plate was centrifuged at 200 x g for 5 min to enhance attachment process. Then, neutrophils were stimulated with 25 nM phorbol 12-myristate 13-acetate (PMA) for 3 h to induce NETs. For PAD inhibition, neutrophils were first treated with 100 μM Cl-amidine for 1 h under the same incubation conditions before the induction of NETs or 2 h after PMA stimulation. In some experiments, neutrophils were pre-treated with 5 μM native or different modified forms of LL-37 for 1 h before the induction of NETs with PMA for 3 hours. Anti-LL-37 antibodies (10 μg/ml) were added 2 h post PMA activation in specified experiments. Induction of NETs by pathogen was performed using *Staphylococcus aureus* (Newman strain). Bacteria were grown overnight in Tryptic Soy Broth culture at 37°C in an orbital shaker at 180 rev./min. The bacterial cultures were centrifuged at 4,500 x g at 4°C for 5 min after overnight incubation. Pellet was washed twice with PBS and centrifuged at the same condition as mentioned above. After the last wash, the pellet was resuspended with 5 ml of PBS and centrifuged at 800 x g at 4°C for 2 min and supernatant that contains live bacteria was collected. The number of *S. aureus* bacterial cells was determined based on previously established growth curve of colony forming units (CFU) calibrated to the optical density of the bacteria suspension. Isolated neutrophils were infected with *S. aureus* at the MOI of (1:10) and incubated for 1 hour.

After stimulation as described above, supernatant containing released NETs was collected for subsequent analysis.

6.2.18. Quantification of NETs

The release of extracellular NET-DNA was quantified using PicoGreen dye. Assays were performed in black 96-well microplates. A working solution of the PicoGreen reagent was prepared by diluting the reagent with TE buffer at 1:200. Ninety µl of working solution was added to 10 µl of tested samples and fluorescent of NET-DNA were measured using a spectrofluorometer with excitation wavelengths 480 nm and emission 520 nm.

6.2.19. Western blot

Protein concentration in NETs was determined using the BCA protein assay (as described in section 6.2.15.) to calculate an equal amount of proteins in each sample that was subjected to SDS-PAGE. SDS-PAGE for the separation of proteins was done according to Schagger and Von Jagow [96] with the gel composition shown in **Table IV**.

	Resolving Gel 16%	**Stacking Gel 4%**
Acrylamide/Bisacrylamide	4.88 ml	1.00 ml
Buffer for gel	5.00 ml	3.10 ml
glycerol	2.00 ml	-
dH_2O	3.03 ml	8.33 ml
10% w/v APS	75 µl	60 µl
TEMED	7.5 µl	6 µl

Table IV. Polyacrylamide gel composition according to Schagger and Von Jagow system.

Samples were incubated at 95°C for 5 min with sample loading buffer (Pierce™ Lane Marker Reducing Sample Buffer) containing DTT and separated on a 16% polyacrylamide gel at 100 V for 2 hours. After electrophoresis, separated proteins were transferred to a methanol-activated PVDF membrane at 60 V for 180 min at 4°C. Non-specific binding sites on the membrane were blocked with 5% skimmed milk in TTBS buffer for 4 h at room temperature before overnight incubation with anti-human LL-37 monoclonal antibody diluted 1,500-fold in TTBS buffer containing 3% BSA. The membrane was washed three times, each for 5 min, with TTBS buffer before incubation with anti-mouse IgG (1:20,000 dilution in TTBS buffer

containing 3% BSA) for 2 h at room temperature. This step was followed by 5 washes with TTBS buffer before the blots were developed with ECL.

6.2.20. Detection of citrullinated proteins with anti-modified citrulline antibody (AMC ab)

Proteins in NET samples were resolved on SDS-PAGE at the same conditions as described in section 6.2.19. and transfer onto PVDF membrane. Citrullinated proteins were visualized using anti-modified citrulline detection kit according to the manufacturer's protocol. Briefly, the membrane was blocked with 0.1% ovalbumin in TBS at room temperature for 15 minutes. Next, the membrane was subjected to chemical modification at highly acidic pH by incubating the membrane for 7 h at 37 °C with 1:1 solution from mixture A (0.025% $FeCl_3$ solubilized in 98% H_2SO_4 and 85% H_3PO_4) and mixture B (0.25% antipyrine, 0.5% 2,3-butanedione monoxime and 0.5 M acetic acid). The membrane was incubated with 3% skimmed milk in TBS (TBS-MLK) for 30 min after thorough rinsed with water. Antibodies specific for chemically modified citrulline (AMC ab) diluted 1,000-fold in TBS-MLK were incubated with the membrane overnight at 4°C. After washing the membrane with water, it was incubated with 5,000-fold diluted goat anti-rabbit HRP-conjugated IgG in TBS-MLK for 1 h at room temperature with agitation. After final wash with water (twice) and 0.05% Tween 20 in TBS-MLK (twice, each 5 minutes), the membrane was developed with ECL detection reagent.

6.2.21. Rhodamine-phenylglyoxal citrulline-labelled probes

To investigate protein citrullination in NETs, we used a citrulline specific chemical probe, rhodamine-phenylglyoxal (Rh-PG), which is highly sensitive and react with any citrulline in proteins and peptides [97]. NET samples (100 µl) in 50 mM HEPES (pH 7.6) were treated with 20% trichloroacetic acid, followed by the incubation with 0.5 mM Rh-PG at 37°C for 30 minutes. The reaction was quenched by treating samples with 100 mM citrulline in HEPES (pH 7.6) for 30 min at 37°C. This was followed by incubating samples on ice for 30 min to facilitate protein precipitation with trichloroacetic acid. Samples were then centrifuged at 16,000 x g for 15 min at 4°C. The pellet was washed with 250 µl ice-cold acetone, centrifuged at 16,000 x g for 10 min at 4°C and left to dry for 10 min. Then, 20 µl of 100 mM

arginine in HEPES (pH 7.6) were added to quench the residual free probe, followed by 2 x 5 sec interval sonication. Samples were incubated at 95°C for 5 min before storage at -20°C. Samples were run on 16% polyacrylamide gel at 120 V and fluorescent bands were visualized using Bio-Rad Gel Imager with a Rhodamine filter (560/50).

6.2.22. Mass spectrometry

NanoESI-MS/MS analyses were performed by Carsten Scavenius, Ph.D. from Interdisciplinary Nanoscience Center, Aarhus University according to the procedure described below. For measurement, either an EASY-nLC II system (ThermoScientific) connected to a TripleTOF 5600 mass spectrometer (AB Sciex) or a NanoLC 415 (Eksigent) connected to a TripleTOF 6600 mass spectrometer (AB Sciex) was used. The micro-purified peptides were dissolved in 0.1% formic acid, injected and trapped on an in-house packed trap column (2 cm x 100 μm i.d.) with RP ReproSil-Pur C18-AQ 3 μm resin (Dr. Maisch GmbH). Peptides were eluted from the trap column and separated on a 15 cm analytical column (75 μm i.d.) packed in-house in a pulled emitter with RP ReproSil-Pur C18-AQ 3 μm resin (Dr. Maisch GmbH). Elution from the analytical column was performed with a linear gradient from 5% to 35% phase B (90% acetonitrile with 0.1% formic acid) over 20 or 50 minutes. The collected MS files were converted to Mascot generic format (MGF) using the AB SCIEX MS Data Converter beta 1.1 (AB SCIEX) and the "proteinpilot MGF" parameters. The generated peak lists were searched against the swiss-prot database or a local database containing mature LL-37 using in-house Mascot search engine (matrix science). Search parameters were adjusted to the applied protease and either propionamide (SDS-PAGE) or carbamidomethyl (iodoacetamide) was set as a fixed modification with peptide tolerance and MS/MS tolerance set to 10 ppm and 0.1 Da respectively.

6.2.23. The estimation of LL-37 half-life in biological fluids

Stability of citrullinated forms of LL-37 added to NETs, inflamed sera and the synovial fluid obtained from rheumatoid arthritis patients was determined by Prof. Adam Lesner, Ph.D. from Faculty of Chemistry, University of Gdansk. Human probes of inflamed serum and the synovial fluid were performed according to the agreement of the Committee of Ethics at the University of Bergen (nr. 242.06) and a courtesy from Piotr Mydel, D. Sc., MD. Briefly, all

biological samples were centrifuged at 16,000 x g for 15 min to remove lipids and precipitated material. Supernatants (900 µl) were mixed with 100 µl peptides (1 mg/ml solution in PBS). Peptides mixed with PBS were used as a control. Samples were incubated at 37°C and at different time points, aliquots (50 µl) were withdrawn and treated with 50 µl of 6 M urea and 50 µl 6% TFA to denature all proteins in a sample. Next, samples were centrifuged at 16,000 x g for 15 min and peptides in supernatants were separated by UPLC Nexera (Shimadzu Japan) on the C8 analytical column (Aeris) equilibrated with 0.1 TFA in water at flow rate 0.4 ml/minutes. Peptides were eluted with acetonitrile gradient up to 55% developed in 12 minutes. Proteinaceous material eluted from the column was detected at 208 nm.

6.2.24. Detection of LL-37 in NETs with immunofluorescence microscopy

Neutrophils were isolated as described in section 6.2.16. and seeded at density of 1×10^5 cells on coverslips treated with syringe-filtered 1% BSA. After 30 min incubation to allow cell adherence, neutrophils were either pre-treated with or without 100 µM Cl-A for 1 h prior stimulation with 25 nM PMA for 3 h. Cells were fixed with 3.7% paraformaldehyde for 10 min at room temperature and after 3 washes with PBS, coverslips were incubated with mouse anti-human LL-37 (1:50 dilution factor) for 1 h at room temperature. This was followed by 45 min incubation with Alexa-Fluor-647 goat anti-mouse antibody (1:1000) and subsequent staining with 1 µg/ml Hoechst 33342 for 10 minutes. Then, coverslips were visualized with a fluorescence microscope at 20 x magnification.

6.2.25. Activation of antigen-presenting cells by NETs

Human monocyte-derived macrophages (hMDMs) were obtained as described in section 6.2.8. Cells were primed with 100 ng/ml LPS for 4 h prior to stimulation with either: synthetic native, differentially citrullinated forms of LL-37 and mixtures of synthetic modified forms of LL-37 (mPAD2 and mPAD4); or NETs collected from either PMA or *S. aureus* activated neutrophils treated with Cl-A or without as described in section 6.2.17. Two hours later media were collected and quantification of IL-1β was performed with commercially available ELISA as mentioned in section 6.2.13.

Plasmacytoid DCs were seeded in a density of 0.8×10^5 cells/well in 96-well plate before an overnight stimulation with NETs and anti-LL-37 antibodies (10 µg/ml), native LL-

37 (5 μM) or hArg-LL-37 (5 μM). Secreted IL-6 in the supernatant of pDCs was quantified with commercially available ELISA as described in section 6.2.13., whilst cells were lysed, and RNA were isolated and used for analysis of IFN-α dependent genes (*MxA*) expression as described in following sections.

6.2.26. RNA isolation

RNA was isolated with TRIzol method as per manufacturer's instructions. Briefly, 200 μl of TRIzol reagent was added to each well and cells were lysed by pipetting the cells up and down a few times. Homogenized samples were collected and stored at -20°C before proceeding to phase separation on the next day. Forty μl of chloroform was added to the homogenized samples, samples were incubated for 5 min at room temperature and then shook vigorously by hand for 15 seconds. After incubating for 2 min at room temperature, samples were centrifuged at 12,000 x g for 15 min at 4°C. Colourless, upper aqueous phase containing RNA was carefully collected, 120 μl of 100% cold isopropanol was added and probes were incubated at room temperature for 10 min, followed by centrifugation 12,000 x g for 10 min at 4°C. Supernatant was carefully removed, the RNA pellet was washed with 1 ml 75% cold ethanol and centrifuged at 7,500 x g for 5 min at 4°C. Supernatant was discarded and the pellet was air dried for 10 min before resuspended with 20 μl RNase-free water. The samples were incubated at 56°C for 15 min and concentration of RNA was quantified with NanoDrop 1000 device.

6.2.27. cDNA synthesis

cDNA was prepared from up to 700 ng of total RNA isolated using high-capacity cDNA reverse transcription kit. Random primers scheme was used for initiating cDNA synthesis. Master mix of required reagents prepared as according to manufacturer's instructions (described as in **Table V**) was mixed with 10 μl of RNA. cDNA synthesis was carried out in room temperature for 10 minutes, then 37°C for 2 h and finished in 85°C for 5 minutes. cDNA samples were stored at -20°C until further use.

Components	Volume/Reaction (μl)
10x RT buffer	2.0
25x dNTP Mix (100 mM)	0.8
10x RT Random Primers	2.0
Reverse Transcriptase	1.0
Nuclease-free water	4.2

Table V. Master mix for cDNA synthesis.

6.2.28. Real-time PCR

To evaluate the activation of IFN-α dependent gene expression, we selected genes regulated by that signalling pathway, as *MxA*. Its expression was analyzed using Bio-Rad CFX96 Real-Time PCR Detection System and SYBR Green-based JumpStart™ Taq ReadyMix™. The relative expression of *MXA* (5′-ACTCTGTCCAGCCCCGTAGAC-3′ (Forward); 5′ TCACAGCTTCCTGCTAAATCACC-3′ (Reverse)) was normalized to the expression of *EF2* (5'-GACATCACCAAGGGTGTGCAG-3'(Forward); 5'-TTCAGCACACTGGCATAGAGGC-3' (Reverse)). Five μl (15 ng) of cDNA was first pipetted to each well before 10 μl of the master mix (as listed in **Table VI**) was added. After the denaturation step (5 min at 95 °C), conditions for cycling were: 39 cycles of 30 sec at 95°C, 30 sec at 56°C and 45 sec at 72°C. The fluorescence signal was measured after the extension step at 72°C and a melting curve was generated to verify the specificity of the PCR product after the end of the PCR cycling. All samples were run in triplicates. Means threshold cycle (C_t) values were calculated and analyzed using the $\Delta\Delta C_t$ method [98].

Component	Volume per reaction (μl)
Nuclease-free water	1.5
Forward primer (10 μM; Sigma)	0.5
Reverse primer (10 μM; Sigma)	0.5
SyBR Green	7.5

Table VI. PCR reaction master mix and volumes

Patient Studies

6.2.29. Patient study group and serum sampling

Rheumatoid arthritis patients that fulfilled the criteria of 2010 Rheumatoid Arthritis Classification Criteria of the American College of Rheumatology / European League Against Rheumatism Collaborative Initiative were recruited from Department of Rheumatology, Clinical Immunology and Allergology of the University Hospital of Bern. Periodontitis patients and control donors (patients without RA and periodontitis) were selected from Department of Periodontology and Department of Preventive, Restorative and Paediatric Dentistry, School of Dental Medicine, University of Bern respectively. The study cohort was reviewed and approved by the Ethical Committee of the Canton Bern, Switzerland (KEK approval # 236/10). All individuals' consent was obtained before the participation in the study. Serum from all individuals were collected after centrifugation of venous blood samples at 400 x g for 10 min and were stored at -20°C until further analysis.

6.2.30. Identification of antibodies against LL-37 and citrullinated LL-37

A non-competitive indirect ELISA to detect the levels of IgG antibodies against native and citrullinated LL-37 was performed on human sera. Plates were first coated with 10 μg/ml of either native and citrullinated LL-37 in coating buffer and incubated overnight at 4°C. After washing 4 times with washing buffer, remaining peptide-binding sites were blocked with blocking buffer for 2 hours. Serum samples diluted 1:100 in RIA buffer were added to wells after discarding blocking buffer. Plates were incubated for 1.5 h followed with 4 times of washing before peroxidase-conjugated mouse anti-human IgG (diluted 1:5,000 in RIA buffer) were added to each well. After 1 hour, wells were washed 4 times with washing buffer and TMB substrate solution were pipetted into each well for substrate colour development. Absorbance was measured immediately at 450 nm after a uniform yellow colour was formed in each well after the addition of stop solution (1 M sulphuric acid).

6.2.31. Statistical analysis

Results obtained under different experimental conditions were analyzed for statistical significance using unpaired Student's *t* tests when independent variables were being assessed or by ANOVA when analyses of trends were being determined. All values are expressed as means ± standard deviation (SD) and results were considered to be significant at $p < 0.05$. Statistical analysis for level of antibodies against citrullinated and native LL-37 in patient studies were analyzed using Mann-Whitney test. Ratio IgGs against LL-$37_{\text{all cit.}}$/LL-37 in healthy donors and patients with inflammatory diseases was conducted. Statistical analysis was performed using GraphPad Prism 7.0.

7. Results

7.1. Citrullination affects the interaction of LL-37 with DNA

7.1.1. The binding of LL-37 to DNA

The common feature of LL-37 being cationic and having high affinity for nucleic acids enable the peptide to form complexes with DNA [80]. However, LL-37 may be deiminated upon released into the inflammatory milieu in the presence of PADs, what modifies the function of the peptide [67][68]. Therefore, we assumed that the process of peptide deimination, which strongly decreases the cationic character of LL-37 may influence the binding of nucleic acids. To verify our hypothesis initially we established the optimal molar ratio of binding between LL-37 and DNA using bacterial nucleotide sequence of 148 bp amplified from *T. forsythia* genomic DNA. The fluorometric assay utilizing PicoGreen, an ultra-sensitive fluorescent nucleic acid stain to quantify DNA was applied. The special feature of PicoGreen is that the dye itself shows no fluorescence until binds to DNA. Free DNA binds the dye most efficiently, whereas the process is inhibited upon the interaction of nucleic acid with proteins and peptides, including LL-37. Decrease of fluorescence intensity is an important indication that complexes between DNA and LL-37 are formed [99]. As such, the optimal molar ratio of the DNA-LL-37 complex formation can be determined. Therefore in our study, DNA was mixed with LL-37 at different molar ratio (DNA:LL-37 = 1:0.5; 1:2; 1:10) and incubated for 10 minutes. A reduction of PicoGreen fluorescence was observed with the increased ratio of LL-37 to DNA. The complex formation of LL-37 with DNA was dose dependent and 10-fold excess of peptide to nucleic acid nearly completely silenced the emission of fluorescence (**Fig. 8**).

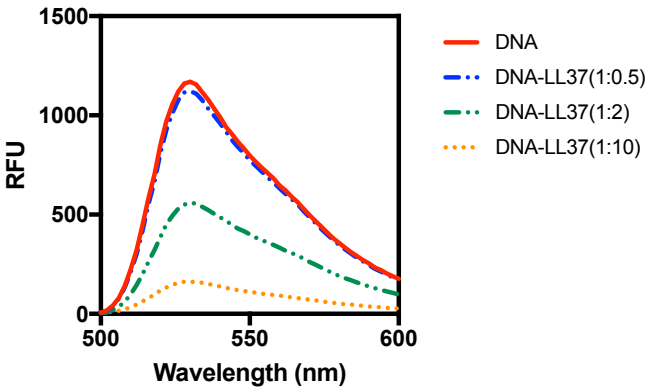

Fig. 8. The fluorescence of DNA after binding to LL-37. The optimum ratio between DNA and LL-37 was established by incubating the molecules at different molar ratio of 1:0.5, 1:2, 1:10 (DNA:peptide) respectively for 10 min at room temperature prior spectral analysis using fluorescent dye PicoGreen to measure the unbound DNA. Data is shown as relative fluorescence units (RFU) and the results are representative of 3 independent experiments. (Copyright 2018. The American Association of Immunologists, Inc.)

7.1.2. The role of LL-37 deimination (catalysed by PADs) on binding to DNA

PADs are capable to modify positively charged peptidyl arginine and methylarginine residues inside a peptide chain to uncharged citrulline [97]. LL-37 consists of 5 arginines making the peptide a favourable substrate for PAD enzymes, what has been already shown by Koziel *et al.* [67]. Hence, we investigated the time dependent effect of PADs mediated citrullination of LL-37 on DNA binding. PAD2 and PAD4 were chosen, as they are released in inflammatory conditions [100] and their activities are positively correlated with disease severity [67].

By using the fluorometric assay as described above (7.1.1.), we determined that both PADs exert time dependent effect on LL-37 binding to DNA. LL-37 was first incubated with PAD2 and PAD4 for a different time (0, 15, 30 and 120 min), before added to DNA for another 10 minutes. Unbound DNA was quantified by spectral analysis using PicoGreen as described in 7.1.1. Higher fluorescence was observed with the increased incubation time of peptide with PADs, revealing the decreased affinity between DNA and LL-37 (**Fig. 9 A & 9 B**). On the other hand, we also observed that PAD2 appeared to be more efficient in LL-37 citrullination compared to PAD4, which requires twice more time (PAD2 : PAD4 – 30 min : 60 min) to achieve the same effects as PAD2 (**Fig. 10**). Obtained data suggests the gradual dissipation of the cationic charge of the peptide due to the conversion of arginine residues to citrulline. Higher

DNA-PicoGreen fluorescence signal is detected with the increased of time, as less LL-37 binds to DNA, allowing the DNA-PicoGreen interaction. The role of citrullination in regulating the formation of DNA-LL-37 complexes was further confirmed by using hArg-LL-37, containing homo-Arg guanidinium side chains that are insensitive to enzymatic citrullination (sequence of hArg-LL-37 is shown in section 6.1.20.). As a control we applied the scrambled version of LL-37 (sequence of sLL-37 is shown in section 6.1.20.). Both peptides (sLL-37 and hArg-LL-37) were incubated with PAD2 for 2 h, as mentioned earlier. We found that sLL-37 did not bind to nucleic acids (**Fig. 11 A**) indicating that the interaction of the peptide with DNA strongly depended on amino acids sequence. The citrullinated counterpart of sLL-37 also remained unbound. Moreover, we observed that hArg-LL-37 interacted equally efficient with DNA regardless of treatment with PAD2 (**Fig. 11 B**) due to inability of PADs to deiminate guanidium side chain in hArg. All together, the presented data revealed that the LL-37 interaction with nucleic acids is not limited to the peptide cationicity but depends on the proper distribution of guanidinium side chains of Arg (hArg) in the context of the native sequence of LL-37.

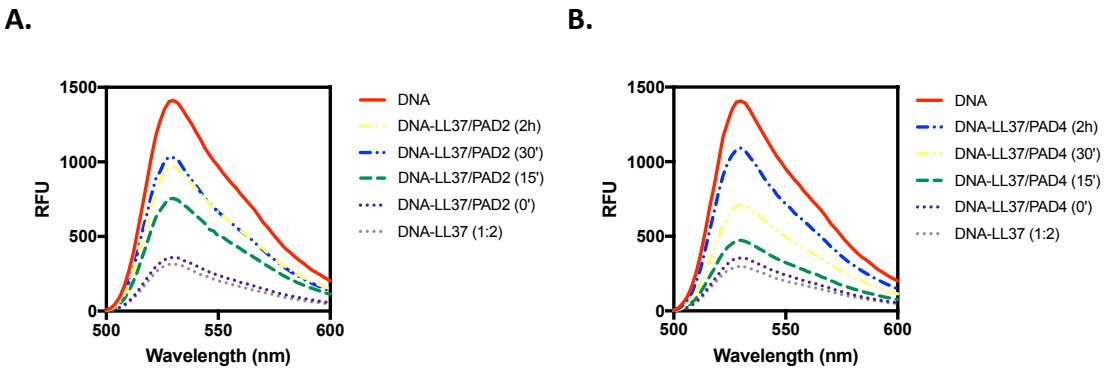

Fig. 9. Time dependent effect of LL-37 incubated with PAD2 (A) and PAD4 (B) on DNA binding. The capability of citrullinated LL-37 binding to DNA was analyzed using PicoGreen fluorescent dye by incubating DNA with LL-37 exposed to PADs at different incubation time: 0, 15, 30 and 120 min respectively. Unbound DNA was quantified with spectral analysis using PicoGreen and is shown as relative fluorescence units (RFU). Data shown are representative of 3 independent experiments. (Copyright 2018. The American Association of Immunologists, Inc.)

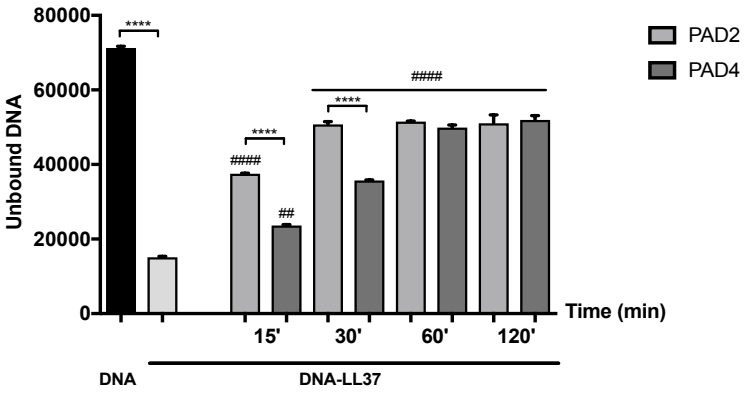

Fig. 10. The time dependent effect of LL-37 citrullination by PAD2 and PAD4 on the capability of peptide to bind DNA. Data collected over the fluorescence range (500 – 600 nm) from Figure 9 was analysed using Prism's area-under-the-curve (AUC) analysis. Statistical significance was evaluated by one-way ANOVA, followed by Tukey's multiple comparisons post-test (****p<0.0001; ##p<0.01; ####p<0.0001- comparing to the control DNA-LL-37 (second bar from left)). Data shown are collective of 3 independent experiments. (Copyright 2018. The American Association of Immunologists, Inc.)

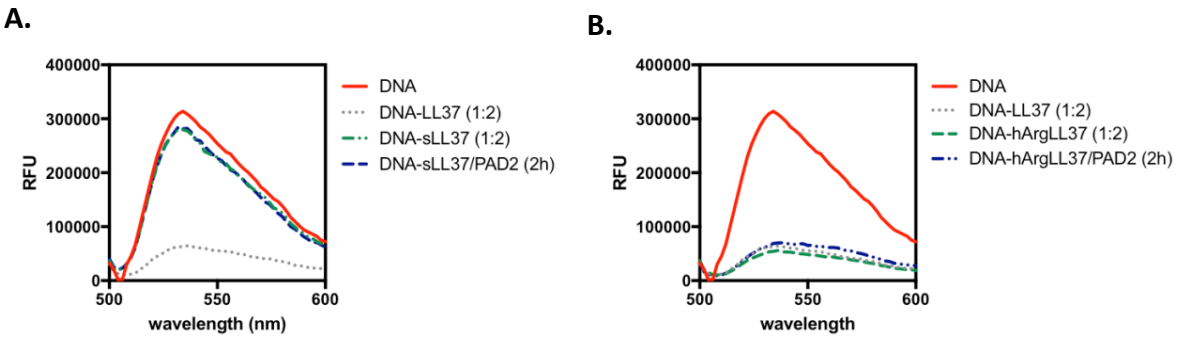

Fig. 11. The enzymatic deimination of modified forms of LL-37 on formation of DNA-LL-37 complexes. DNA binding by scrambled version of LL-37 (sLL-37) (**A**) and peptide with homo-Arg guanidinium side chains (hArg-LL-37) (**B**) with or without preincubation with PAD2. Unbound DNA was quantified with the spectral analysis using PicoGreen and is shown as relative fluorescence units (RFU). Data shown are representative of 3 independent experiments. (Copyright 2018. The American Association of Immunologists, Inc.)

7.1.3. Interaction of synthetic citrullinated LL-37 with oligonucleotides

Having observed that citrullination of LL-37 catalysed by PADs influences its binding to DNA, we expanded our studies implementing synthetic, differentially citrullinated forms of LL-37 harbouring different numbers of citrullinated arginine residues ($Arg^{7}Cit$ = LL-37_{7}; $Arg^{7,29,34}Cit$ = LL-$37_{7,29,34}$; $Arg^{7,19,23,29,34}Cit$ = LL-$37_{all\ cit}$), which sequences are shown in section 6.1.20. Above mentioned peptides were selected based on the data published by Koziel *et al*., where the citrullination profile exerted upon enzymatic modification of native LL-37 by PAD2 enzyme was determined by automated Edman degradation [67].

As described previously [80], the complex formation between anionic nucleic acids (DNA) and the cationic peptide LL-37 is based on the electrostatic interaction between both molecules, therefore we apply a classical electrophoresis mobility shift assay (EMSA) [95]. The assay is not limited to nucleic acid sizes and structures, thus provides a straightforward measure on protein-DNA interaction [101]. The unbound, negatively charged DNA migrates towards the anode when electric current is applied, however DNA bound with peptide retains in the well and couldn't migrate as corresponding to the free nucleic acid (**Fig. 12 A**). Interestingly, the intensity of the bands with mobility that resemble free DNA increased with the number of citrullinated arginine residues of LL-37, revealing the decreased binding of DNA with more citrullinated forms of LL-37 (**Fig. 12 A**). We also applied CpG oligonucleotides, which are short single-stranded synthetic DNA molecules that mimic bacterial DNA. CpG ODN 2216, a class A CpG was selected for our study as it was reported to elicit a substantial immunological response on TLR9-expressing cells [82], which we were interested to introduce for subsequent *in vitro* studies. Using CpG oligonucleotides we confirmed the observation of decreased nucleic acids binding together with the increase level of LL-37 citrullination (**Fig. 12 B**).

To quantify the interaction of citrullinated peptides with DNA, surface plasmon resonance (SPR) analysis was performed in the Department of Comparative Biochemistry and Bioanalytics, Jagiellonian University. The amount of DNA bound by respective native and modified LL-37 was measured at 210RU. As expected, native LL-37 bound DNA tightly and the affinity of such interaction decreased about 3-fold, with just a single arginine residue substitution at position 7 in LL-37 (**Fig. 13**). In case of fully citrullinated peptide the binding to DNA was totally abolished (**Fig. 13**). As citrullination of LL-37 by PAD2 and PAD4 generates the different profile of citrullinated peptides [68], we tested two mixtures of synthetic modified forms of LL-37, which composition resembles the final products of LL-37

citrullination generated by PAD2 (mPAD2) and PAD4 (mPAD4) (**refer Table VII**). The SPR analysis has shown that the global DNA binding by the peptides in the mixture was a result of additive binding of the individual modified peptides (**Fig. 14**). This excludes any interaction between the peptides themselves and argues that deimination of particular arginine residues within LL-37 does not affect the peptide interactions.

Taken together, citrullination of LL-37 diminishes the binding of the peptide to DNA, as we confirmed by both enzymatic deimination (**Fig. 9, 10**) and using synthetic peptides (**Fig. 12, 13**). The interaction between DNA and LL-37 strongly depends on the numbers of citrulline residues within the peptide. PAD enzymes may variably affect the level of citrullination, as shown by amino acid sequence analysis of the peptide incubated with PAD2 and PAD4 [67].

Peptide	mPAD2	mPAD4
LL-37	1%	49%
$LL\text{-}37_{7}$	77.5%	35%
$LL\text{-}37_{7,29,34}$	20%	14%
$LL\text{-}37_{\text{all cit.}}$	1.5%	2%

Table VII. Mixture composition of synthetic modified forms of LL-37 that resembles the catalytic modification of LL-37 by PAD2 (mPAD2) and PAD4 (mPAD4). (Copyright 2018. The American Association of Immunologists, Inc.)

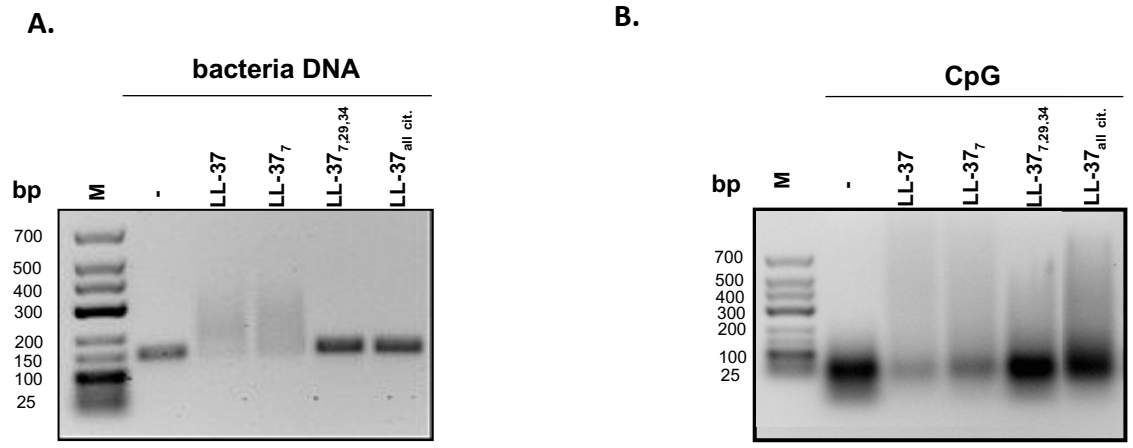

Fig. 12. Binding efficiency of bacteria (*T. forsythia*) genomic DNA and synthetic oligonucleotide CpG with synthetic native and citrullinated forms of LL-37 determined by EMSA. Synthetic native or differentially modified forms of LL-37 were mixed with bacteria genomic DNA or CpG, respectively, at a 1:5 (DNA-peptide) molar ratio and incubated at room temperature for 10 min prior running samples on 1.5% agarose gel. Decreased intensity

of DNA band and its retardation are indicative for the complex formation with the peptide. Data shown are representative of 3 independent experiments. (Copyright 2018. The American Association of Immunologists, Inc.)

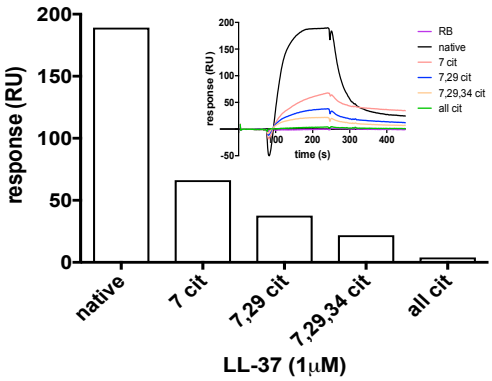

Fig. 13. The efficiency of DNA binding by native and differentially citrullinated forms of LL-37 (LL-37$_7$, LL-37$_{7,29}$, LL-37$_{7,29,34}$, and fully citrullinated LL-37) determined by SPR. CpG biotinylated at the 5′ end of the antisense strand was immobilized on the SA sensor chip (GE Healthcare) with streptavidin covalently attached to the dextran. Next, a series of native and modified LL-37 peptide samples were injected over the sensor surface at 30 μL/min flow rate using 2 min interval for association and for dissociation process. Binding efficiency was evaluated with SPR analysis (LL-37 1 μM/Bt-DNA 210RU). Data shown are amounts of immobilized DNA corresponding to 210 response units (RU). Sensorgram (insert) showed an overview of binding curves between DNA and peptides. Analysis was performed in the Department of Comparative Biochemistry and Bioanalytics, Jagiellonian University. (Copyright 2018. The American Association of Immunologists, Inc.)

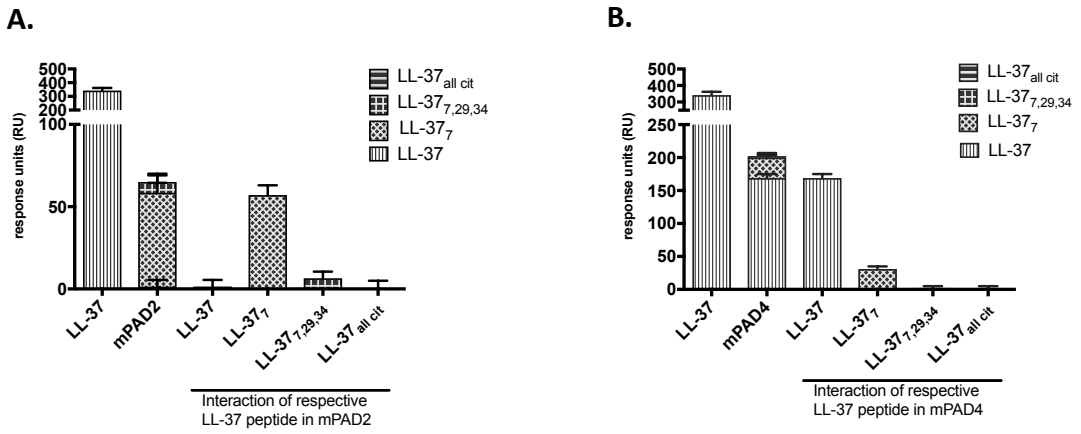

Fig. 14. Efficiency of DNA binding by mixtures of synthetic peptides resembles catalytic modification of LL-37 by PAD2 (mPAD2 - A) and PAD4 (mPAD4 - B) respectively. The binding efficiency of DNA by mixtures of synthetic native and differentially citrullinated forms of LL-37 (composition see Table VII) was analysed by SPR. The R max values of the mixtures were compared with the quota determined separately for the mixed components at the same concentration level. Response units (RU) were used to describe the amounts of immobilized DNA. Analysis was performed in the Department of Comparative Biochemistry and Bioanalytics, Jagiellonian University. (Copyright 2018. The American Association of Immunologists, Inc.)

7.1.4. Evaluation of specificity of studied interaction

7.1.4.1. Binding of murine cathelicidin to DNA

We next explored if deimination of cathelicidin originated from different species than human also interferes with their ability to bind DNA. We examined native and deiminated variants of CRAMP (sequences as shown in section 6.1.20.), a murine analog of human LL-37, on its binding affinity with nucleic acids. CRAMP contains a single Arg residue so the citrullinated form of CRAMP also encompasses only a single deiminated arginine residue.

Results of the gel retardation assay has revealed the ability of CRAMP to form complexes with nucleic acids, and reduced binding with the citrullinated form of peptide manifested by a slight band of released DNA (**Fig. 15**). This observation revealed that decreased complex formation between modified cathelicidin and nucleic acids is not species-specific. It occurs regardless the origin of the peptide. Moreover, these data revealed decrease of DNA binding by modified CRAMPs mimicking the effect documented for a single

substitution of Arg in the sequence of LL-37 (**Fig. 12**).

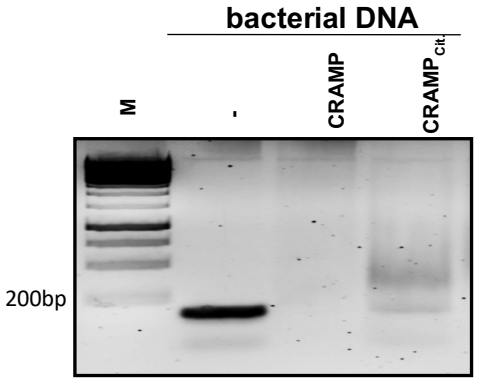

Fig. 15. Binding of CRAMP and its deiminated form to DNA. Bacterial genomic DNA (*T. forsythia*) was incubated with either the native (CRAMP) or the citrullinated peptide ($CRAMP_{cit.}$) in molar ratio (1:5) at room temperature for 10 min prior running samples on 1.5% agarose gel. DNA can bind with CRAMP, murine analogue of LL-37, but less efficiently than the citrullinated form of the peptide. Data shown are representative of 3 independent experiments. (Copyright 2018. The American Association of Immunologists, Inc.)

7.1.4.2. Interaction of LL-37 with other molecules - apolipoprotein A-1

Electrostatic character of proteins determines their reciprocal charge-dependent interactions. Therefore, we decided to investigate how citrullination of LL-37 will affect its binding with other molecules. For that purpose, the serum apolipoprotein A-1 (ApoA-1) has been chosen as it can form the complex with LL-37 [102]. The interaction was analyzed with SPR, which was performed in the Department of Comparative Biochemistry and Bioanalytics, Jagiellonian University. We confirmed concentration-dependent binding of LL-37 binding affinity to ApoA-1 with the increasing concentration of LL-37, ranging from 0 – 20 μM (**Fig. 16**). Next, we examined the effects of citrullination on the formation of ApoA-1-peptide complexes, finding the reduced affinity of modified LL-37 for ApoA-1 (**Fig. 17**). Complete citrullination of LL-37 attenuated its ability to bind with ApoA-1. However, the amount of ApoA-1 coupled with deiminated LL-37 increased with the peptide concentration. To conclude, deimination of LL-37 affecting its interaction with other molecules is not limited to DNA.

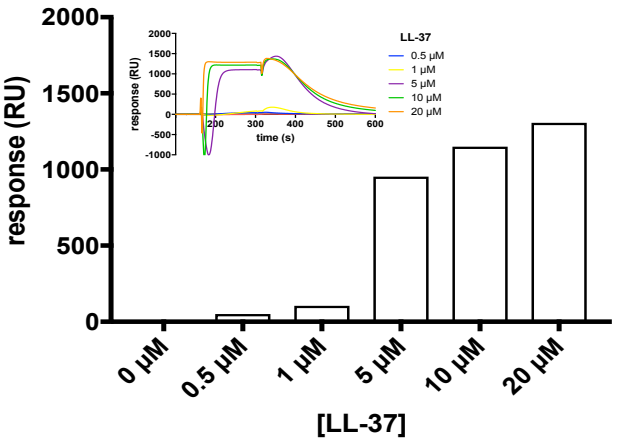

Fig. 16. Interaction of LL-37 with apolipoprotein A-1. ApoA-1 was incubated with different concentrations of synthetic native LL-37 ranging from 0 – 20 μM and the binding efficiency was estimated with SPR analysis. Data shown are amounts of coupled ApoA-1 corresponding to 270 response units (RU). The sensogram (insert) showed an overview of binding curves in the interaction between ApoA-1 and LL-37. Analysis was performed in the Department of Comparative Biochemistry and Bioanalytics, Jagiellonian University.

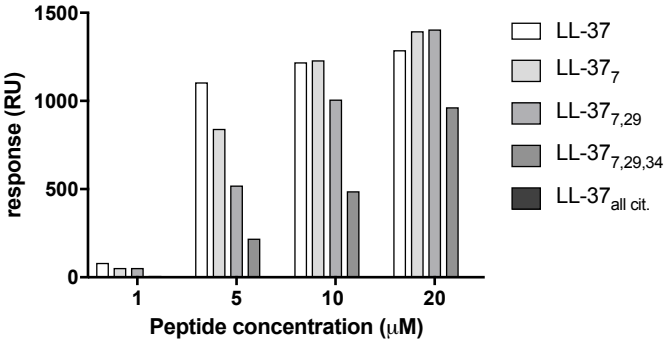

Fig. 17. Comparison of concentration-dependent interaction of LL-37 in native and citrullinated forms with ApoA-1. ApoA-1 immobilized on a sensor chip was interacting with native and differentially citrullinated forms of LL-37 (LL-37$_7$, LL-37$_{7,29}$, LL-37$_{7,29,34}$, and LL-37$_{all\ cit.}$) applied at 1, 5, 10 and 20 μM concentration and the binding was estimated with SPR analysis. Data shown are amounts of coupled ApoA-1 correspond to 270 response units (RU). Analysis was performed in the Department of Comparative Biochemistry and Bioanalytics, Jagiellonian University.

7.1.4.3. Specificity of posttranslational modifications on the binding affinity of LL-37 to DNA

We have shown that citrullination of LL-37 and CRAMP efficiently abolished the interaction of these antibacterial peptides with nucleic acid. We now investigated how other modifications affecting e.g. charge of the peptide influence LL-37 interaction, with DNA. To this end, we focused on carbamylation process since this posttranslational modification of proteins/peptides is well known for its association with inflammatory diseases [103]. Of note, carbamylation is a chemical reaction that converts lysine into homocitrulline, leading the decrease of peptides' positive charge. LL-37, which contains six lysine residues, serves as potentially highly susceptible substrate for carbamylation, which alter its cationic and amphipathic nature. Thus, we next analyzed if DNA binding is affected by LL-37 carbamylation. Koro *et al.* [51] documented that in the presence of physiological concentrations of cyanate, three different carbamylated forms of LL-37 are generated (Sequences see section 6.1.20.).

Each of the three forms of synthetic carbamylated LL-37 (K1, K2 and K3) was incubated with DNA at room temperature for 10 min before proceeding to gel electrophoresis analysis. Interestingly, the binding affinity between modified LL-37 and DNA was not affected by carbamylation (**Fig. 18**), suggesting the importance of Arg but not Lys residues in LL-37 interaction with DNA. That conclusion was fully confirmed by the results of another experiment (**Fig. 19)**, showing that preincubation of carbamylated forms of LL-37 with PAD2 totally abolished their binding ability to DNA. Taken together, the formation of complexes between LL-37 and DNA was dependent on the positively charged guanidinium groups of Arg residues but not on the global cationicity of LL-37 or the peptide amphipathic nature.

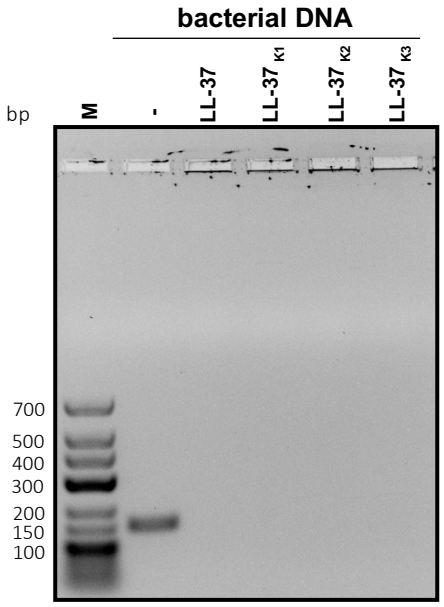

Fig. 18. Gel retardation assay using carbamylated LL-37 peptides. Bacterial DNA from *T. forsythia* was incubated with different forms of carbamylated LL-37 (K1, K2 and K3) at the molar ratio 1:5 (DNA-peptide) at room temperature for 10 min prior to electrophoresis. Data shown are representative of 3 independent experiments. (Copyright 2018. The American Association of Immunologists, Inc.)

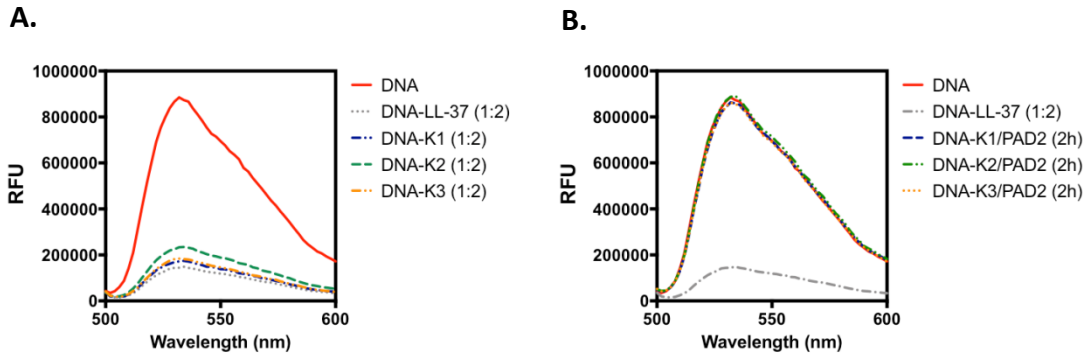

Fig. 19. Effect of enzymatic deimination of arginines in native and carbamylated forms of LL-37 on binding to DNA. The binding of different variants of LL-37 to DNA before (**A**) and after (**B**) preincubation with PAD2. Amount of unbound DNA was quantified with spectral analysis using PicoGreen and is shown as relative fluorescence units (RFU). Data shown are representative of 3 independent experiments. (Copyright 2018. The American Association of Immunologists, Inc.)

7.1.5. Effects of LL-37 citrullination on protection of DNA complexed with peptide

As it was described previously the interaction of LL-37 to DNA protects bound nucleic acid against nucleases [80]. Therefore, we decided to analyze if citrullination of LL-37 can influence that process. For experiment we have chosen the modified form of LL-37 with only one substituted Arg residue (LL-37_7), since in case of more extensive modification we observed practically no binding to DNA. DNA was incubated with either native or modified LL-37 (LL-37_7) for 10 minutes ensuring the complex formation. Then, the complex was exposed to DNase for 60 minutes, after which fluorometric assay using Picogreen dye was applied to determine the residual amount of DNA. Percentage of intact DNA complexed with LL-37 and LL-37_7 before DNase treatment was normalized to 100% and the percentage of residual DNA after DNase treatment was calculated against appropriate control. Our results have showed that native LL-37 can protect DNA from nuclease activity with ~70% of DNA staying intact, as compared to the modified LL-37, where only ~35% DNA of initially bound DNA was detached (**Fig. 20**). Based on these results, we can conclude the citrullination of LL-37 not only diminished the binding of DNA, but also reduced the protection of entrapped nucleic acid from degradation. Possibly such complex might have a more relaxed structure than that with native LL-37.

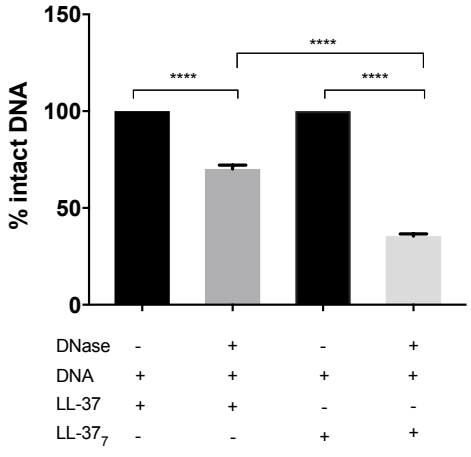

Fig. 20. Citrullination of LL-37 diminishes protection of complexed DNA against degradation of DNase. The efficiency of native and modified LL-37 to protect DNA against degradation is represented as the percentage of DNA bound to the peptide after 60 min of DNase treatment. Percentage of intact DNA before DNase treatment for native LL-37 and modified LL-37 (LL-37_7) was normalized to 100% respectively and the percentage of

remaining DNA after DNase treatment was calculated by dividing the treatment values with its' corresponding control values. Data shown are representative of 3 independent experiments. Statistical significance was evaluated by one-way ANOVA, followed by Tukey's multiple comparisons post-test (****P<0.0001). (Copyright 2018. The American Association of Immunologists, Inc.)

In summary, citrullination interferes the interaction of LL-37 with DNA, and deimination of even a single Arg residue has a significant effect on the peptide ability to form complexes with DNA.

7.2. The role of citrullinated LL-37 on immune cells activation by oligonucleotides

Nucleic acids are usually rapidly degraded in the extracellular environment, however, LL-37 increases the immunogenic potential of DNA by acting as a carrier molecule. In addition, this facilitates the internalization of bacterial or self-DNA molecules into the endosomal compartment of pDCs. Large amount of IFN-α is secreted when pDCs are exposed to such complexes (DNA-LL-37) [80]. Therefore, we attempt to investigate how citrullination can affect LL-37-dependent DNA-mediated activation of myeloid cells.

7.2.1. The activation of human plasmacytoid dendritic cells (pDCs) by oligonucleotides (CpG) in the presence of deiminated peptides

Human plasmacytoid dendritic cells (pDCs) characterized by elevated expression of TLR9 were chosen in that part of study, as they are highly sensitive to oligonucleotides recognition. Those cells provide protective immunity by generating type I IFNs [104]. Oligonucleotides used in this study CpG ODN 2216 is a class A of CpG, which is known to induce higher and longer secretion of IFN-α in pDCs [105] as compared to CpG class B. In addition, the nuclease-resistant phosphorothrioate-modified backbone of CpG oligonucleotides (typical for both classes) improves their cellular uptake. Lande *et al.* reported in 2007, that the activation of pDCs upon the exposure of complexes formed between DNA and LL-37 is manifested by a robust IFN-α expression [80]. This observation has prompted us to apply the same model to investigate the effect of deiminated LL-37 on pDCs activation induced by DNA. Initially, after stimulation of pDC cultures with mixture of CpG (3 μM) : peptides (6.4 μM)

(native or different modified forms of LL-37), we examined the morphology of cells. Bright-field microscopy analysis has revealed the formation of cell clumps, a distinct feature of pDCs activation, which was observed mainly after stimulation of cells with CpG-LL-37 (**Fig. 21 C**). We also documented, that the amount of cell clumps decreased with the increase numbers of citrullinated Arg residues as depicted in **Fig. 21 D-F**, with the least clumping of cells reported for cells treated with CpG alone (**Fig. 21 B)** or mixture of CpG with fully citrullinated LL-37 (**Fig. 21 F)**. Taken together, we assumed that citrullination of LL-37 affects the DNA-induced activation of the myeloid cells.

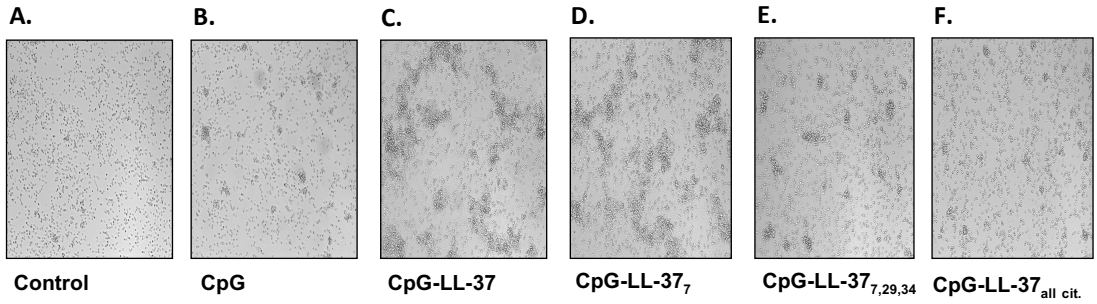

Fig. 21. Morphology of pDCs culture exposed to oligonucleotides (CpG) in the presence of the native and deiminated forms of LL-37. CpG alone (final concentration 3 μM) or CpG with synthetic native and modified forms of LL-37 (final concentration 6.4 μM) were incubated for 15 min before pDCs were washed with PBS for 3 times and incubated overnight with fresh RPMI medium supplemented with gentamycin. Formation of cell clumps reflects the activation of human pDCs. Images shown are representative of 3 independent experiments. (Copyright 2018. The American Association of Immunologists, Inc.)

7.2.2. The induction of cytokine expression in pDCs by DNA in the presence of native and citrullinated forms of LL-37

The inverse relationship on the degree of cell clumping with the level of peptide citrullination in the presence of CpG (**Fig. 21**) has prompted us to verify the level of pDCs activation by analyzing the cytokines expression induced by CpG in the presence of native and citrullinated LL-37. Human pDCs were exposed to CpG complexed with either native LL-37 or different forms of modified LL-37 for 15 minutes as published previously by Hurtado *et al*. [82]. In this report authors shown that a short exposition of cells to DNA complexed with LL-37 was sufficient to induce elevated cytokine secretion. Accordingly, we confirmed high level

of IFN-α generated by pDCs upon stimulation with the CpG-LL-37 complexes as compared to native LL-37 or CpG alone (**Fig. 22 A**). Such observation indicates that cell activation mediated by CpG is strongly enhanced by LL-37. In corroboration with our findings, citrullination interferes with DNA binding. Interferon-α released by DNA-LL-37 were reduced when CpG was mixed with LL-37_7 or LL-$37_{7,29,34}$, or fully-citrullinated LL-37 (LL-$37_{\text{all cit.}}$). The latter complex led to approximately 3-fold reduction of IFN-α secretion compared to the CpG-LL-37 (**Fig. 22 A**). We have also included controls: the scrambled form of LL-37 (sLL-37), hArg-LL-37 and carbamylated forms of LL-37 (K1-K3) in our study. Our analysis has showed that scrambled LL-37 peptide, which does not bind DNA (**Fig. 11**), could not promote immunoregulatory effect on pDCs compared to the native peptide. However, hArg-LL-37 and carbamylated forms of LL-37 exerted effects similar to the native peptide when complexed with CpG. The secretion of IL-6 showed totally different pattern in comparison to IFN-α response (**Fig. 22 B**). The elevated level of IL-6 was mainly observed in cell culture exposed to CpG alone or when CpG was accompanied by fully citrullinated LL-37. In conclusion, DNA-LL-37 complexes induced nearly inverse effects on pDCs response regarding on the secretion of IFN-α and IL-6.

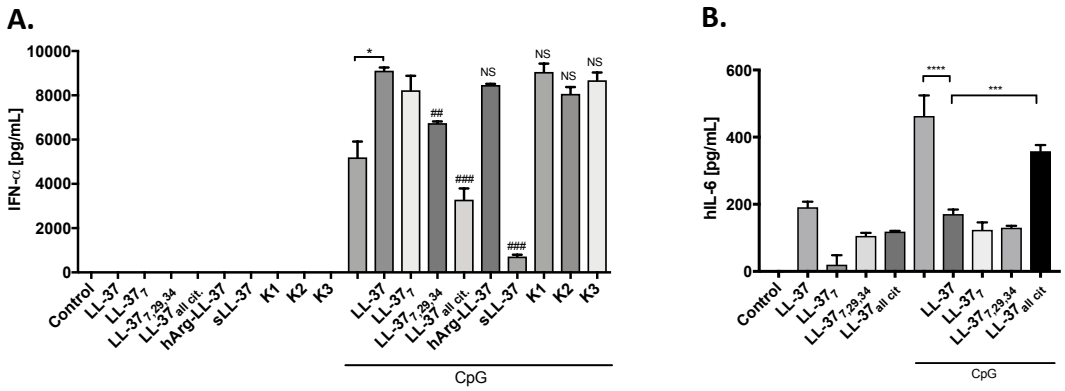

Fig. 22. Cytokines expression in pDCs after short contact with CpG combined with native or citrullinated LL-37. Primary human pDCs (8 x 10^5 per well/200 μL) were incubated with CpG (3 μM) or CpG combined with differentially citrullinated forms of LL-37 (6.4 μM) for 15 minutes. Thereafter cells were washed 3 times with PBS and incubated for additional 20 hours. (**A**) IFN-α and (**B**) IL-6 levels were measured by ELISA in culture supernatant. Statistical significance was evaluated by one-way ANOVA, followed by Tukey's multiple comparisons post-test (*P<0.05, ***P<0.001, ****P<0.0001- comparing to CpG alone; ##P<0.01, ###P<0.001, NS, non-significant- comparing to CpG-LL-37). Results shown are representative of 3 independent experiments. (Copyright 2018. The American Association of

Immunologists, Inc.)

In the follow up experiment we decided to prolong the time exposure of pDCs to tested complexes that resembles *in vivo* conditions. Human pDCs were treated overnight with CpG alone or with a mixture of CpG and either the native or 3 deiminated forms of LL-37. Similarly, as before, CpG-LL-37 mixture induced the strongest IFN-α secretion and the effect was significantly weaker when pDCs were exposed to CpG complexed with modified forms of LL-37 (**Fig. 23 A)**. The profile of IL-6 secretion was also similar to that observed after short-time exposition to pDCs complexes, with respect to high level of IL-6 released by cells only in response to CpG alone (**Fig. 23 B**). Together, the prolonged incubation with the CpG-native LL-37 complex enhanced secretion IFN-α by ~10-fold comparing to CpG alone (**Fig. 23 A**), apparently in the arginine guanidinium dependent-manner (**Fig. 23 A, B)**.

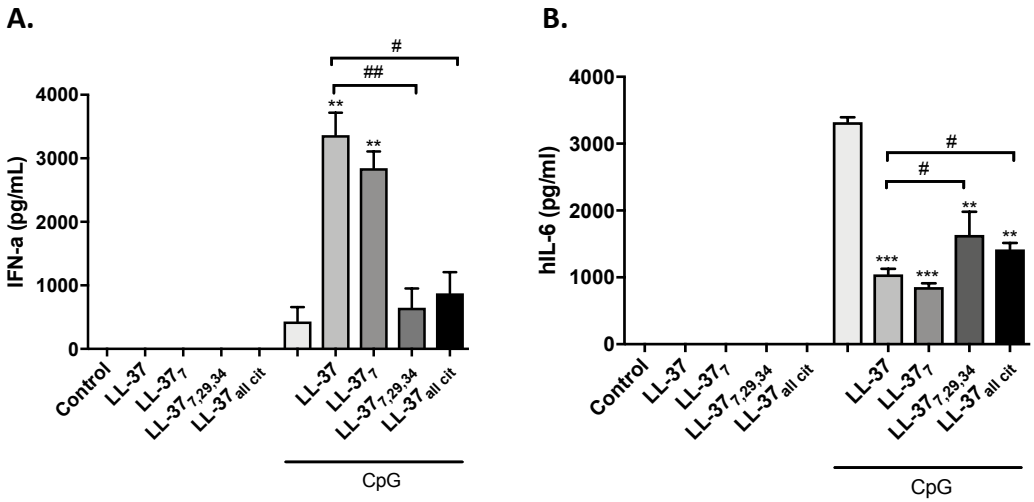

Fig. 23. Cytokines expression in pDCs after prolonged contact with CpG combined with native or citrullinated LL-37. (**A**) IFN-α and (**B**) IL-6 levels measured by ELISA in conditioned media after overnight incubation with CpG-LL-37 complexes or mixture of CpG with different modified forms of LL-37. Primary human pDCs (8 x 10^5 cells/200 μl) were incubated overnight with CpG (3 μM) or CpG combined with differentially citrullinated LL-37 forms (6.4 μM). Results shown are representative of 3 independent experiments. Statistical significance was evaluated by one-way ANOVA, followed by Tukey's multiple comparisons post-test (**P<0.01, ***P<0.001- comparing to CpG alone; #P<0.05, ##P<0.01, comparing to CpG-LL37).

7.2.3. The activation of macrophages by oligonucleotides (CpG) in the presence of deiminated peptides

Having observed the effects of LL-37 citrullination on activation of pDCs by CpG, we next explored another immune cell subset that expresses TLR9. Murine macrophages model (RAW264.7) was chosen for the study as this cell line was reported to be sensitive for CpG activation [106]. We challenged RAW264.7 with mixtures of CpG with the native/modified forms of LL-37 as described previously for pDCs (section 7.2.1.). We found that CpG-LL-37 complexes triggered RAW264.7 to secrete high amount of TNF-α. On the other hand, an inverse relationship of TNF-α secretion was observed with the mixture of CpG with the increase numbers of citrullinated arginine residues (**Fig. 24**), which is similar to results obtained for pDCs. Of note, the complex containing LL-37_7 induced a strong stimulatory effect in macrophages. The TNF-α secretion level in response to treatment with a mixture of CpG with control peptides (sLL-37, hArg-LL-37, K1-K3) was similar to that observed in pDCs, with sLL-37 being unable to sensitize macrophages to nucleic acid recognition. In contrast hArg-LL-37, similar to native peptide and carbamylated variants of LL-37 (K1-K3) stimulated the secretion of high amounts of TNF-α, in the latter case the effect was exerted despite the diminished cationic character ot the peptide with carbamylated Lys residues (**Fig. 24**). We also applied the murine form of cathelicidin – CRAMP. As expected, complexes of native CRAMP with CpG activated RAW264.7, but the effect was absent in the presence of modified CRAMP (**Fig. 25**). Taken together, our results have shown that deimination of arginine residues in native LL-37 affects the proinflammatory response of APCs to cell-free DNA.

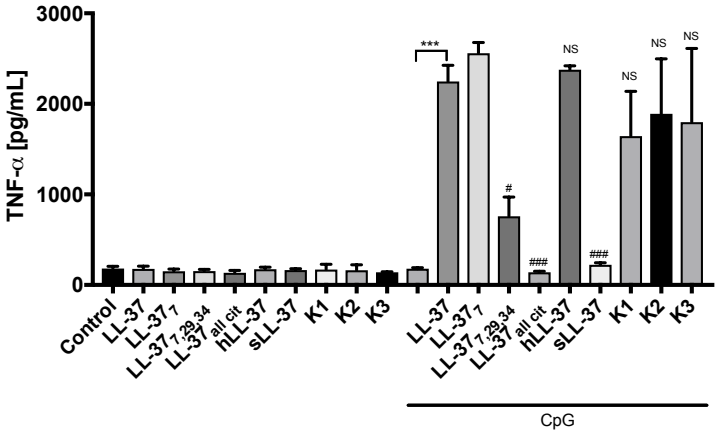

Fig. 24. Activation of murine macrophages by CpG in the presence of the native and deiminated or carbamylated LL-37. RAW264.7 cells were stimulated with either CpG (final concentration 3 μM) alone or mixtures of CpG with the native and modified forms of LL-37 (final concentration 6.4 μM) for 15 minutes. Cells were washed with PBS and TNF-α level in conditioned medium was measured with ELISA after overnight activation. Data shown are representative of 3 independent experiments. Statistical significance was evaluated by one-way ANOVA, followed by Tukey's multiple comparisons post-test (***P<0.001- compared to CpG alone; #P<0.05, ###P<0.001, NS, non-significant- compared to CpG-LL-37). (Copyright 2018. The American Association of Immunologists, Inc.)

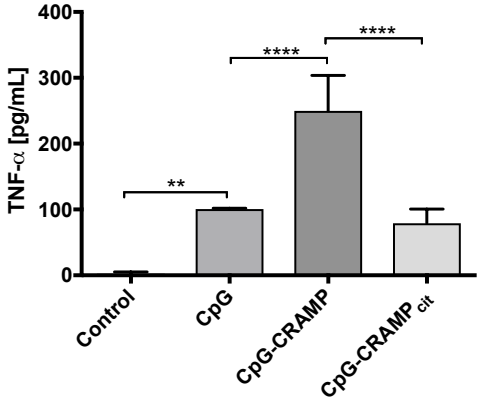

Fig. 25. The expression of TNF-α in murine macrophages upon exposition to CpG alone or mixed with the native or citrullinated murine cathelicidin (CRAMP). RAW264.7 cells were stimulated with either CpG (final concentration 3 μM) alone or CpG with murine native (CRAMP) or modified cathelicidin ($CRAMP_{cit}$) (final concentration 6.4 μM) for 15 minutes. Cells were washed with PBS and cultured overnight. TNF-α secretion to the conditioned medium was measured with ELISA. Data shown are representative of 3 independent experiments. Statistical significance was evaluated by one-way ANOVA, followed by Tukey's

multiple comparisons post-test (**P<0.01, ****P<0.0001). (Copyright 2018. The American Association of Immunologists, Inc.)

7.2.4. Effect of CpG binding and internalization by phagocytes in the presence of LL-37 or its modified forms

Lande *et al.* [80] has showed that the activation of pDCs by CpG-LL-37 is a consequence of the internalization of the complex, and thus we next wanted to determine the degree of complex penetration into cells. Firstly, we studied such effects on RAW264.7 by incubating the cells with FITC-labeled CpG in the presence or absence of LL-37 or LL-37$_{\text{all cit.}}$ and showed significant internalization of CpG only in the complex with native LL-37. The modified peptide had no effect on engulfment process (**Fig. 26**). This remarkable finding has prompted us to proceed the study with human pDCs.

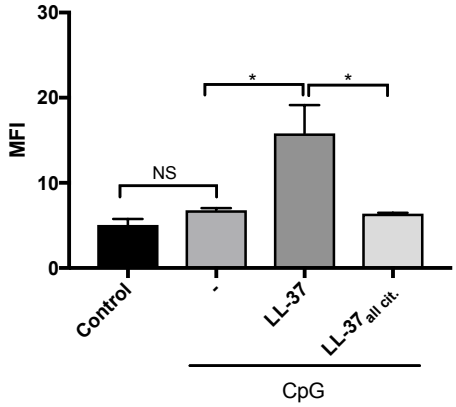

Fig. 26. LL-37 enhances the uptake of CpG. RAW264.7 were treated with either CpG-FITC or CpG-FITC + LL-37 or LL-37$_{\text{all cit.}}$ for 15 minutes. Cells were washed with PBS and analyzed for FITC fluorescence by flow cytometry. Data are shown as mean fluorescence intensity (MFI) of gated cells. Statistical significance was evaluated by one-way ANOVA, followed by Tukey's multiple comparisons post-test (*P<0.05, NS, non-significant).

Human pDCs were exposed to mixture of FITC labelled CpG with either native or differentially citrullinated peptides, washed with PBS and analyzed by FACS as described previously. We found that internalization of CpG was reduced as the level of peptide citrullination increased (**Fig. 27 A**). The same staining profile in the presence and absence of cytochalasin D has suggested that the impairment of CpG internalization was due to the weaker binding affinity of oligonucleotide to the cell membrane in the presence of citrullinated

peptides (**Fig. 27 B**). This implies that citrullination affects nucleic acids access into the intracellular/endosomal compartment of pDCs.

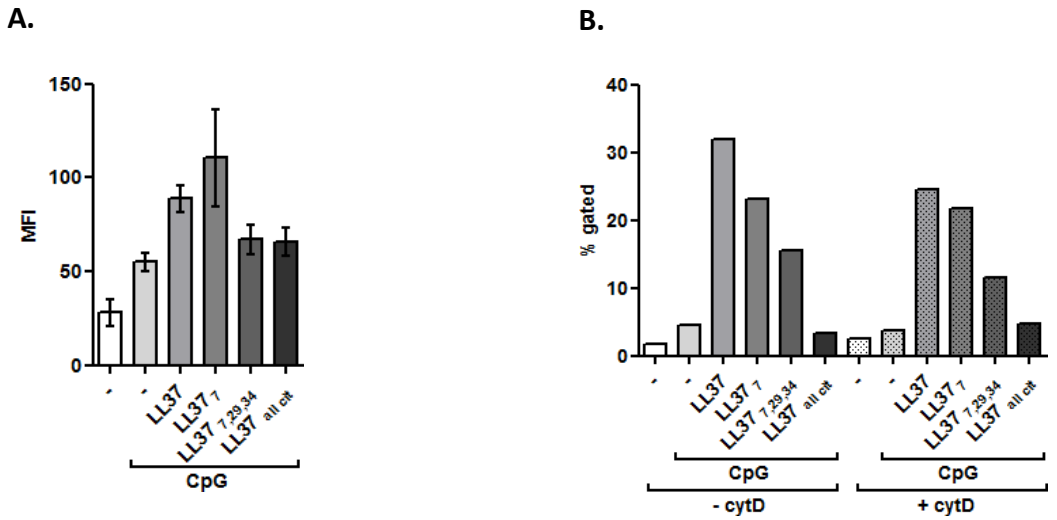

Fig. 27. The effect of LL-37 or its' modified forms on CpG binding and internalization by pDCs. (**A**) Human pDCs were treated with either FITC-labeled CpG alone or mixture of CpG-FITC with native or modified forms of LL-37 for 15 min before FACS analysis; (**B**) Staining profile showing the uptake of CpG-FITC in the presence or absence of cytochalasin D. Data are shown as mean fluorescent intensity (MFI) of gated cells or percentage of FITC positive cells respectively. (Copyright 2018. The American Association of Immunologists, Inc.)

7.2.5. The mechanism of regulation of the CpG-induced inflammatory response by native or citrullinated LL-37

7.2.5.1. Effects of LL-37 citrullination on NF-κB transcription factor activation induced by oligonucleotides

As our results have shown (**Fig. 24, 25**) the differentiated role of native and modified LL-37 on TNF-α secretion induced by DNA thus, we analyzed the activation of transcription factor NF-κB that regulates the expression of TNF-α [107]. Initially, we used an ELISA-based kit, which can detect and quantify NF-κB activation. Nuclear extracts were isolated from RAW264.7 cells after stimulation with the mixtures (CpG with native or different citrullinated LL-37) for 15 minutes, however we observed no activation of NF-κB signalling as shown in **Fig. 28**.

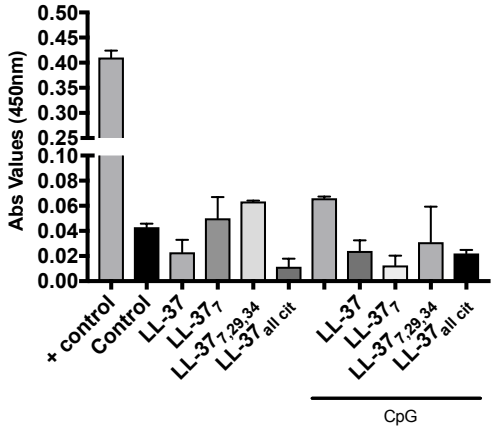

Fig. 28. Effects of LL-37 citrullination on NF-κB activation induced by CpG measured by ELISA. RAW264.7 were incubated for 15 min with CpG (final concentration 3 μM) or mixtures of CpG with the native and variable modified forms of LL-37 (final concentration 6.4 μM). Then cells were washed 3 times with PBS and subjected to 1.5 h incubation before nuclear extraction. The active form of NF-κB containing in the nuclear cell extract was quantifified using commercial NF-κB calorimetric kit and the activation was measured at OD 450nm. Positive control of the nuclear extract was provided in the kit. Data shown are collective of 3 independent experiments.

We next employed another method to quantitate the signal transduction pathway by measuring the luciferase activity in RAW264.7, which were transduced with lentiviral particles expressing NF-κB reporter constructs. Macrophages were incubated with CpG-LL-37 or mixture of CpG with different modified forms of LL-37 for 1.5 h and 6 h respectively. We noted enhanced activation of NF-κB in response to CpG in the presence of native peptide, while with the increase number of citrullinated arginine residues the effect was reduced (**Fig. 29 A**). The prolonged to 6 h stimulation of cells revealed sustain activation of cells in the presence of the partly citrullinated peptides (LL-37_7, LL-$37_{7,29,34}$) with significantly strong upregulation observed for LL-37_7 (**Fig. 29 B**). These findings indicate that citrullination of LL-37 diminish ability of the peptide to enhance the oligonucleotide-induced NF-κB signalling pathway and subsequent expression of inflammatory genes in cells briefly exposed to the complex, with the prolonged exposition partly reversing that effect.

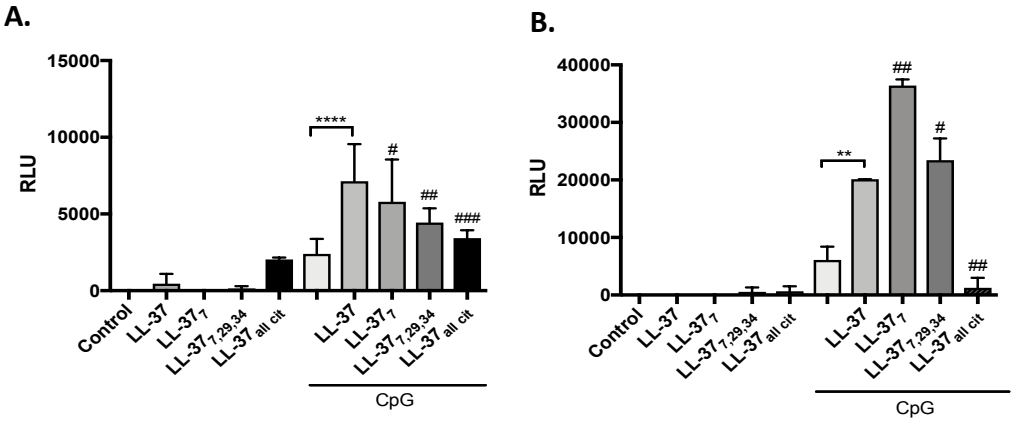

Fig. 29. Effects of LL-37 citrullination on the CpG induced NF-κB activity. Activation of the NF-κB pathway was determined in RAW264.7 cells transduced using Cignal Lenti Reporter Assay. Activity of NF-κB was measured after 1.5 h (**A**) and 6 h (**B**) incubation with CpG-LL-37 complex or mixtures of CpG with different forms of modified LL-37. Cells were lysed and assayed for luciferase activity (RLU). Data shown are representative of 3 independent experiments. Statistical significance was evaluated by one-way ANOVA, followed by Tukey's multiple comparisons post-test (**p<0.05, ****p<0.0001- compared to CpG alone; #p<0.05, ##p<0.01, ###p<0.001- compared to CpG-LL-37).

7.2.5.2. Effects of LL-37 citrullination induced by oligonucleotides on IRF7 transcription factor activation

We next evaluated IRF7 activity in human pDCs, given that IFN-α production (**Fig. 22 - 23**) depends on the activation and translocation of IRF7 to the nucleus. For this study, we used an ELISA-based kit, which can detect and quantify IRF7 transcription factor activation. Initially we treated human pDCs with either CpG alone or CpG-LL-37 for 15 minutes before cells were washed three times with PBS, followed by 3 h cultivation with fresh media. Then nuclear extraction was performed and subsequent ELISA analysis according to manufacturer's instructions. Although IRF7 was reported to express at very high levels in pDCs upon stimulation with CpG [108], we did not observe IRF7 activation even after exposition of cells to CpG complexed with LL-37 (**Fig. 30**).

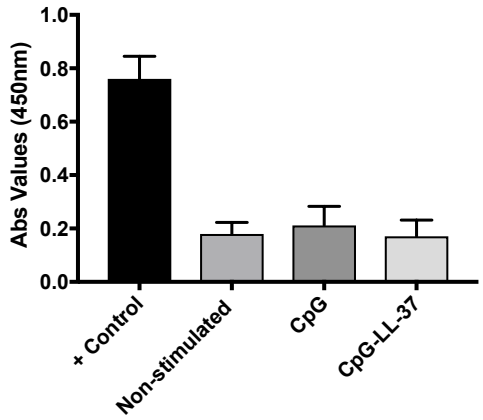

Fig. 30. IRF7 activity upon pDCs treatment with oligonucleotides. Human pDCs were incubated with either CpG alone or CpG-LL-37 for 15 min before cells were washed three times with PBS, followed by 3 h cultivation with fresh media. Nuclear extractions of pDCs were performed and subjected to analysis of IRF7 activity as per manufacturer's instructions. Positive control is the nuclear extract of IRF-7 transfected Cos-7 (fibroblast-like cell-lines) provided in the kit. Data shown are collective of 3 independent experiments.

To sum up, our findings indicate that citrullination of LL-37 strongly and specifically affects the immunostimulatory potential of the native peptide complexed with DNA abolishing (dendritic cells) or delaying (macrophages) activation of myeloid cells. The observed effect is due to reduced recognition of nucleic acids by the intracellular receptor (TLR9) as a consequence of limited penetration via cell membrane.

7.3. Identification of citrullinated LL-37

7.3.1. Direct identification of citrullinated LL-37 in NETs

Neutrophils have been demonstrated to form web-like structures, termed NETs (neutrophil extracellular traps), which contains de-condensed DNA decorated with histones and proteins originated from dying neutrophils. High concentration of antimicrobial components, such as myeloperoxidase, neutrophil elastase and cathelicidin LL-37 has been reported as released during the event of NETosis [32]. Thus, NET structures serve as a good model for our study to identify the presence of citrullinated LL-37, given that both LL-37 and active PAD enzymes co-exist at relatively high concentrations. Apart from that, various studies have associated NETs with inflammatory diseases, such as psoriasis, systemic lupus

erythematoses (SLE) and rheumatoid arthritis (RA), where NETs play a role as a source for citrullinated antigens [84].

7.3.1.1. Using Rh-PG to detect protein citrullination

First, we used a citrulline specific chemical probe, Rh-PG (rhodamine-phenylglyoxal), which chemoselectively reacts with citrulline thus fluorescently labelling citrullinated LL-37. Cl-amidine, which is known to be an inhibitor of NETs formation, was used as a control for our study. Fluorescent imaging of NETs stimulated by PMA, revealed a faint band similar molecular mass or electrophoretic mobility as the exogenous, citrullinated LL-37 added to NETs (**Fig. 31**). A decreased intensity of this band in Cl-amidine treated PMN corroborates our prediction that LL-37 is at least partially citrullinated in NETs.

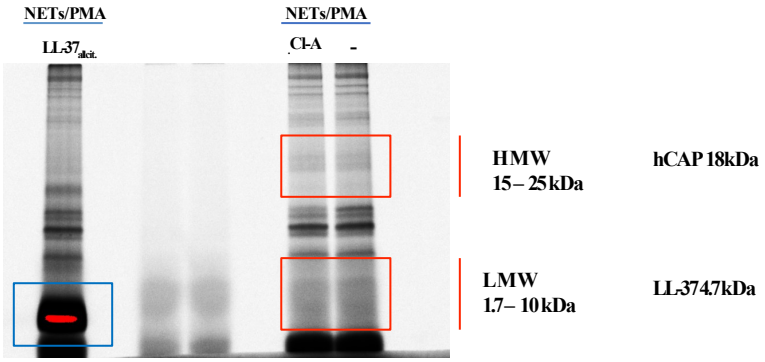

Fig. 31. A profile of citrullinated proteins labelled with the Rh-PG labelling probe in NETs. PMA induced NETs in the presence and absence of PAD inhibitor (Cl-A) were treated with Rh-PG probe and thereafter separated with SDS-PAGE. NETs supplemented with synthetic fully citrullinated LL-37 ($LL\text{-}37_{\text{all cit.}}$) was used as the control for citrullinated LL-37 migration in the gel (blue bracket). Red rectangles indicate modified human cathelicidin hCAP18/LL-37 in PMA induced NETs in the presence or absence of Cl-A. Data shown are representative of 3 independent experiments. (Copyright 2018. The American Association of Immunologists, Inc.)

7.3.1.2. Detection of LL-37 in NETs samples with mass spectrometry analysis

To confirm our observation (7.3.1.1.), we employed mass spectrometry to detect LL-37 and citrullinated forms of the peptide in PMA-induced NETs. The analysis was performed in Interdisciplinary Nanoscience Center, Denmark. Bands corresponded to cathelicidin were excised, in-gel digested with trypsin and analyzed by MS. N-terminal peptide LLGDFFRK, indicator of mature LL-37, was identified in the samples (**Fig. 32**), however, no citrullinated variant of LL-37 was detected. Next, we tried another approach by ultra-filtrating and treating the samples (supernatant containing PMA-induced NETs) with LysC endopeptidase, resulting in identification of N- terminal (**Fig. 33 A**) and C-terminal (**Fig. 33 B**) fragments of the LL-37 peptide, but not citrullinated forms of LL-37. Different methods have been used, such as in-gel digestion, precipitation, ultrafiltration, and combination of the mentioned methods, all reported failure in detection of peptides derived from modified forms of LL-37. Since inability to detect modified LL-37, we examined the stability of synthetic peptides in cooperation with Prof. Adam Lesner, from Faculty of Chemistry, University of Gdansk. Those studies were conducted in different conditions. We verified peptides stability in sera from healthy and RA patients, synovial fluid from RA patients and NET samples in the presence and absence of protease inhibitor. Different synthetic forms of native and modified LL-37 were incubated in tested biological fluids and their half-life was estimated. As revealed, LL-37 was equally stable as $LL\text{-}37_{7}$, but we observed significant decrease of the life span in case of LL-37 that contained more than two deiminated arginine residues ($LL\text{-}37_{7,29,34}$ and $LL\text{-}37_{\text{all cit}}$), which was most marked in synovial fluid from RA patients (**Fig. 34 A**).

Intriguingly, the half-life for all native and modified forms of LL-37 in the NET samples was significantly lower, when compare to sera or synovial fluid. The stability of the peptide strongly increased in the presence of protease inhibitors (**Fig. 34 B**), thus we decided to analyze the role of neutrophil elastase (HNE), which is a major serine protease released during NET formation in observed phenomenon. We found that all modified LL-37 peptides have shorter half-life compared to the native LL-37 when added to HNE. In the presence of a HNE inhibitor, the half-life of the modified LL-37 peptides was comparable to the native LL-37 (**Fig. 34 B**). All these findings might be the plausible explanation why direct detection of citrullinated LL-37, especially in NETs, failed.

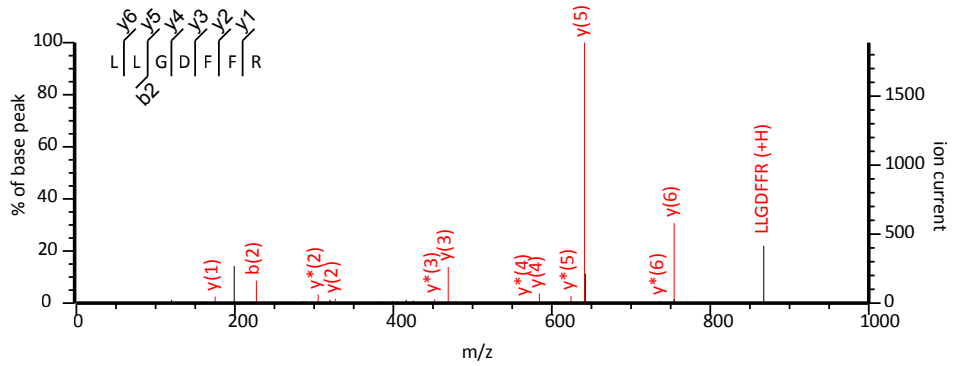

Fig. 32. MS/MS spectra of the LL-37 N-terminal tryptic peptide (LLGDFFR), confirming the presence of mature LL-37. The analysis was performed in Interdisciplinary Nanoscience Center, Denmark. (Copyright 2018. The American Association of Immunologists, Inc.)

A.

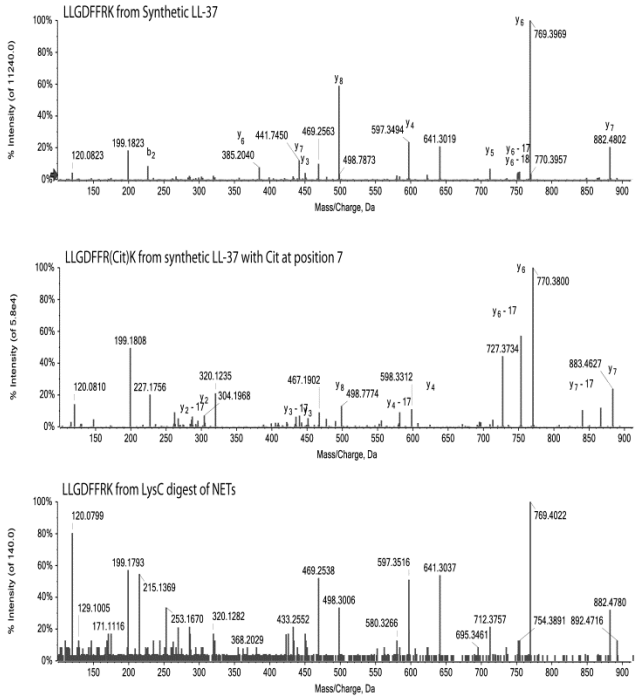

B.

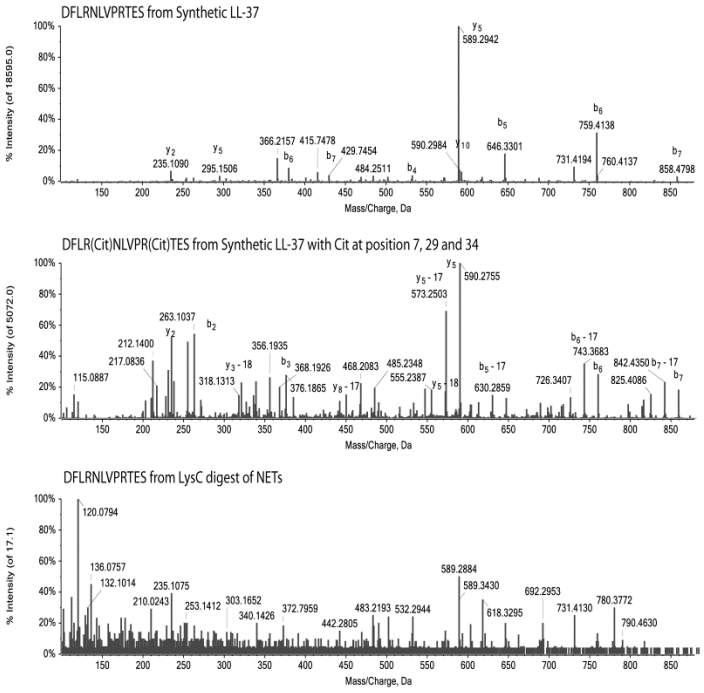

Fig. 33. MS/MS data of the LysC generated N- and C-terminal peptide of LL-37. NETs sample digested with LysC were compared with MS/MS spectra of (**A**) N-terminal unmodified (top) and modified (middle) peptide LLGDFFRK; and (**B**) C-terminal unmodified (top) and modified (middle) peptide DFLRNLVRPTES. NETs samples digested with LysC produced a

weak signal of the unmodified version of the peptide. The analysis was performed in Interdisciplinary Nanoscience Center, Denmark. (Copyright 2018. The American Association of Immunologists, Inc.)

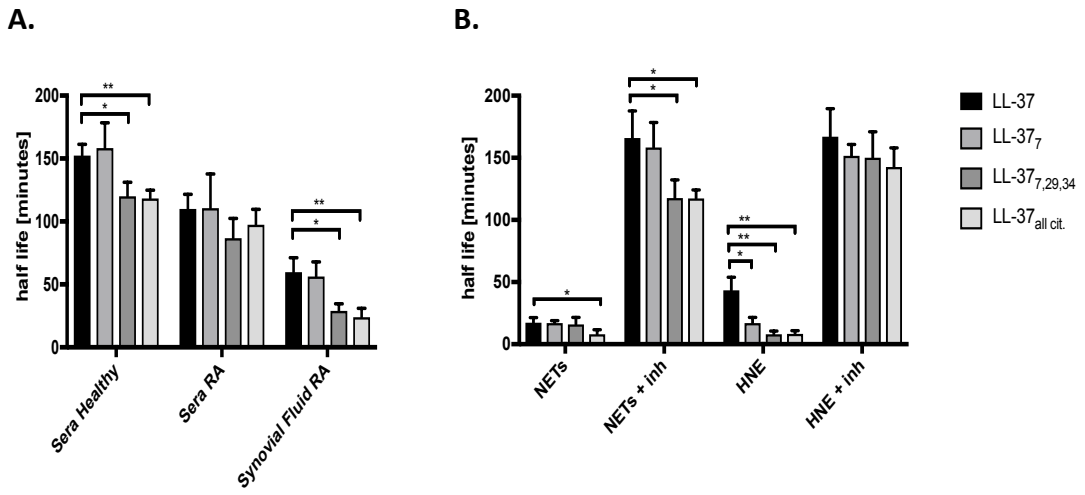

Fig. 34. The half-life of the native LL-37 and its variably citrullinated forms in different biological fluids. The half-life of LL-37 and its citrullinated forms was estimated in healthy and inflamed sera (RA serum), synovial fluid of RA patients (**A**); NETs in the presence or absence of protease inhibitors (inh) and HNE in the presence or absence of a HNE inhibitor (inh) (**B**). The analysis was performed in Faculty of Chemistry, University of Gdansk. Unpaired t-test was used to calculate the *p* values between groups (*p<0.05; **p<0.01).

7.3.1.3. Estimation of specificity of antibody against native LL-37 towards modified forms of peptides

We next validated specificity of available antibodies to recognize the native LL-37 and the fully citrullinated forms of the peptide. To this end, synthetic native and fully citrullinated LL-37 were subjected to western blot analysis using antibodies against native LL-37 (LL37 ab) and antibodies reacting with chemically modified citrulline residues in proteins or peptides (AMC ab). Blotted membrane was cut into 3 pieces in the middle of lanes with resolved antigens to allow the testing of both antibodies respectively on the same loaded sample. As shown in **Fig. 35** (left part of the blot), no reaction of fully citrullinated LL-37 was detected with antibody against native LL-37. This indicates that reactivity of this antibodies depends on recognition of epitopes containing Arg side chains. Apparently, conversion of Arg to citrulline destroyed these epitopes and, the citrullinated peptide can be now detected using AMC ab,

antibodies specific chemically derivatized citrulline residues (**Fig. 35**- middle part of the blot). Furthermore, we found in both Western blot (**Fig. 36**) and ELISA (**Fig. 37**) that the affinity of antibody against native LL-37 decreased as the number of citrullinated arginine residues increased in the peptide. **Figure 36** shows that intensity of the bands for synthetic LL-37_7 and LL-$37_{7,29}$ was less than native LL-37 and no bands were observed when LL-37 consisted of more than two citrullinated arginine residues. This observation was supported by a commercial ELISA assay. The antibodies used in this ELISA kit were able to recognize native LL-37 and certain differentially citrullinated synthetic LL-37 peptides (LL-37_7, LL-$37_{7,29}$, and LL-$37_{7,29,34}$), but not fully citrullinated synthetic LL-37 peptide (LL-$37_{\text{all cit.}}$) (**Fig. 37**). Taken together, antibody specific for the native LL-37 failed to detect the modified forms of LL-37.

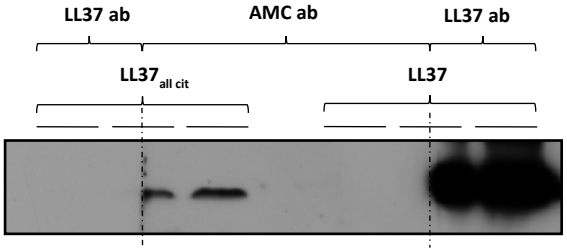

Fig. 35. Specificity of antibody against the native LL-37 and its fully citrullinated form of the peptide. Shown are representative western blot analysis of the native and fully citrullinated LL-37 using antibodies against native LL-37 (LL37 ab) and chemically modified citrulline (AMC ab). Detection of citrullinated LL-37 can only be recognized by anti-citrulline (modified) polyclonal antibodies but not anti-LL-37 antibodies. The dashed line showed the section where the membrane was cut to allow the incubation of different antibodies. (Copyright 2018. The American Association of Immunologists, Inc.)

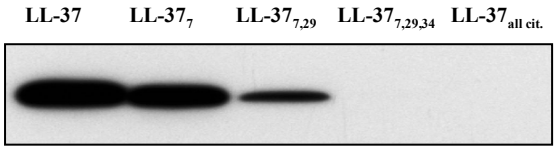

Fig. 36. Recognition of citrullinated LL-37 by antibodies against the native LL-37 using Western Blot. Shown are representative Western Blot analysis of native and citrullinated forms of LL-37 using antibodies against native LL-37. (Copyright 2018. The American Association of Immunologists, Inc.)

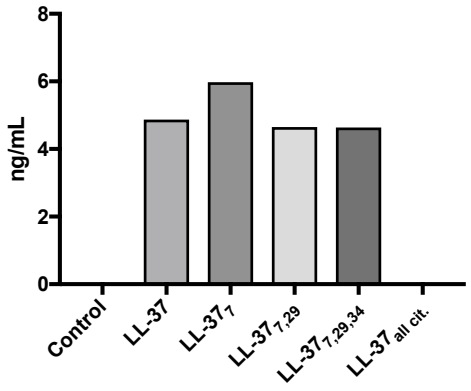

Fig. 37. Recognition of the citrullinated LL-37 by antibodies against the native LL-37 using commercial ELISA kit. Wells of a microtiter plate were coated with 10 ng/ml of the native LL-37 or LL-37 forms harbouring different numbers of citrulline residues (LL-37_7, LL-$37_{7,29}$, LL-$37_{7,29,34}$ and LL-$37_{\text{all cit.}}$) and incubated with antibodies recognizing human LL-37. The analysis was performed as per manufacturer's instructions.

7.3.2. Indirect identification of LL-37 citrullination in NETs

As we were unable to directly determined the presence of citrullinated LL-37 partly due to the short life-span of the modified peptide. Thus, we employed an indirect approach to identify citrullinated LL-37 in NETs. For that purpose, we selected NET structures in which the relatively high concentration of active PAD enzymes and citrullinated proteins was documented. The leading idea was to show that inhibition of citrullination process increase with the level of native peptide, proving indirectly that extensive deamination of LL-37 occurs in NETs. We applied Cl-amidine, a PAD inhibitor, which irreversibly inhibits PADs through covalent modification at the enzyme active site.

7.3.2.1. Immunoblot analysis of the presence of LL-37 in NETs

PAD plays an important role in NET formation by inducing chromatin decondensation and facilitating the formation of web-like structures containing both DNA and antimicrobial peptides. As we would like to apply PAD inhibitor in our study, therefore we first estimated the NETs generation in the presence of Cl-amidine. Picogreen assay was used to measure the released DNA of NETs in supernatant. We noted that neutrophils treated with 25 nM PMA formed NETs in the process partly reduced when neutrophils were treated with 100 μM Cl-A prior stimulation with PMA (**Fig. 38**).

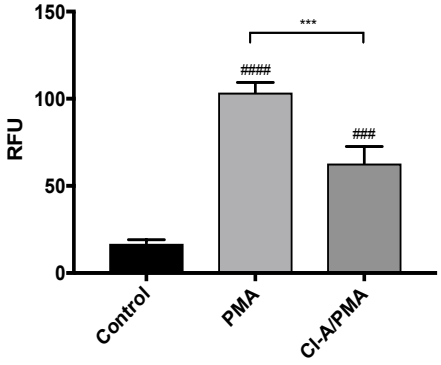

Fig. 38. The reduction of NET formation upon Cl-amidine treatment of neutrophils. Isolated human neutrophils (2 x 10^6 cells/ 400µl) were treated either with or without 100 µM Cl-amidine (Cl-A) for 1 h prior stimulation with or without 25 nM PMA for 3 hours. Formation of NETs was quantified using PicoGreen and shown as relative fluorescence units (RFU). Results shown are representative from 3 independent experiments. Statistical significance was evaluated by one-way ANOVA, followed by Tukey's multiple comparisons post-test (***$p<0.001$; $^{###}p<0.001$, $^{####}p<0.0001$- compared with control). (Copyright 2018. The American Association of Immunologists, Inc.)

Then, we performed immunoblot analysis of PMA-induced NETs. Keeping in mind that antibodies against native LL-37 (LL37 ab) can only recognize the native form of LL-37 (**Fig. 36**), immunoblot to analyze PMA- induced NETs in the presence or absence of Cl-A was conducted. The monoclonal antibody used for Western blot studies can recognize both precursor (hCAP18) and mature form of LL-37, and our results revealed that both forms are externalized during NETosis induced by PMA or *Staphylococcus aureus* (**Fig. 39**). Notably, our observation showed stronger band corresponding to hCAP18 (18 kDa) and LL-37 (4.7 kDa) in neutrophils pre-treated with Cl-A, when compared with samples without PAD inhibitor (**Fig. 39**). Our results suggest that citrullination of mature form of LL-37, as well as its precursor takes place during NET formation.

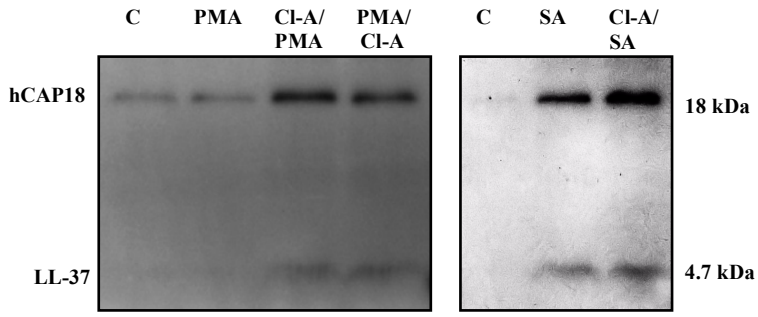

Fig. 39. The identification of the LL-37 in NETs generated in the presence of PAD inhibitor. Shown are representative of Western Blot analysis on the mature peptide (LL-37 - 4.7 kDa) and its precursor (hCAP18 - 18 kDa) in NETs generated in presence/absence of 100 μM Cl-A and PMA (25 nM) or *Staphylococcus aureus* (SA) (MOI 1:10) using antibodies against native LL-37. (Copyright 2018. The American Association of Immunologists, Inc.)

7.3.2.2. Detection of LL-37 in NETs samples with immunofluorescence microscopy

Next, we conducted immunofluorescence analysis to confirm our observation. Neutrophils were added to the coverslips in the presence or absence of PAD inhibitor (Cl-A) for 1 h prior stimulation with PMA for 3 hours. Cells were fixed and stained for native LL-37 with specific antibodies, while Hoechst was used to visualized DNA. As we observed, NETs generated in the presence of Cl-A showed more positive staining corresponding to LL-37 (red) compared to NETs without the inhibitor (**Fig. 40**). The ratio between LL-37-positive staining and amount of NETs revealed that PMA-induced NETs in the presence of Cl-A generated three times more LL-37 fluorescence spots (PMA:Cl-A/PMA=0.136:0.306). Numbers of fluorescence spots of LL-37 was calculated from 20 independent images and presented in **Fig. 41**. This observation correlates with the immunoblot analysis (**Fig. 39**), with more native LL-37 quantified in neutrophils exposed to the PAD inhibitor.

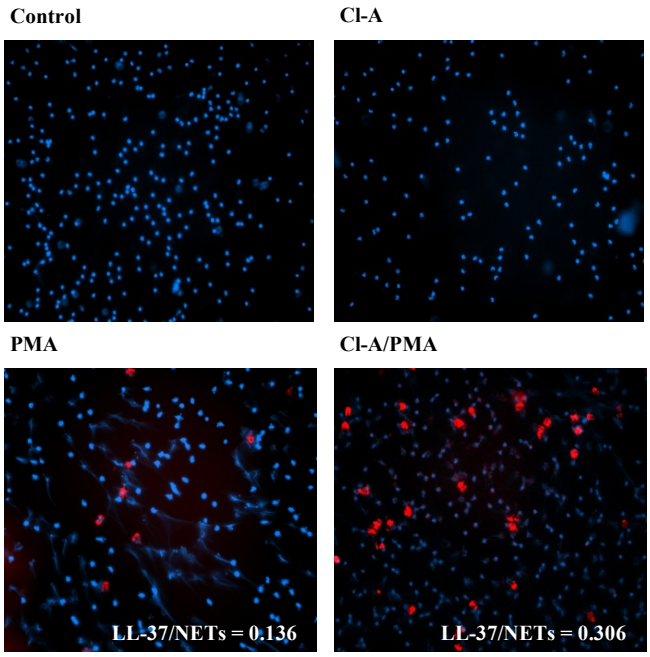

Fig. 40. Immunofluorescence analysis of native LL-37 on PMA-induced NETs in the presence or absence of the PAD inhibitor. Isolated neutrophils were treated either with or without 100 μM Cl-Amidine (Cl-A) for 1 h prior stimulation with or without 25 nM PMA for 3 hours. Formation of NETs and detection of LL-37 was visualized using Alexa Flour 647-labelled antibody against Mouse Anti-human LL-37 (red) and counterstained with Hoechst (blue) and imaged by fluorescent microscopy. The representative images from 3 independent experiments were taken at the magnification x 20. (Copyright 2018. The American Association of Immunologists, Inc.)

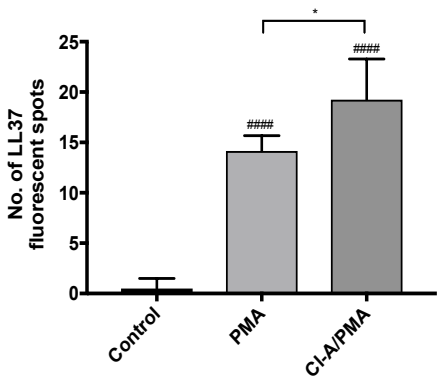

Fig. 41. **The presence of native LL-37 visualized by fluorescent microscopy.** Fluorescence specific for LL-37 visualised by fluorescence microscopy was quantified from 20 independent images and presented as the number of spots. Statistical significance was evaluated by one-

way ANOVA, followed by Tukey's multiple comparisons post-test (*p<0.05; ####p<0.0001-compared with control) (Copyright 2018. The American Association of Immunologists, Inc.)

7.3.3. Identification of LL-37 and citrullinated LL-37 in serum from patients

The conversion of arginine to citrulline can change the structure and function of a protein. Moreover, as citrulline is not a natural amino acid, thus its presence in a protein structure may induce immune response manifested by antibodies generation [60]. Various studies have showed the presence of antibodies against citrullinated proteins/peptides in the development of inflammatory and autoimmune diseases [61]. As it has been previously reported the elevated expression of LL-37 is identified in RA and periodontal disease patients [28]. Therefore, we applied yet another indirect method to show the presence of citrullinated proteins that relies on detection of specific antibodies. According to this we tempt to estimate the level of antibodies directed against LL-37 and/or citrullinated LL-37 in sera obtained from different cohorts of donors, including: healthy individuals, periodontitis patients, rheumatoid arthritis patients, and patients suffer from both RA and periodontitis. Healthy individuals have the highest level of antibodies against native LL-37 compared to other cohorts (**Table VIII**). Although we found no significant difference in the level of antibodies against citrullinated LL-37 among all tested groups (**Fig. 42 A, B**), the ratio of antibodies against citrullinated LL-37/LL-37 had tendency to be elevated but without reaching statistical significance, in patients with inflammatory diseases (periodontitis, rheumatoid arthritis and both RA and periodontitis) (**Fig. 42 C**) compared to control (healthy). All together, obtained data may suggest the presence of deiminated LL-37 in inflamed patients that leads to the generation of relevant antibodies.

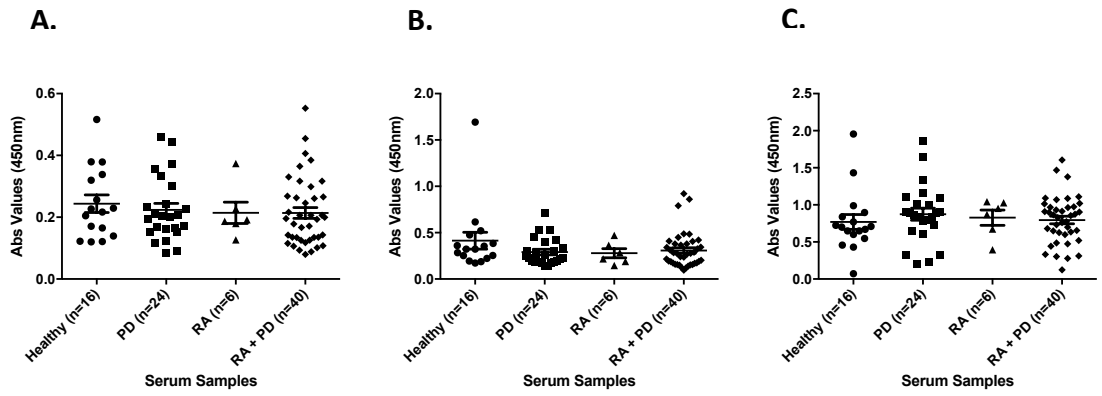

Fig. 42. The antibody response to citrullinated and native LL-37. The level of antibodies against citrullinated **(A)** and native LL-37 **(B)** in sera of healthy donors and patients with inflammatory diseases (periodontitis (PD), rheumatoid arthritis (RA), RA patients with periodontitis (RA + PD)) were analyzed using an ELISA method. (**C**) Ratio of antibodies against citrullinated LL-37 and LL-37 for respective different cohorts of donors. The black line indicates median corresponding for OD 450 nm.

	Healthy (n=16)	**PD (n=24)**	**RA (n=6)**	**RA + PD (n=40)**
	Median (Range)			
LL-37$_{\text{all cit.}}$ (OD)	0.24 (0.12-0.52)	0.22 (0.08-0.46)	0.21 (0.13-0.37)	0.21 (0.08-0.55)
LL-37 (OD)	0.41 (0.17-1.69)	0.29 (0.14-0.71)	0.28 (0.15-0.47)	0.31 (0.10-0.92)
LL-37$_{\text{all cit.}}$/LL-37 (OD)	0.77 (0.07-1.96)	0.87 (0.21-1.65)	0.83 (0.4-1.04)	0.80 (0.12-1.61)

Table VIII. Analysis for antibody levels against citrullinated (LL-37$_{\text{all cit.}}$) and native LL-37 (LL-37) in sera of healthy donors and patients with inflammatory diseases by calculating the ratio of IgG against LL-37$_{\text{all cit.}}$/LL-37.

To conclude, our observation suggested the presence of modified forms of LL-37 within inflammatory milieu, especially in NETs, given that NETs generated in the presence of PAD inhibitor revealed more native LL-37 than control NETs.

7.4. Biological confirmation of the presence of citrullinated LL-37 in NETs

Results of our experiments strongly argue for the presence of citrullinated LL-37 in the NETs structures. Therefore, we applied several methods to explore the immunomodulatory potential of LL-37 citrullination within NETs, which may regulate the functions of phagocytic cells.

7.4.1. NETs induction by anti-LL-37 antibodies

Lande *et al.* [32] have demonstrated that anti-LL-37 Abs can trigger NETosis upon specific binding to LL-37 released by neutrophils isolated from SLE patients [32]. We could not replicate such observation using neutrophils from healthy donors in the PMA-induced NETs model. However, the effect was visible when neutrophils were pretreated with PAD inhibitor, Cl-A. We found that incubation of PMA-induced NETs with anti-LL-37 Abs did not enhance NETosis. The significantly enhanced NETosis was however observed in the presence of Cl-A (**Fig. 43**). Keeping in observation that anti-LL-37 Abs can only recognize the native form of the peptide (**Fig. 36**), this result suggests that higher amount of the native LL-37 was present in neutrophils exposed to Cl-A. Moreover, our findings showed that Cl-A itself did not contribute to the increased NETosis with the presence of anti-LL-37 Abs (**Fig. 44**). These data have suggested that LL-37 are citrullinated by PADs during NET formation, and Cl-A-treatment of neutrophils led to NETs containing higher amount of native LL-37.

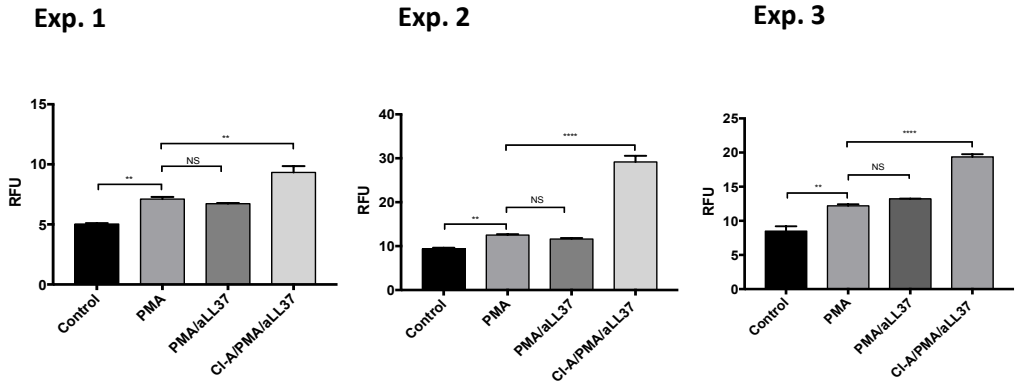

Fig. 43. Antibodies against LL-37 enhanced PMA-induced NETosis in the presence of PAD inhibitor. Neutrophils from 3 different healthy donors were pre-treated either with or without 100 μM Cl-Amidine (Cl-A) for 1 h prior stimulation with or without 25 nM PMA for 3 h. Anti-LL-37 antibodies (aLL37) were added 2 h post PMA activation. Formation of NETs

was quantified using PicoGreen. Statistical significance was evaluated by one-way ANOVA, followed by Tukey's multiple comparisons post-test (**P<0.01; ****p<0.0001; NS, non-significant). Data shown are from 3 different donors.

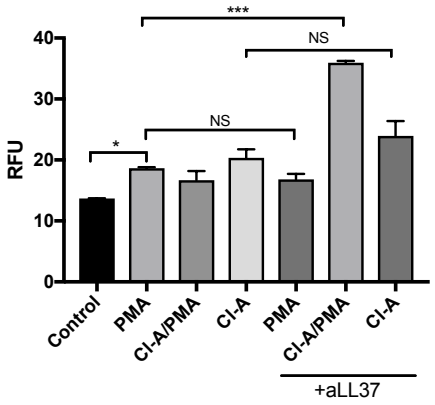

Fig. 44. PAD inhibitor (Cl-A) alone did not enhance NETosis in the presence of anti-LL-37 Abs. Neutrophils were pre-treated either with or without 100 μM Cl-Amidine (Cl-A) for 1 h prior stimulation with or without 25 nM PMA for 3 h; or 100 μM Cl-Amidine (Cl-A) alone. Anti-LL-37 antibodies (aLL37) were added 2 h post PMA activation. Formation of NETs was quantified using PicoGreen. Results shown are representative from 3 independent experiments. Statistical significance was evaluated by one-way ANOVA, followed by Tukey's multiple comparisons post-test (*p<0.05; ***P<0.001; NS, non-significant).

7.4.2. Activation of the inflammasome pathway in macrophages by NETs

We next identified the presence of citrullinated LL-37 within NETs in an indirect approach by using a model described by Kahlenberg *et al.* [30]. In this model, priming of hMDMs with LPS increases surface expression of the P2X7 receptor thus sensitizing macrophages to respond to LL-37. The activation of P2X7 upon stimulation with LL-37 leads to the release of high level of IL-1β. As LL-37 is one of the major NETs components that can activate the P2X7 receptor-signalling pathway, we decided to apply this model in our studies. First, we determined the effects of the synthetic, modified forms of LL-37 on promoting the capacity of hMDMs in releasing IL-1β. Our results have showed that citrullination of LL-37 decreased the response measured as the level of secreted IL-1β in the citrullination-degree dependent manner as demonstrated in **Fig. 45**. Moreover, we stimulated primed macrophages with mixtures of the synthetic modified forms of LL-37, that resembles the composition of peptides obtained after enzymatic modification of LL-37 by PAD2 or PAD4 (mixture

composition as per **Table VII** in section 7.1.3.) and observed a significant reduction in the ability of such mixtures to stimulate the release of IL-1β. Our results confirmed that citrullination of LL-37 abrogated the secretion of IL-1β by primed macrophages.

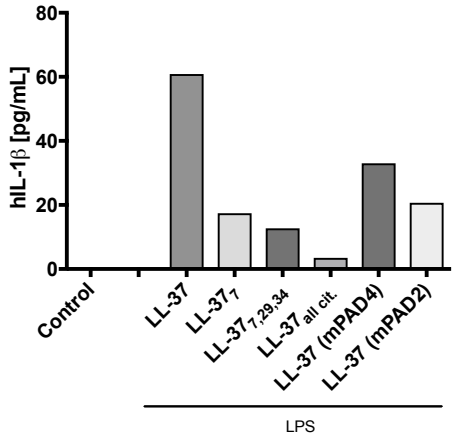

Fig. 45. The release of IL-1β from primed macrophages in response to LL-37 and deiminated forms of the peptide. Human macrophages were primed with or without LPS for 4 h, then treated with the synthetic native or differentially citrullinated forms of LL-37 (LL-37$_7$, LL-37$_{7,29,34}$, and fully citrullinated LL-37) or mixtures of synthetic modified forms of LL-37 (mPAD2 and mPAD4). Supernatants were collected and secretion of IL-1β was quantified using commercial ELISA. Results shown are representative of 3 independent experiments. (Copyright 2018. The American Association of Immunologists, Inc.)

Next, we compared the effects of NETs generated by PMA or *S. aureus* in the absence or presence of Cl-A, on the ability to promote the release of IL-1β from LPS-primed macrophages. We found, that NETs derived from Cl-A pretreated neutrophils induced higher expression of IL-1β in LPS-primed macrophages than "native" NETs (**Fig. 46 A and B**). Taken together, the inhibition of citrullination in NETs potentiated their proinflammatory potential in the applied model, probably via maintaining of the high level of native LL-37.

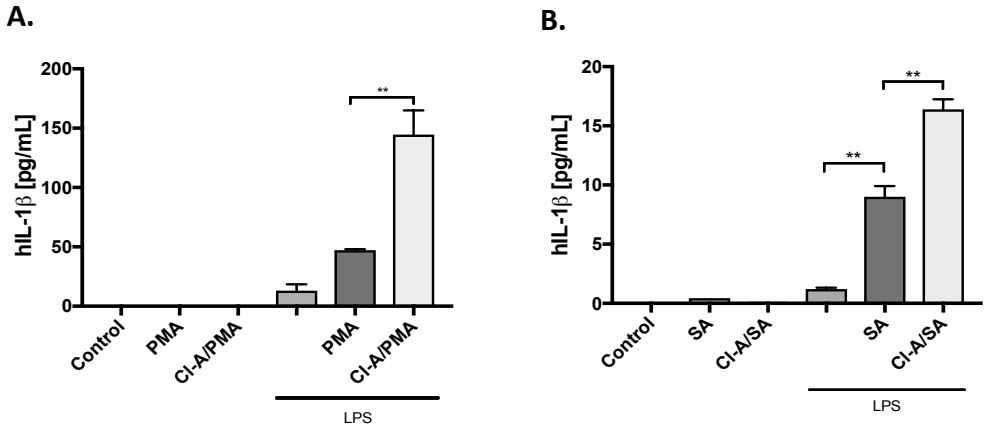

Fig. 46. The activation of IL-1β release from macrophages by NETs. Macrophages primed with or without LPS were treated with NETs triggered by PMA (**A**) or *S. aureus* (SA) (**B**) in the presence or absence of Cl-A. Supernatants were collected and concentration of IL-1β was quantified by ELISA. Results shown are representative from 3 independent experiments. Statistical significance was evaluated by one-way ANOVA, followed by Tukey's multiple comparisons post-test (**P<0.01). (Copyright 2018. The American Association of Immunologists, Inc.)

7.4.3. Activation of pDCs by NETs

To further explore the immunomodulatory role of LL-37 citrullination in NETs we examined the effect of NETs on human pDCs. Taking into account the possibility of NETs being the source of citrullinated LL-37 and the fact that LL-37 is required for the activation of pDCs by nucleic acids, we sought to investigate the pDC activation by PMA-induced NETs with the presence or absence of Cl-A. Activation of pDCs is manifested by characteristic aggregation of cells. We documented such morphology when phagocytes were exposed to CpG complexed with LL-37 (**Fig. 47 B**). Aggregation was also clearly visible upon exposition of pDCs to PMA-induced NETs but the effect was much stronger if neutrophils were pretreated with Cl-A (**Fig. 47 D, E**). This finding collaborates the contention that LL-37 is citrullinated in NETs.

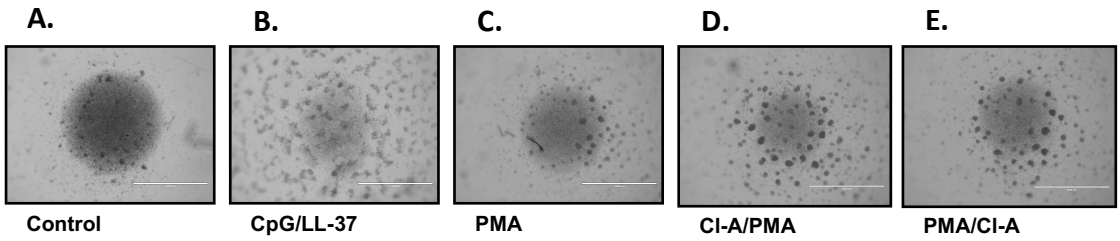

Fig. 47. Activation of pDCs by NETs with differential content of citrullinated proteins. pDCs were incubated with CpG (final concentration 3 μM) with native LL-37 (final concentration 6.4 μM) (**B**); NETs induced by PMA (25 nM) (**C**); NETs induced by PMA (25 nM) from neutrophils pretreated with 100 μM Cl-A (Cl-A/PMA: Neutrophils preincubated with Cl-A for 1 h before stimulation with PMA for 3 hours **(D)**; PMA/Cl-A: Cl-A was added after 2 h of PMA stimulation **(E**)). Morphology of the cell clumps formation reflecting the activation of human pDCs. Images taken were representative of 3 independent experiments. (Copyright 2018. The American Association of Immunologists, Inc.)

We next assessed the molecular parameters of pDCs activation by PMA-induced NETs collected from neutrophils pre-treated with or without Cl-A. Initially, we analyzed the secretion of IFN-α. However, this approach failed as the level of IFN-α was below detection range of the commercial ELISA (**Fig. 48**). Thus, we decided to analyze the expression of genes dependent on type I IFN-α using real-time PCR. *MxA* was chosen, as the gene highly expressed after the engagement of the type I IFN-α receptor. Our data has shown the upregulation of *MxA* gene expression occurred only when pDCs were exposed to PMA-induced NETs in the presence of Cl-A (Cl-PMA). Remarkably, NETs induced without Cl-A pretreatment or if the PADs inhibition was added to pre-formed NETs did not affect the *MxA* gene expression (**Fig. 49**).

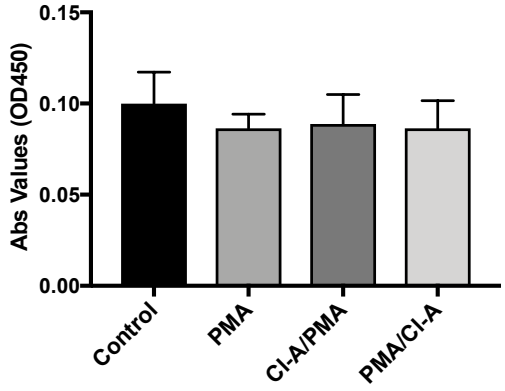

Fig. 48. The IFN-α level secreted by pDCs incubated with NETs. pDCs were exposed to NETs as described in Fig. 47. Production of IFN-α in supernatants collected from pDCs was measured with commercial ELISA. Data shown are representative of 3 independent experiments.

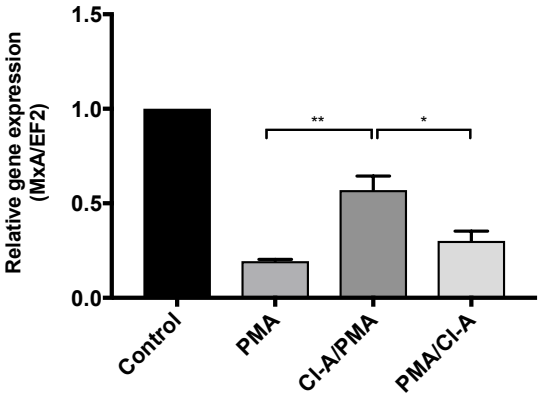

Fig. 49. Expression of the type I IFN-α dependent *MxA* gene in pDCs. The level of *MxA* gene expression was measured by real-time PCR and quantified in relation to the house-keeping gene *EF2*. Statistical significance was evaluated by one-way ANOVA, followed by Tukey's multiple comparisons post-test (*P<0.05, **P<0.01). Results shown are representative from 3 independent experiments. (Copyright 2018. The American Association of Immunologists, Inc.)

Another hallmark of pDC activation is the secretion of IL-6. Although we observed upregulation of that cytokine in conditioned medium of pDCs incubated with PMA-induced NETs, nonetheless a higher IL-6 level was noticed for pDCs treated with NETs obtained in the presence of Cl-A (**Fig. 50**). The data correlates with the observation of cell clumping in **Fig. 47**.

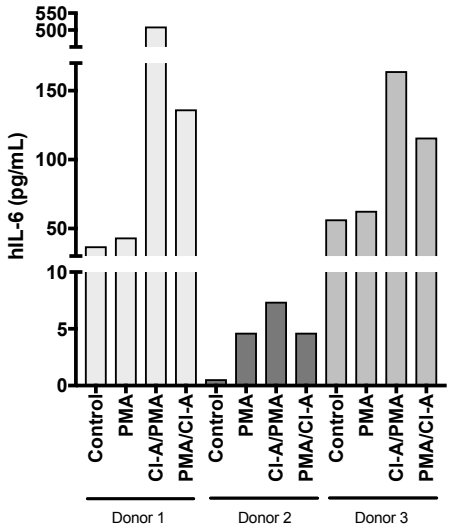

Fig. 50. Activation of pDCs with NETs induced by PMA without any additional treatment (PMA) or from neutrophils pretreated with Cl-A (Cl-A/PMA) or preformed NETs treated with Cl-A (PMA/Cl-A). pDCs were seeded and stimulated overnight with PMA-activated NETs. Production of IL-6 in supernatants was measured with ELISA. Data shown are from 3 different donors. (Copyright 2018. The American Association of Immunologists, Inc.)

To confirm that citrullination of LL-37 in NETs abolish inflammatory reaction of pDCs (**Fig. 47, 49, 50**), we supplemented NETs with either the native LL-37 or its peptide resistant for citrullination - hArg-LL-37. Intriguingly, pDCs treated with NETs containing hArg-LL-37 induced the substantial inflammatory response manifested by both *MxA* expression (**Fig. 51**) and IL-6 secretion (**Fig. 52**) compared to native LL-37.

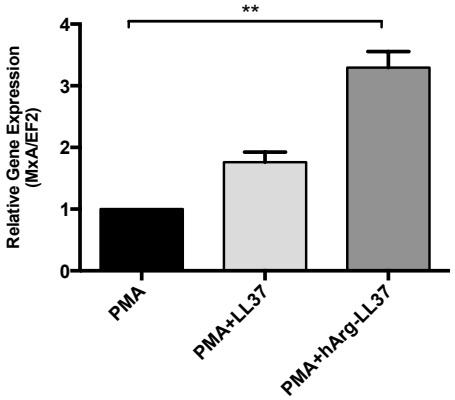

Fig. 51. Activation of pDCs by NETs supplemented with LL-37 or hArg-LL-37. The level of *MxA* gene expression in relative to the house-keeping gene, *EF2* in pDCs measured by real-time PCR. Statistical significance was evaluated by one-way ANOVA, followed by Tukey's

multiple comparisons post-test (**P<0.01). Results shown are representative from 3 independent experiments. (Copyright 2018. The American Association of Immunologists, Inc.)

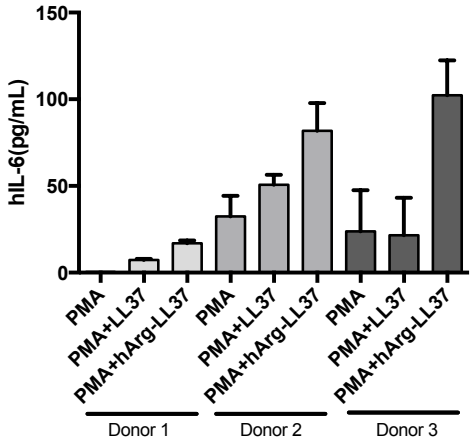

Fig. 52. Activation of pDCs by NETs supplemented with LL-37 or hArg-LL-37. The level of IL-6 in pDCs were measured with ELISA as per manufacturer's instructions. Data shown are from 3 different donors. (Copyright 2018. The American Association of Immunologists, Inc.)

7.4.4. The role of LL-37 citrullination in the generation of NETs

Expression of LL-37 is augmented during inflammatory response. The peptide is secreted by epithelial cells, but also released from dying neutrophils. Recently, LL-37 was reported to increase NETs activation upon exposure to PMA [109]. We confirmed that phenomenon in our studies (**Fig. 53**), but keeping in mind that citrullination of LL-37 occurs in NETosis, we examined also NETs formation induced by PMA in the presence of citrullinated LL-37. Our results showed that neutrophils pre-treated with the modified peptides before exposition to PMA underwent accelerated NETosis, which intensity positively correlated with the amount of substituted arginines (**Fig. 53**). Next, we confirmed the above observation using other stimulant of NETs formation – gingipain RgpA, the virulence factor of *Porphyromonas gingivalis* (data not shown). As in the case of PMA stimulation we observed, a slight but the significant increased level of NETs upon preincubation of neutrophils with some modified peptides.

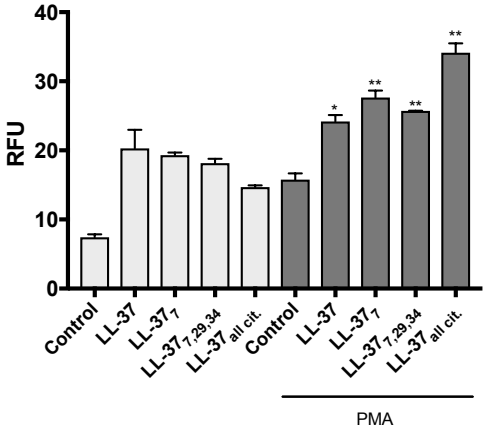

Fig. 53. The intensity of NETs formation induced by PMA in the presence of the native or citrullinated LL-37 peptides. Neutrophils were pre-treated with 5 μM native or modified forms of LL-37 for 1 hour, followed by 3 h incubation in the presence or absence of 25 nM PMA. NETs were collected and quantified with PicoGreen Assay. Results were representative of 3 independent experiments. Unpaired t-test was used to calculate the *p* values (*p<0.05; **p<0.01- compared with control in the presence of 25 nM PMA).

Taken together our studies revealed that the process of LL-37 citrullination occurs in NETs affecting the inflammatory potential of those structures. On the other hand, we documented that citrullinated peptides intensify the process of NETs formation what can be considered as a mechanism of positive feedback what might promote further uncontrolled inflammation.

8. Discussion

The innate immune system plays a crucial role to safeguard the host from invading microorganisms. Initiation of the immune response occurs via pattern recognition receptors (PRR), which recognize an array of pathogen associated molecular patterns (PAMPs), including among other nucleic acids. Nucleic acids are common inherent molecular signatures present in both pathogen and host, leading to the potential risk of self-recognition by innate immune receptors. Few studies have emphasized the deleterious consequences of self-DNA recognition, which has established a link to many autoimmune diseases. Our studies focused on a human peptide LL-37, that displays natural antimicrobial activity but can elicit an immune response in the absence of an infection by binding with high affinity to released nucleic acids. This pathway is likely a key driver of autoimmune diseases, which are enhanced by LL-37, by facilitating DNA uptake into the endosomal compartment of APCs via the recognition of genomic DNA by intracellular TLR9 receptors. Through binding of nucleic acid to LL-37, a condensed aggregate structure is formed and translocated to the early endosomes thus upregulating the production of IFN-α. Altogether, it leads to the overwhelming pro-inflammatory responses such as in the case of systemic lupus erythematosus and psoriasis patients [32][80]. On the other hand, the enhanced recognition of nucleic acids with CpG motifs by LL-37 benefits our immune system especially in the event of bacterial infection, as LL-37 is capable to form complexes with nucleic acids released from lysed bacterial cells, sufficient to protect them from nucleases degradation and deliver them into host cells [110].

Recent observations have highlighted the denoting effect of posttranslational modifications (PTM) in the regulation of the inflammatory reaction. Posttranslational regulation of protein function and activity is one of the mechanisms developed by the host to avoid uncontrolled innate inflammatory responses and also to regulate PRR signalling. One of the most extensively studied PTM is phosphorylation which plays an important role in regulating the activation and deactivation of multiple TLR-dependent signalling molecules such as MAPKs, NF-κB inhibitor kinases and IRF3, that is essential in the antiviral response [111]. Another common PTM that is important in controlling innate immunity and inflammatory responses is ubiquitination. Protein ubiquitination is known as the regulatory mechanism for inhibition of TLR signalling, for example, suppressing cytokine signalling 1 (SOCS1) or neuroregulin receptor degradation protein 1 (Nrdp1) [112]. On the other hand, increased level of acetylation and SUMOylation are widely linked to various neurological and cardiac diseases. For instance, acetylation of tau, which is the major microtubule associated

protein (MAP) of a mature neuron, at lysine 174 (K174) affects its stability and toxicity in early stages of the Alzheimer's disease. The alterations in SUMOylation can lead to the heart failure. SUMOylation of Lamin A at lysine 201, which is a critical scaffolding protein important for the nuclear structure, can cause human familial dilated cardiomyopathy (a genetic form of heart disease) [113]. The carbonylation of amino acids like proline, arginine, lysine, threonine, glutamate and aspartate is irreversible and has been reported to act as a mediator in a number of chronic diseases such as chronic renal failure, cystic fibrosis, psoriasis and etc. The elevation of protein carbonyl derivatives (aldehydes and ketones) correlates with the severity of the disease [114]. In this context, we focused on citrullination, a process catalyzed by calcium-dependent PAD enzymes to generate citrulline from arginine residues. As it was documented, LL-37 is susceptible to be citrullinated as it contains five Arg residues [67]. Moreover, it has been reported that such modification of peptide abrogates its anti-inflammatory functions. One of the most significant effect of peptide citrullination is abbrogation of its immunomodulatory activity manifested by neutralization of LPS proinflammatory ability. This may result in the lost of protection against sepsis exerted by the native LL-37 [67]. Furthermore, Klisgård and co-workers have demonstrated that citrullination of LL-37 dampens its bactericidal effect. Authors proposed that citrullination of LL-37 could be enhanced by the increased local production of PAD2 and recruitment of neutrophils containing PAD4 during inflammation suggesting the role of LL-37 deimination in the course of chronic obstructive pulmonary disease (COPD) [68].

LL-37 exerts several immunomodulatory functions that regulate host responses to pathogens. Among them is formation of complexes with negatively charged oligonucleotides derived from both dying host cells and pathogens. Our observation has showed that citrullination affects the affinity with which LL-37 binds DNA. LL-37 is highly susceptible to citrullination by PAD2 and PAD4 [67][68] and our studies showed that both PADs reduced the binding of LL-37 to DNA, with PAD2 to be reported being more efficient. PAD2 has a higher efficiency in citrullinating LL-37 compared to PAD4 which might due to the differences in the catalytic potency of the LL-37 sequence of these two PAD isoforms or their specificity for Arg residues in the context of the specificity exerted on the peptide [115]. In conjunction with the HPLC analysis on the level of citrullination of LL-37, we hypothesized the possibility of differentially modified forms of the peptide being generated *in vivo* as PAD2 and PAD4 has its' own preference in citrullinating peptidylarginines [67]. This is illustrated by the fact that histone H3 is citrullinated by both PAD2 and PAD4, but fibrinogen is predominantly citrullinated by PAD2 [100]. Furthermore, it is broadly proposed that endogenous PADs could

have stricter substrate selection than recombinant enzymes [116]. Our findings were confirmed using synthetic citrullinated LL-37 forms, since their binding to DNA was gradually reduced with the increase number of deiminated arginine residues within the peptide. We have also shown that the affinity of LL-37 to DNA does not depend entirely on the peptide cationicity alone, but also the proper distribution of guanidinium side chains of Arg and specific PTMs. This was illustrated by using carbamylated forms of LL-37 which represents a good example of changes in cationicity of LL-37, since six lysine residues within the peptide are susceptible to carbamylation, which alters the cationic and amphipathic nature of the peptide [51]. Nevertheless, carbamylated LL-37 still had affinity for DNA comparable to that of the native LL-37. Remarkably however, upon enzymatic deimination of Arg residues in carbamylated LL-37, the binding affinity was totally abolished. The role of guanidinium side chains of Arg (hArg) was verified by using hArg-LL-37, which is insensitive to enzymatic deamination [57]. We observed equally efficient binding of hArg-LL-37 to nucleic acids compare to the native peptide, and the binding affinity was not affected upon incubation with PAD2, confirming the role of guanidinium side chains of Arg or hArg residues in LL-37 for DNA binding. In contrast to carbamylated LL-37 and hArg-LL-37, scrambled peptide (sLL-37) did not bind to DNA, similarly to its citrullinated version, revealing that the defined sequence of the amino acids in the polypeptide chain is essential for LL-37 binding to DNA.

Our results obtained with murine analog of LL-37, the CRAMP peptide revealed that even the single Arg residue in CRAMP is essential for DNA binding. The loss of one positive charge that caused the change in protein structure and/or function is a phenomenon not only limited to LL-37. It was also described in case of a myelin basic protein (MBP), which contributes to the pathogenesis of multiple sclerosis. The conversion of arginine to citrulline in the brain carried out by PAD2 has compromised the ability of MBP to interact with lipid bilayer. The reduced ability of the deiminated protein to bind and aggregate lipid vesicles and the presence of such highly deiminated form of MBP caused the fragmentation of lipid vesicles, leading to myelin breakdown in multiple sclerosis. Moreover, the elevated levels of PAD4 observed in the brain might deiminate the arginyl residues of histones and compromise its ability to interact with DNA hence resulting in the induction of apoptosis of oligodendrocytes and suggesting an important role of its citrullination in the pathogenesis of multiple sclerosis [117]. The impairment of binding by citrullination was observed also in chemokines CXCL10 and CXCL11. The heparin binding capacity of citrullinated forms of CXCL10 and CXCL11 was significantly diminished compared to the native chemokines, with just the loss of one positive charge [118].

Our data has shown that citrullination of LL-37 effectively abolished the binding of peptide to DNA irrespectively to the length and origin of nucleic acid, as it was demonstrated using *T. forsythia* DNA, DNA isolated from human epithelial cells (HeLa) and synthetic oligonucleotides containing CpG motifs. Changes in the cationic charge of the peptide efficiently affects also its interaction with other molecules such as lipoproteins e.g. ApoA1. Moreover, we found that the change in the positive overall charge of LL-37 is also essential in stabilizing nucleic acids against nucleases. Such conclusion is supported by results, showing that the modified peptide with a single substituted residue that still binds to nucleic acid shows significantly diminished protection of DNA against nuclease degradation. This phenomenon might be explained by a less condensed structure formed between monocitrullinated LL-37 and nucleic acids, which allow nucleases to access cleavage sites of DNA. Taken together, these data reflect the unique role of deimination in LL-37 that alters the peptide interaction with nucleic acids and ability to provide associated DNA with resistance to nucleases.

Deimination does not only contribute to the significant changes in physiochemical properties of LL-37, but also alters the biological function of the peptide. As reported by Koziel *et al.* [67] and Kilsgard *et al.* [68], modified peptide loses its' antimicrobial and chemotactic activity, including its anti-inflammatory role as an antagonist of TLR-dependent signalling induced by LPS, lipoteichoic acid, and peptidoglycan [67][68]. Our study aimed to investigate the immune response elicited by DNA, a key ligand for the TLR9 receptor. Recent findings have emphasized the role of host DNA in the development of inflammatory and/or autoimmune diseases. This has suggested that the greater level of inflammation correlates with intensity of cell death accompanied with the release of host DNA [119]. Innate immune recognition of bacterial DNA is considered as a beneficial mechanism to confer protection against invading pathogens, however, when host DNA is recognized, it becomes detrimental. Activation of TLR9 by self-DNA is prevented by DNA degradation by nucleases preventing DNA uptake by phagocytes. DNA in inflammatory milieu is usually removed by the action of DNases released by dying cells. However, Lande *et al.* [32] have reported that LL-37 forms complexes with DNA, protecting it against extracellular degradation, acting as a carrier molecule and facilitating the uptake of nucleic acid by immune cells [32]. The cationic charge of LL-37 plays an essential role in binding to DNA via electrostatic interactions and enhance the transfer of DNA over the plasma membrane which involved noncaveolar lipid raft domains, as well as cell surface proteoglycans [81]. Moreover, penetrating complex of DNA with LL-37 induces potent activation of pDCs [82]. As demonstrated in current dissertation this phenomenon is altered, when LL-37 undergoes citrullination. This was illustrated by using different forms of

the synthetic citrullinated LL-37 peptide. Citrullination regulates the LL-37-dependent immune response of APCs to the CpG motifs, in the citrullination-level dependent manner as the degree of activation of cells inversely correlated with numbers of modified Arg residues. This is in accordance with the studies conducted by Lande *et al.* [80], which indicates that DNA uncomplexed with LL-37 does not activate TLR9, as there were less CpG entering the endosomal compartment of pDCs, thereby abolishing the IFN-α production and desensitizing the cells to DNA. Our data mechanistically confirmed such observation as the consequence of reduced complex formation between citrullinated peptides and DNA diminished binding of nucleic acid to the cell membrane.

In presented studies we documented stronger immunostimulatory effect induced by CpG-LL-37 complexes observed after continuous overnight incubation with phagocytes compared to short exposure time (15 min). This might be a result of enhanced recognition of DNA or self-priming of pDCs mediated by type I IFN [120]. Moreover, our data revealed differential induction of inflammatory mediators, while IFN was elevated upon CpG-LL-37 complex recognition, the level of IL-6 was diminished. Few studies have suggested that IFN-α production by pDCs is the consequences of activation of TLR9 signalling in early endosomes, whilst its induction in late endosomes leads to pDC maturation and secretion of IL-6. In accordance with Lande *et al.* [80] observation, CpG in the complex with LL-37 stimulated the production of IFN-α, without inducing pDC maturation, as low levels of IL-6 secretion was observed, suggesting the retainment of complexes in early endosomes. Apart from that, uncomplexed LL-37 was unable to induce pDCs to produce IFN-α but IL-6, suggesting the effects of LL-37 on TLR9 activation solely depends on DNA binding. The carbamylated forms of LL-37 exerted the immunoregulatory effects on pDCs at the same level as native LL-37, with sLL-37 reported to be neutral for pDCs response to DNA. Although carbamylated peptides showed decreased cationicity, such modification did not affect the immunostimulatory potential of DNA complexed with the peptide, emphasizing that citrullination strongly and specifically affects the immunomodulatory function of LL-37. This conclusion corroborates with the idea that PAD regulates the local immune responses through posttranslational modification of immunomodulators [118]. Above described phenomenon was also documented in the model of murine macrophages RAW264.7, cells that express TLR9. Mixture of synthetic modified peptides harboring different deiminated residues mimicking *in vivo* citrullination catalysed by PAD2 and PAD4, respectively, triggered the release of significantly lower level of TNF-α in response to DNA as compared to the native peptide.

Taken together, deimination of LL-37 downregulates host response to nucleic acids, which is not limited only to the reduced cationicity of peptide, but rather related to arginine modification. This was confirmed with the observations of binding affinity of carbamylated peptides and hArg-LL-37 to DNA, suggesting the essential role of the guanidinium side chain of Arg and hArg residues in protein/peptide interaction with DNA, RNA and other proteins [121]. The guanidinium functional group acts as a unique biomolecular recognition property for Arg residues. This group is particularly adept at multidentate hydrogen bonding and electrostatic interactions. Cell-penetrating peptides are reported to be arginine-rich peptides, and thus their properties are dependent on the guanidinium functional groups of the peptides [122].

The diverse induction of the inflammatory response in phagocytes mediated by modified LL-37 and DNA has prompted us to study the cell signalling cascades. First, we wanted to determine how citrullination regulates the inflammatory response by investigating the uptake mechanism of native and citrullinated LL-37. To estimate the interaction of the native and modified LL-37 with cell membrane and intracellular penetration of peptides we tried to adapt the method published by Tang *et al.* [123]. One of the most well-characterized mechanism for the entry of molecules into cells is via early and late endosomes to lysosomes. Lysosome is a major degradation site for internalized material and cellular membrane proteins [124]. And thus, we wanted to establish the mechanism of LL-37 internalization by analyzing the lysosome formation. However, the lysosomes labelling pattern displayed by RAW264.7 cells did not discriminate between the uptake of native and citrullinated LL-37 (data not shown). Further studies utilizing fluorescent-labelled native and citrullinated LL-37 can be done to observe the potential difference in a penetration of such peptides into the host cells.

As we proved differentiated regulation of cytokines secretion in response to CpG combined with the native and citrullinated forms of LL-37, therefore we attempt to identify a signalling pathway. For that purpose, we used both RAW264.7 cells and pDCs, which are both, classified as well-defined *in vitro* models sensitive to CpG [125]. Initially, we attempt to determine the activation of transcription factors. For that purpose, we used RAW264.7 cells transfected with a NF-κB-luciferase reporter plasmid. Exposition of those cells to DNA in a presence of native or modified LL-37 has revealed that NF-κB activation corroborates with TNF-α expression, and regardless of the duration of exposure, similar manner of NF-κB activity was observed. There was a decline of NF-κB activity when the deiminated residues increased within the peptide. Such data states in accordance to our FACS results that have demonstrated that citrullination affects the uptake of CpG into the cell. Based on obtained

results we can conclude that the downstream activation of NF-κB requires first the CpG to be endocytosed and upon endosomal acidification, it is specifically engaged by TLR9 and initiates a signalling cascade [126]. Moreover, this process is most efficient in the presence of native LL-37.

As the regulation of TLR9 activation varies between cell types and culture conditions [82], thus we studied the signalling pathways also in primary cells using CpG DNA well recognized by pDCs. Interestingly, not all known CpG DNA can induce pDCs to produce type I IFNs. We have selected A-type oligonucleotides such as 2216 for our studies as it is reported to be a strong stimulus for type I IFN production and promotes transcriptional activity of IRF-7, triggering an autocrine feedback loop involving the IFN receptor-dependent pathway [127]. Of note, induction of type I IFN genes requires the activation of IRF7 [128]. However, we did not observe IRF7 activation after exposition of cells to CpG-LL-37 complexes. One of the plausible explanations might be that the IRF7 activity was below detection range of the applied ELISA assay. However, we confirmed the role of this pathway observing significant upregulation of type I interferon-dependent genes, including *MxA*. However, the process of pDCs activation should be further examined as Guiducci *et al.* reported that pDCs can induce a different mechanism of cell activation in response to TLR9 ligands, which depends on their location in an intracellular compartment [129]. Kim *et al.* [120] have reported that IRF3 and IRF7 are specific for PRR-triggered type I IFN production, whilst AP-1 and NF-κB components are essential for spontaneous type I IFN production, suggesting type I IFN production by pDCs cannot simply be explained at the cellular or subcellular level. Future studies are needed to verify the endosomal location of CpG-LL-37 complexes in pDCs that will provide a new insight into the mechanism of their activation.

To further explore if LL-37 citrullination plays a role in inflammatory conditions, we employed neutrophils as our study model. LL-37 is found abundantly within the azurophilic granules of neutrophils. While NETs formation facilitates the interaction between bacteria and antimicrobial effectors leading to enhanced bacteria killing, they also contribute to the detrimental effects such as excessive inflammation and tissue damage in the host by release of proinflammatory, immunostimulatory molecules and various autoantigens [130]. The interaction between DNA and LL-37 in NETs was well described in a few studies where the presence of DNA-LL-37 complexes was identified [32][42]. They analyzed NETs released by neutrophils activated for 3 hours with phorbol 12-myristate 13-acetate (PMA) and using confocal microscopy, they show long stretches of DNA filaments of NETs consist DNA

decorated with LL-37. Treatment of NETs with DNase I degraded DNA stretches but not of the globular DNA domains containing LL-37 [32][42]. The important role of LL-37 generated through NETs has been described to have numerous immunomodulatory functions as according to environmental and cellular contexts. Apart from its antimicrobial activity, LL-37 also protects NETs against degradation by bacterial nucleases [109]. Another unique function of LL-37 in NETs was reported to induce inflammasome via the activation of the P2X7R inflammatory signalling pathway in macrophages and monocytes [30]. Moreover, upon NETs formation, the presence of enzymatically active PAD [131] might catalyse the citrullination process of LL-37 exposed on DNA fibers. Thus, we tried to identify modified forms of LL-37 in NETs directly with a citrulline specific chemical probe, rhodamine-phenylglyoxal (Rh-PG), however, only faint band correspond to the band size of citrullinated LL-37 was observed. And thus, we proceed with another approach by using mass spectrometry analysis. Nonetheless, our attempts failed with this method, which might be an effect of peptide degradation catalysed by the neutrophil proteases. This conclusion is strongly supported with our finding that LL-37 stability was increased in the presence of a general inhibitor of proteases. As far as we documented the protective effect of elastase inhibitors one may propose that it is one of the crucial enzymes responsible for degradation of the peptide in NETs. Moreover, all modified LL-37 peptides have shorter half-life compared to the native LL-37 when added to HNE. The presence of HNE was documented in NETs and synovial fluid from RA patients. Of note enhanced NETosis was reported in synovial fluid from RA patients [84]. O'Donoghue and co-workers have demonstrated in their study that NETs are enriched in serine proteases, with HNE (neutrophil elastase) and PR3 (neutrophil proteinase 3) as the main contributors to NETs associated proteolytic activity [132]. As both enzymes are released from vacuoles upon the event of NETosis, their activity may no longer spacially restricted leading to enhanced local proteolysis of liberated proteins [132]. This can be an explanation why the proteomic analysis might have failed to identify citrullinated LL-37. Apart from that, the oxidative environment created from myeloperoxidase activity during NETosis can lead to further modification on citrulline and other residues in LL-37 [103], and thus interfering with identification of citrullinated LL-37 by mass spectrophotometry due to mass shift. Of note, both native and modified forms of LL-37 have a longer half-life in healthy donor's sera. Keeping in mind that less proteolytic activity occurs in healthy sera, this suggest that proteolytic degradation can be a cause to a short half-life of modified LL-37 in NETs. Such conclusion supports the studies conducted by Klisgard *et al.*, where the citrullinated LL-37 peptide is rapidly degraded due to the change of its' molecular structure [68]. Hahn and co-workers recently documented the role

of neutrophils and NETs in the regulation of the life-span of the immunoregulators. They reported the immunoregulatory effects of neutrophil serine proteases [133] whihch degrade several cytokines/chemokines, such as IL-1β, IL-6, MCP-1 and IL-8. Described degradation of proinflammatory mediators dampens the inflammation in gout and an animal model of lupus [134][135]. This implies a strategy of the host to interrupt the self-positive feedback loop with neutrophil recruitment and activation, providing a safeguard of neutrophilic inflammation [133].

Experiments using antibodies against native LL-37 have revealed that more unmodified LL-37 was found in NETs generated in the presence of a nonselective PAD inhibitor – chloramidine (Cl-A) [130]. We confirmed this using fluorescent microscopy as well as Western blot analysis. Moreover, the increase level of hCAP18 was found in neutrophils pretreated with Cl-A in our immunoblot analysis, suggesting the inhibition of hCAP18 deimination by PADs. These data have strongly suggested that both cathelicidin and mature LL-37 are citrullinated by PADs during NET formation, both *in vitro* and *ex vivo*. This observation was further supported by examining the biological effect of the native peptide on macrophages using a model based on an approach published by Kahlenberg *et al.* [30]. The authors reported that primed human monocyte-derived macrophages with increased surface expression of the P2X7 receptor released high levels of IL-1β upon stimulation with LL-37. As LL-37 is one of the major NETs components that can activate the P2X7 receptor-signalling pathway, our results can serve as a strong evidence of the presence of modified LL-37 in NETs, where NETs pretreated with Cl-A had stronger effect on primed macrophages, as shown by the IL-1β secretion, compared to native NETs.

Few studies have reported the role of citrullinated proteins/peptides in the onset of inflammatory responses, such as in rheumatoid arthritis, multiple sclerosis and systemic lupus erythematosus patients. Apparently citrullination leads to the generation of antibodies against citrullinated proteins/peptides. NETs are known as an important source of autoantigens that contribute to autoinflammatory conditions and in concordance we found an elevated antibody response against citrullinated LL-37 in RA patients, which elevated levels of NETs have been reported in RA patients [136]. Our studies have shown the slight increase of the ratio of IgGs against citrullinated LL-37/LL-37 in patients with inflammatory disease (periodontitis and rheumatoid arthritis), suggesting the presence of citrullinated LL-37 and induction of adaptive immunity in the response to this peptide. The explanation of observed phenomenon is likely chronic inflammation typical for both groups of patients [137]. Moreover, in both diseases the

detrimental role of NETs is postulated [84]. A study conducted by Kienhöfer *et al.* [138] has showed a significant difference in the level of IgGs against LL-37 between healthy controls and SLE patients, but not in RA, which corroborates with our results. They also showed that autoantibodies to LL-37 in sera of the two tested cohorts did not correlate with the disease activity, organ involvement or treatment. That suggested that the autoreactivity against exposed cathelicidins is an epiphenomenon due to extensive disease-induced overexpression. However, further studies involving a larger cohort of patients shall be conducted for better explanation of above observation. Darrah *et al.* [115] have reported that PAD enzymes are active extracellularly in RA. That raised the possibility of LL-37 citrullination and presentation of modified antigens to T cells. Such modifications may alter the processing and presentation on antigen by antigen presenting cells and thus production of IgGs might be triggered. NETosis was observed to be enhanced in RA patients which elevates the members of this cascade, such as the increased intracellular ROS production, enhanced expression of HNE and MPO, increased nuclear translocation of PAD4, and citrullination of proteins/peptides [115], providing the immune system with access to abundant sources of citrullinated proteins.

Finally, one cannot exclude the possibility that citrullination of LL-37 can be executed by peptidyl deiminase expressed by *P. gingivalis,* the only one PAD ortholog identified in prokaryotes [139]. Studies conducted by Bielecka *et al.* [140] have showed the effect of bacterial citrullination on proinflammatory functions of anaphylatoxin C5a, where a reduced chemotactic activity for neutrophils and impairment to induce calcium influx in a myeloid-derived cell line (U937) transfected with C5aR (C5a receptors) were observed [140]. Moreover, Moelants and co-workers have suggested that chemokine citrullination such as CXCL8 by bacterial PAD (PPAD) may lead to negative feedback on local leukocyte-mediated inflammation and bacterial clearance [141]. Besides that, Wegner *et al.* [56] have demonstrated the citrullination of host peptides (human fibrinogen and α-enolase) by *P. gingivalis*, where the host peptides were first subjected to proteolytic cleavage by arginine-gingipains followed by citrullination of carboxy-terminal arginines by PPAD. This has led to the generation of antigens driving autoimmune response in RA. *P. gingivalis* can also induce NETs formation, as an increased NETosis have been reported in gingival crevicular fluid from periodontitis patients. This has opened the window of possibilities that enhanced citrullination and NETosis induced in the oral cavity by *P. gingivalis* could be an initial event that leads to the generation of autoantigens and autoantibodies corroborating an autoimmune response in RA patients [142]. Taken together, we postulate that citrullinated LL-37 is generated during NETs formation.

Several studies have reported the crosstalk between neutrophils and DCs [32][42][143]. Neutrophils death, such as apoptosis, necrosis and NETosis has contributed to the potential resource of self-DNA in patients with autoimmune diseases. Besides that, psoriasis is characterized by the overexpression of LL-37. LL-37 was also found to be present at high levels in the blood of SLE patients. The presence of the LL-37 in such disorder has suggested the involvement of DNA-LL-37 complexes in the disease pathogenesis. Thus LL-37 can be considered a stable ligand that promotes loss of tolerance and TLR9 stimulation in pDCs [32][80]. Furthermore, SLE patients selectively develop antibodies against LL-37 derived from neutrophils, which in turn could activate neutrophils to release NETs containing complexes of DNA and the antimicrobial peptide. These autoantibodies were also reported to enhance the uptake of DNA-antimicrobial peptide complexes into pDCs by enhancing FcγRII recognition of the DNA complexes, leading to the release of IFN-α and exacerbating the inflammation and disease [32].

Collectively our studies have shown the critical role of citrullinated LL-37 in the host response. There's a growing interest on the role of PTM in the context of NETs and its link with autoimmunity. The presence of modified forms of LL-37 which are released abundantly during NETosis play an important role in modulating myeloid cell response to nucleic acids. APCs exposed to NETs generated in the presence of a PAD inhibitor exhibit stronger activation compared to native NETs, suggesting the protective role of protein citrullination, including LL-37 on the enhanced response of myeloid cells to host DNA. Above statement is strongly supported by results of efficient pDCs activation by NETs supplemented with resistant to deimination hArg-LL-37. Thus, we postulate that the proinflammatory potential of NETs could be regulated at the level of posttranslational modification of proteins associated with nucleic acids. Such regulation of protein activity and stability by the host can provide the control of inflammatory reaction needed for elimination of pathogens without triggering further proinflammatory response. This can be critical in the context of immune system regulation and in the development of autoimmune diseases, especially in cases where self-DNA molecules triggered an excessive inflammatory response [32]. This has led to the hypothesis that posttranslational modification by citrullination may act to protect the host against inflammatory activity of proteins associated with DNA fibers [100]. Moreover, small quantities of citrulline-containing proteins and the soluble PAD2 protein have been detected in healthy human subjects, suggesting the physiological roles of these enzymes under healthy conditions, although the exact physiological functions still remain unknown [144]. However, this maybe a disadvantage

during bacterial infection, since the abrogation of LPS neutralization by citrullinated LL-37 leads to an exacerbated inflammatory response in the endotoxin-induced model of sepsis [67]. Thus, the hArg-LL-37 peptide resistant for deimination might serve a potential candidate for apical treatment in patients suffering with microbial related infections such as periodontitis or infected wounds. Moreover, a study conducted by Biron *et al.* has shown that the inhibition of Histone 3 citrullination by Cl-Amidine improves survival in murine sepsis model by decreasing the proinflammatory response [130].

Interestingly, presented data have revealed that citrullination of LL-37 is crucial not only for the regulation of the immune response to DNA. We also documented that neutrophils pre-treated with citrullinated proteins/peptides exhibited an increased response to further stimulation with NETs inducers (PMA or RgpA). Those data corroborate with unpublished results of Danuta Bryzek, Ph.D. She proved that some forms of deiminated LL-37 act proinflammatory in contrast to native peptide. As she documented human monocyte-derived macrophages (hMDMs) produce an elevated level of pro-inflammatory cytokines upon stimulation with some forms of citrullinated LL-37. The effect was observed for monocitrullinated LL-37 ($LL\text{-}37_7$), while the strongest induction was executed by $LL\text{-}37_{7, 29, 34}$. This might be a plausible explanation of the amplified inflammation observed in autoimmune disease patients. This phenomenon was observed in RA, that is characterized by the increased NETs level and production of autoantibodies to citrullinated protein antigens (ACPAs), with citrullinated antigens being mostly derived from NETs [145]. Intriguingly, autoantibodies against antimicrobial peptides were found also to activate neutrophils, and thus perpetuating a vicious circle of NETs production that maintains the delivery of modified autoantigens to the immune system even in the absence of infections. One may propose, that modified proteins/peptides released during NETosis might lead to neutrophil priming and heightens neutrophil responses manifested by extruding a greater amount of DNA. These observations may suggest the amplifying mechanism exerted by citrullinated proteins/peptides, which further promote NETs enhancement and exacerbate autoimmune responses [84]. Taken together, citrullination in NETs strongly modified the inflammatory potential of those structures, changing the primary functions of its proteinaceous components. Thus, our observations suggest that the design of PAD inhibitors as therapeutic targets for inflammatory diseases must be considered carefully.

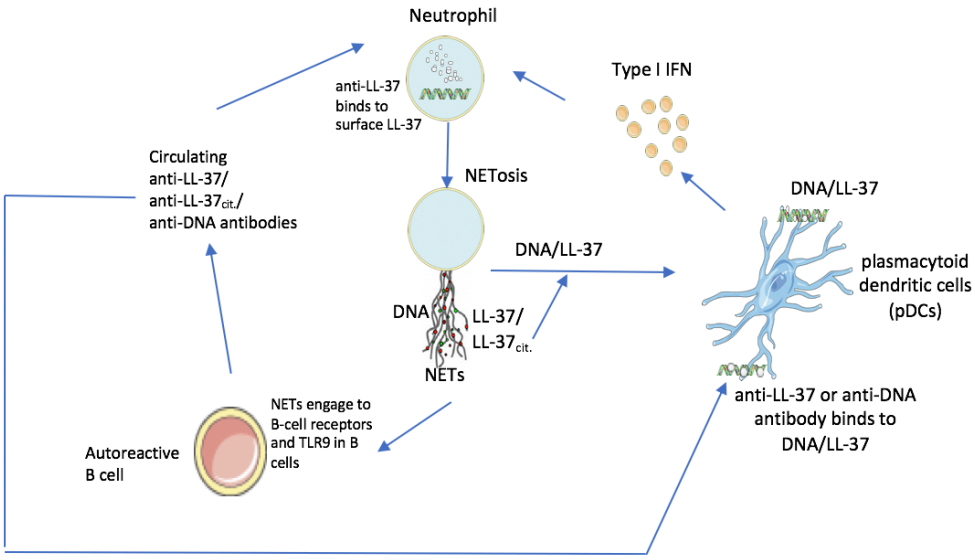

Fig. 54. An overview of the cross-talk between neutrophils and dendritic cells. All the necessary ingredients to trigger the adaptive immune system through a self-amplifying pathogenic loop. NETs containing DNA-LL-37 complexes released from dying neutrophils are taken up by plasmacytoid dendritic cells and signal via TLR9 in endosomes, leading to the release of IFN-α which could prime mature neutrophil and allow the formation of NETs. Development of antibodies against both DNA and antimicrobial peptides in NETs could promote their transport into pDCs, leading to the amplification of IFN-α production. Abundant NET creation also prompts autoreactive B-cell activation, leading to the release of anti-LL-37/anti-LL-$37_{cit.}$ which might trigger the activation of neutrophils, providing the mechanism of continuous release of NETs and augments the inflammatory response.

9. Overall Conclusions

1. LL-37 is highly susceptible to be citrullinated by PAD2 and PAD4 during inflammatory milieu, with the former being more efficient. Citrullination of LL-37 has a marked effect on its affinity for nucleic acids, which is largely dependent on the number of modified Arg residues within the peptide. The strength of binding to DNA is inversely proportional to the number of citrullinated residues in the peptide. Peptide-DNA binding capacity does not depend entirely on the positive charge of LL-37, as illustrated by preincubation of carbamylated LL-37 with PAD2, which abrogated the peptide's ability to bind DNA. On the contrary, guanidinium side chain of Arg residues (homo-Arg) in the peptide, which cannot be deiminated, is essential for the LL-37 interaction with DNA, with results shown to bind DNA with the efficiency similar to native LL-37.

2. Deimination of LL-37 also leads to alteration of the peptide interactions with other molecules than DNA, such as lipoprotein, Apo-A1. In the latter case, however, it must be examined if the citrullination affects the interaction as specificly as in case of DNA.

3. Deimination of arginine residues within LL-37 strongly and specifically affects the immunogenic potential of DNA in the citrullination level-dependent manner. The proinflammatory response of APCs sensitive to nucleic acid-induced signalling, inversely correlated with the increase number of citrulline residues within the peptide. The impairment of APCs activation is caused by the reduced interactions between DNA and LL-37. This hinders the delivery of nucleic acids into the intracellular/endosomal compartment, diminishing the activation of NF-κB and IRF signalling pathway.

4. The generation of citrullinated forms of LL-37 occurs in NETs. The problems with direct identification of modified forms of LL-37 could be related to susceptibility of the citrullinated peptides to proteolytic cleavage.

5. Citrullination in NETs regulates the inflammatory potential of those structures, changing the primary functions of its proteinaceous components. That phenomenon can be important in protecting the host against over-activation of the immune system in the

development of autoimmune diseases but on the other hand detrimental, affecting the cellular responses to microbial components.

6. Modified LL-37 probably plays a broader immunomodulatory role, as citrullinated LL-37 itself enhances the generation of NETs formation suggesting the positive feedback mechanism.

10. List of Tables

11. List of figures

12. References

[1] Akira S, Hemmi H, 2003. Recognition of pathogen-associated molecular patterns by TLR family. *Immunol Lett.*, 85(2): 85-95.

[2] Hato T and Dagher PC, 2015. How the innate immune system senses trouble and causes trouble. *Clin J Am Soc Nephrol.*, 10(8):1459-1469.

[3] Hancock RE, Haney EF, Gill EE, 2016. The immunology of host defence peptides: beyond antimicrobial activity. *Nat Rev Immunol.*, 16(5):321-334.

[4] Pasupuleti M, Schmidtchen A, Malmsten M, 2012. Antimicrobial peptides: key components of the innate immune system. *Crit Rev Biotechnol.,* 32(2):143-171.

[5] Hurdle JG, O'Neill AJ, Chopra I, Lee RE, 2011. Targeting bacterial membrane function: an underexploited mechanism for treating persistent infections. *Nat. Rev. Microbiol*.,9:62–75.

[6] Hilchie, AL, Wuerth K, Hancock, REW, 2013. Immune modulation by multifaceted cationic host defense (antimicrobial) peptides. *Nat Chem Biol.*, 9(12): 761-768.

[7] Durr UH, Sudheendra US, and Ramamoorthy A, 2006. LL-37, the only human member of the cathelicidin family of antimicrobial peptides. *Biochim Biophys Acta*, 1758(9):1408-1425.

[8] Birgitta A, Charo J, Werr J, Olsson B, Idali F, Lindbom L, Kiessling R, Jörnvall H, Wigzell, H, and Gudmundsson GH, 2000. The human antimicrobial and chemotactic peptides LL-37 and α-defensins are expressed by specific lymphocyte and monocyte populations. *Blood*, 96:3086-3093.

[9] Wang G, 2010. Structure, dynamics and mapping of membrane-binding residues of micelle-bound antimicrobial peptides by natural abundance (13)C NMR spectroscopy. *Biochim Biophys Acta*, 1798(2):114-121.

[10] Wang G, 2014. Human antimicrobial peptides and proteins. *Pharmaceuticals (Basel)*, 7(5): 545-594.

[11] De Smet K, Contretas R, 2005. Human Antimicrobial peptides: defensins, cathelicidins and histatins. *Biotechnol Lett*., 27(18):1337-47.

[12] Kościuczuk EM, Lisowski P, Jarczak J, Strzałkowska N, Jóźwik A, Horbańczuk J, Krzyżewski J, Zwierzchowski L, Bagnicka E, 2012. Cathelicidins: family of antimicrobial peptides. A review. *Mol Biol Rep.*, 39(12): 10957-10970.

[13] Adamczak M, and Niemir Z, 2014. Cathelicidin- Its structure, function and the role in autoimmune diseases. *Adv Cell Biol.*, 4(2):83-96.

[14] Vandamme D , Landuyt B, Luyten W, Schoofs L, 2012. A comprehensive summary of LL-37, the factotum human cathelicidin peptide. *Cell Immunol.*, 280(1):22-35.

[15] Zelezetsky I, Pontillo A, Puzzi L, Antcheva N, Segat L, Pacor S, Crovella S, Tossi A, 2006. Evolution of the primate cathelicidin. Correlation between structural variations and antimicrobial activity. *J Biol Chem.*, 281(29):19861-19871.

[16] Johansson J, Gudmundsson GH, Rottenberg ME, Berndt KD, Agerberth B, 1998. Conformation-dependent antibacterial activity of the naturally occurring human peptide LL-37. *J Biol Chem.*, 273(6):3718-3724.

[17] Wang Y, Agerberth B, Löthgren A, Almstedt A, Johansson J, 1998. Apolipoprotein A-I binds and inhibits the human antibacterial/cytotoxic peptide LL-37. *J Biol Chem*, 273(50):33115-33118.

[18] Wang G, 2008. Structures of human host defense cathelicidin LL-37 and its smallest antimicrobial peptide KR-12 in lipid micelles. *J Biol Chem*, 283(47):32637-32643.

[19] Oren Z, Lerman JC, Gudmundsson GH, Agerberth B, and Shai Y, 1999. Structure and organization of the human antimicrobial peptide LL-37 in phospholipid membranes:

relevance to the molecular basis for its non-cell-selective activity. *Biochem J*, 341(Pt 3):501-513.

[20] Sørensen O, Arnljots K, Cowland JB, Bainton DF, Borregaard N, 1997. The human antibacterial cathelicidin, hCAP18, is synthesized in myelocytes and metamyelocytes and localized to specific granules in neutrophils. *Blood*, 90(7):2796-2803.

[21] Campbell Y, Fantacone M, and Gombart A, 2012. Regulation of antimicrobial peptide gene expression by nutrients and by-products of microbial metabolism. *Eur J Nutr.*, *51*(8), 899–907.

[22] Brogden KA, 2005. Antimicrobial peptides: pore formers or metabolic inhibitors in bacteria. *Nat Rev Microbiol*., 3(3):238-250.

[23] Overhage J, Campisano A, Bains M, Torfs EC, Rehm BH, Hancock RE, 2008. Human host defence peptide LL-37 prevents bacterial biofilm formation. *Infect Immun*., 76(9):4176-4182.

[24] Chromek M, Slamová Z, Bergman P, Kovács L, Podracká L, Ehrén I, Hökfelt T, Gudmundsson GH, Gallo RL, Agerberth B, Brauner A, 2006. The antimicrobial peptide cathelicidin protects the urinary tract against invasive bacterial infection. *Nat Med*., 12(6):636-641.

[25] Pütsep K, Carlsson G, Boman HG, Andersson M, 2002. Deficiency of antibacterial peptides in patients with morbus Kostmann: an observation study. *Lancet*., 360(9340):1144-1149.

[26] Yasin B, Pang M, Turner JS, Cho Y, Dinh NN, Waring AJ, Lehrer RI, Wagar E, 2000. Evaluation of the inactivation of infectious herpes simplex virus by host defense peptides. *Eur J Clin Microbiol Infect Dis.*, 19(3): 187-194.

[27] Bergman P, Walter-Jallow L, Broliden K, Agerberth B, Söderlund J, 2007. The antimicrobial peptide LL-37 inhibits HIV-1 replication. *Curr HIV Res.*, 5(4):410-415.

[28] Kahlenberg JM, Kaplan MJ, 2013. Little peptide, big effects: the role of LL-37 in inflammation and autoimmune disease. *J Immunol.*, 191(10):4895-4901.

[29] van der Does AM, Beekhuizen H, Ravensbergen B, Vos T, Ottenhoff TH, Dissel JT, Drijfhout JW, Hiemstra PS, Nibbering PH, 2010. LL-37 directs macrophage differentiation toward macrophages with a proinflammatory signature. *J Immunol.*, 185(3):1442-1449.

[30] Kahlenberg JM, Carmona-Rivera C, Smith CK, Kaplan MJ, 2013. Neutrophil extracellular trap-associated protein activation of the NLRP3 inflammasome is enhanced in lupus macrophages. *J Immunol.*, 190(3):1217-1226.

[31] Gilliet M, Cao W, and Liu YJ, 2008. Plasmacytoid dendritic cells: sensing nucleic acids in viral infection and autoimmune diseases. *Nat Rev Immunol.*, 8(8):594-606.

[32] Lande R, Ganguly D, Facchinetti V, Frasca L, Conrad C, Gregorio J, Meller S, Chamilos G, Sebasigari R, Riccieri V, Bassett R, Amuro H, Fukuhara S, Ito T, Liu YJ, Gilliet M, 2011. Neutrophils activate plasmacytoid dendritic cells by releasing self-DNA-peptide complexes in systemic lupus erythematosus. *Sci. Transl. Med.,* 3: 73ra19.

[33] Chen X, Takai T, Xie Y, Niyonsaba F, Okumura K, Ogawa H, 2013. Human antimicrobial peptide LL-37 modulates proinflammatory responses induced by cytokine milieus and double-stranded RNA in human keratinocytes. *Biochem Biophys Res Commun*, 433(4):532–537.

[34] Di Nardo A, Braff MH, Taylor KR, Na C, Granstein RD, McInturff JE, Krutzik S, Modlin RL, Gallo RL, 2007. Cathelicidin antimicrobial peptides block dendritic cell TLR4 activation and allergic contact sensitization. *J Immunol.*, 178(3):1829-1834.

[35] Barlow PG, Li Y, Wilkinson TS, Bowdish DME, Lau YE, Cosseau C, Haslett C, Simpson AJ, Hancock REW, Davidson DJ, 2006. The human cationic host defense

peptide LL-37 mediates contrasting effects on apoptotic pathways in different primary cells of the innate immune system. *J Leukoc Biol*., 80(3): 509–520.

[36] Hing TC, Ho S, Shih DQ, Ichikawa R, Cheng M, Chen J, Chen X, Law I, Najarian R, Kelly CP, 2013. The antimicrobial peptide cathelicidin modulates *Clostridium difficile*-associated colitis and toxin A-mediated enteritis in mice. *Gut*, 62: 1295–1305.

[37] Sørensen OE, Cowland JB, Theilgaard-Mönch K, Liu L, Ganz T, Borregaard N, 2003. Wound healing and expression of antimicrobial peptides/polypeptides in human keratinocytes, a consequence of common growth factors. *J Immunol.*, 170(11):5583-5589.

[38] Shaykhiev R, Beisswenger C, Kändler K, Senske J, Püchner A, Damm T, Behr J, Bals R, 2005. Human endogenous antibiotic LL-37 stimulates airway epithelial cell proliferation and wound closure. *Am J Physiol Lung Cell Mol Physiol.*, 289(5):L842-848.

[39] Koczulla R, von Degenfeld G, Kupatt C, Krötz F, Zahler S, Gloe T, Issbrücker K, Unterberger P, Zaiou M, Lebherz C, Karl A, Raake P, Pfosser A, Boekstegers P, Welsch U, Hiemstra PS, Vogelmeier C, Gallo RL, Clauss M, Bals R., 2003. An angiogenic role for the human peptide antibiotic LL-37/hCAP-18. *J Clin Invest.*, 111(11):1665-1672.

[40] Döring Y, Manthey HD, Drechsler M, Lievens D, Megens RT, Soehnlein O, Busch M, Manca M, Koenen RR, Pelisek J, 2012. Auto-antigenic protein-DNA complexes stimulate plasmacytoid dendritic cells to promote atherosclerosis. *Circulation,* 125(13): 1673-1683.

[41] Reinholz M, Ruzicka T, Schauber J, 2012. Cathelicidin LL-37: an antimicrobial peptide with a role in inflammatory skin disease. *Ann. Dermatol.*, 24(2): 126–135.

[42] Garcia-Romo GS, Caielli S, Vega B, Connolly J, Allantaz F, Xu Z, Punaro M, Baisch J, Guiducci C, Coffman RL, 2011. Netting neutrophils are major inducers of type I IFN production in pediatric systemic lupus erythematosus. *Sci. Transl. Med*, 3(73): 73ra20.

[43] Denny MF, Yalavarthi S, Zhao W, Thacker SG, Anderson M, Sandy AR, McCune WJ, Kaplan MJ, 2010. A distinct subset of proinflammatory neutrophils isolated from patients with systemic lupus erythematosus induces vascular damage and synthesizes type I IFNs. *J Immunol.*, 184: 3284–3297.

[44] Hoffmann MH, Bruns H, Bäckdahl L, Neregård P, Niederreiter B, Herrmann M, Catrina AI, Agerberth B, Holmdahl R, 2013. The cathelicidins LL-37 and rCRAMP are associated with pathogenic events of arthritis in humans and rats. *Ann. Rheum. Dis.*, 72: 1239–1248.

[45] Mann M, Jensen ON, 2003. Proteomic analysis of post-translational modifications. *Nat Biotechnol*, 21(3):255-261.

[46] Sieprawska-Lupa M, Mydel P, Krawczyk K, Wójcik K, Puklo M, Lupa B, Suder P, Silberring J, Reed M, Pohl J, Shafer W, McAleese F, Foster T, Travis J, Potempa J, 2004. Degradation of human antimicrobial peptide LL-37 by staphylococcus aureus-derived proteinases. *Antimicrob Agents Chemother.*, 48(12):4673-4679.

[47] Rosen G, Sela MN, Bachrach G, 2012. The antibacterial activity of LL-37 against Treponema denticola is dentilisin protease independent and facilitated by the major outer sheath protein virulence factor. *Infect Immun.*, 80(3):1107-1114.

[48] Koziel J, Karim AY, Przybyszewska K, Ksiazek M, Rapala-Kozik M, Nguyen KA, Potempa J, 2010. Proteolytic inactivation of LL-37 by karilysin, a novel virulence mechanism of Tannerella forsythia. *J Innate Immun.*, 2(3):288-293.

[49] Schiemann F, Brandt E, Gross R, Lindner B, Mittlestädt J, Sommerhoff CP, Schulmistrat J and Petersen F, 2009. The cathelicidin LL-37 activates human mast

cells and is degraded by mast cell tryptase: counter-regulation by CXCL4. *J Immunol.*, 183(4):2223-2231.

[50] Bergsson G, Reeves EP, McNally P, Chotirmall SH, Greene CM, Greally P, Murphy P, O'Neill SJ, McElvaney NG, 2009. LL-37 complexation with glycosaminoglycans in cystic fibrosis lungs inhibits antimicrobial activity, which can be restored by hypertonic saline. *J Immunol*, 183(1):543-551.

[51] Koro C, Hellvard A, Delaleu N, Binder V, Scavenius C, Bergum B, Główczyk I, Roberts HM, Chapple IL, Grant MM, Rapala-Kozik M, Klaga K, Enghild JJ, Potempa J, Mydel P, 2016. Carbamylated LL-37 as a modulator of the immune response. *Innate Immun.*, 22(3):218-229.

[52] Nilsson L, Lundquist P, Kagedal B, Larsson R, 1996. Plasma cyanate concentrations in chronic renal failure. *Clin. Chem.* 42:482-483.

[53] Wang Z, Nicholls SJ, Rodriguez ER, Kummu O, Hörkkö S, Barnard J, Reynolds WF, Topol EJ, DiDonato JA, Hazen SL, 2007. Protein carbamylation links inflammation, smoking, uremia and atherogenesis. *Nat Med.*, 13(10):1176-1184.

[54] Shi J, van Veelen PA, Mahler M, Janssen GM, Drijfhout JW, Huizinga TW, Toes RE, Trouw LA, 2014. Carbamylation and antibodies against carbamylated proteins in autoimmunity and other pathologies. *Autoimmun Rev.*, 13(3):225-230.

[55] Jaisson S, Pietrement C, Gillery P, 2018. Protein Carbamylation: Chemistry, pathophysiological involvement and biomarkers. *Adv Clin Chem*, 84:1-38.

[56] Wegner N, Lundberg K, Kinloch A, Fisher B, Malmström V, Feldmann M, Venables PJ, 2010. Autoimmunity to specific citrullinated proteins gives the first clues to the etiology of rheumatoid arthritis. *Immunol Rev.*, 233(1):34-54.

[57] Witalison EE, Thompson PR, Hofseth LJ, 2015. Protein arginine deiminases and associated citrullination: physiological functions and diseases associated with dysregulation. *Curr Drug Targets*, 16(7):700-710.

[58] Zhou Y, Mittereder N, and Sims GP, 2018. Perspective on protein arginine deiminase activity- Bicarbonate is a pH-independent regulator of citrullination. *Front Immunol.*, 9:34.

[59] Vossenaar ER, Zendman AJ, van Venrooij WJ, Pruijn GJ, 2003. PAD, a growing family of citrullinating enzymes: genes, features and involvement in disease. *Bioessays*, 25(11):1106-1118.

[60] Bicker KL, Thompson PR, 2013. The protein arginine deiminases: structure, function, inhibition, and disease. *Biopolymers*, 99(2):155-163.

[61] György B, Tóth E, Tarcsa E, Falus A, Buzás EI, 2006. Citrullination: a posttranslational modification in health and disease. *Int J Biochem Cell Biol.*, 38(10):1662–1677.

[62] Chavanas S, Mechin MC, Nachat R, Adoue V, Coudane F, Serre G, Simon M, 2006. Peptidylarginine deiminases and deimination in biology and pathology: relevance to skin homeostasis. *J Dermatol Sci.*, 44:63–72.

[63] Harris SL, and Levine AJ. 2005. The p53 pathway: positive and negative feedback loops. *Oncogene*, 24:2899–2908.

[64] Hsu PC, Liao YF, Lin CL, Lin WH, Liu GY, Hung HC, 2014. Vimentin is involved in peptidylarginine deiminase 2-induced apoptosis of activated Jurkat cells. *Mol Cells*, 37(5):426-434.

[65] Hagiwara T, Hidaka Y, Yamada M, 2005. Deimination of histone H2A and H4 at arginine 3 in HL-60 granulocytes. *Biochemistry*, 44(15):5827-5834.

[66] Valesini G, Gerardi MC, Iannuccelli C, Pacucci VA, Pendolino M, Shoenfeld Y, 2015. Citrullination and autoimmunity. *Autoimmun Rev.*, 14(6):490-497.

[67] Koziel J, Bryzek D, Sroka A, Maresz K, Glowczyk I, Bielecka E, Kantyka T, Pyrć K, Svoboda P, Pohl J, Potempa J, 2014. Citrullination alters immunomodulatory

function of LL-37 essential for prevention of endotoxin-induced sepsis. *J Immunol.*, 192(11):5363-5372.

[68] Kilsgård O, Andersson P, Malmsten M, Nordin SL, Linge HM, Eliasson M, Sörenson E, Erjefält JS, Bylund J, Olin AI, Sørensen OE, Egesten A, 2012. Peptidylarginine deiminases present in the airways during tobacco smoking and inflammation can citrullinate the host defense peptide LL-37, resulting in altered activities. *Am J Respir Cell Mol Biol.*, 46(2):240-248.

[69] Picchianti M, Russo C, Castagnini M, Biagini M, Soldaini E, Balducci E, 2015. NAD-dependent ADP-ribosylation of the human antimicrobial and immune-modulatory peptide LL-37 by ADP-ribosyltransferase-1. *Innate Immun.*, 21(3):314-321.

[70] Strömstedt AA, Pasupuleti M, Schmidtchen A, Malmsten M, 2009. Evaluation of strategies for improving proteolytic resistance of antimicrobial peptides by using variants of EFK17, an internal segment of LL-37. *Antimicrobial Agents Chemother.*, 53(2):593-602.

[71] Fairman R, Shoemaker KR, York EJ, Stewart JM, and Baldwin RL, 1989. Further studies of the helix dipole model: effects of a free alpha-NH3+ or alpha-COO− group on helix stability. *Proteins* 5:1-7.

[72] Takeshita F, Leifer CA, Gursel I, Ishii KJ, Takeshita S, Gursel M, Klinman DM, 2001. Cutting edge: Role of toll-like receptor 9 in CpG DNA-induced activation of human cells. *J Immunol.*, 167(7):3555-3558.

[73] Ishii KJ, Akira S, 2006. Innate immune recognition of, and regulation by, DNA. *Trends Immunol.*, 27:525–532.

[74] Klechevsky, E, 2015. Functional diversity of human dendritic cells. *Adv Exp Med Biol.*, 850:43-54.

[75] Abbas AK, Lichtman AH, and Pillai S, 2012. *Cellular and molecular immunology*. Philadelphia: Saunders/Elsevier.

[76] Merad M, Sathe P, Helft J, Miller J, Mortha A, 2013. The dendritic cell lineage: ontogeny and function of dendritic cells and their subsets in the steady state and the inflamed setting. *Ann Rev Immunol.*, 31:563-604.

[77] Moresco EM, Lavine D, Beutler B, 2011. Toll-like receptors. *Curr Biol.*, 21(13):R488-493.

[78] Blasius AL, Beutler B, 2010. Intracellular toll-like receptors. *Immunity*, 32(3):305-315.

[79] Colonna M., Trinchieri G, Liu YJ, 2004. Plasmacytoid dendritic cells in immunity. *Nat Immunol.*, 5(12):1219-1226.

[80] Lande R, Gregorio J, Facchinetti V, Chatterjee B, Wang YH, Homey B, Cao W, Wang YH, Su B, Nestle FO, Zal T, Mellman I, Schröder JM, Liu YJ, Gilliet M, 2007. Plasmacytoid dendritic cells sense self-DNA coupled with antimicrobial peptide. *Nature*, 449(7162):564-569.

[81] Sandgren S, Wittrup A, Cheng F, Jönsson M, Eklund E, Busch S, Belting M, 2004. The human antimicrobial peptide LL-37 transfers extracellular DNA plasmid to the nuclear compartment of mammalian cells via lipid rafts and proteoglycan-dependent endocytosis. *J Biol Chem.*, 279(17):17951-17956.

[82] Hurtado P, Peh, CA, 2010. LL-37 promotes rapid sensing of CpG oligodeoxynucleotides by B lymphocytes and plasmacytoid dendritic cells. *J Immunol.*, 184(3):1425-1435.

[83] Ganguly D, Chamilos G, Lande R, Gregorio J, Meller S, Facchinetti V, Homey B, Barrat FJ, Zal T, Gilliet M, 2009. Self-RNA-antimicrobial peptide complexes activate human dendritic cells through TLR7 and TLR8. *J Exp Med.*, 206(9):1983-1994.

[84] Khandpur R, Carmona-Rivera C, Vivekanandan-Giri A, Gizinski A, Yalavarthi S, Knight JS, Friday S, Li S, Patel RM, Subramanian V, Thompson P, Chen P, Fox DA, Pennathur S, Kaplan MJ, 2013. NETs are a source of citrullinated autoantigens and stimulate inflammatory responses in rheumatoid arthritis. *Sci Transl Med.*, 5(178):178ra40.

[85] Britigan BE, Lewis TS, Waldschmidt M, McCormick ML, Krieg AM, 2001. Lactoferrin binds CpG-containing oligonucleotides and inhibits their immunostimulatory effects on human B cells. *J Immunol.*, 167(5):2921-2928.

[86] Kenny EF, Herzig A, Krüger R, Muth A, Mondal S, Thompson PR, Brinkmann V, Bernuth HV, Zychlinsky A, 2017. Diverse stimuli engage different neutrophil extracellular trap pathways. *Elife*, 2017;6:e24437.

[87] Fuchs TA, Abed U, Goosmann C, Hurwitz R, Schulze I, Wahn V, Weinrauch Y, Brinkmann V, Zychlinsky A., 2007. Novel cell death program leads to neutrophil extracellular traps. *J Cell Biol.*, 176(2):231-241.

[88] Lewis HD, Liddle J, Coote JE, Atkinson SJ, Barker MD, Bax BD, Bicker KL, Bingham RP, Campbell M, Chen YH, Chung CW, Craggs PD, Davis RP, Eberhard D, Joberty G, Lind KE, Locke K, Maller C, Martinod K, Patten C, Polyakova O, Rise CE, Rüdiger M, Sheppard RJ, Slade DJ, Thomas P, Thorpe J, Yao G, Drewes G, Wagner DD, Thompson PR, Prinjha RK, Wilson DM, 2015. Inhibition of PAD4 activity is sufficient to disrupt mouse and human NET formation. *Nat Chem Biol.*, 11(3):189-191.

[89] Pinegin B, Vorobjeva N, Pinegin V, 2015. Neutrophil extracellular traps and their role in the development of chronic inflammation and autoimmunity. *Autoimmun Rev.*, 14(7):633-640.

[90] Sørensen OE, and Borregaard N, 2016. Neutrophil extracellular traps- the dark side of neutrophils. *J Clin Invest.*, 126(5):1612-1620.

[91] Darrah E, and Andrade F, 2012. NETs: the missing link between cell death and systemic autoimmune diseases? *Front Immunol*, 3:428.

[92] Bosch, X, 2011. Systemic lupus erythematosus and the neutrophil. *N Engl J Med.*, 365(8):758-760.

[93] Lande R, Chamilos G, Ganguly D, Demaria O, Frasca L, Durr S, Conrad C, Schröder J, Gilliet M, 2015. Cationic antimicrobial peptides in psoriatic skin cooperate to break innate tolerance to self-DNA. *Eur J Immunol.*, 45(1):203-213.

[94] Gestermann N, Di Domizio J, Lande R, Demaria O, Frasca L, Feldmeyer L, Di Lucca J, Gilliet M, 2018. Netting neutrophils activate autoreactive B cells in Lupus. *J Immunol*, 200(10):3364-3371.

[95] Chuang CM, Monie A, Wu A, Mao CP, Hung CF, 2009. Treatment with LL-37 peptide enhances antitumour effects induced by CpG oligodeoxynucleotides against ovarian cancer. *Hum Gene Ther*, 20(4):303-313.

[96] Schagger H and von Jagow G, 1987. Tricine-sodium dodecyl sulfate-polyacrylamide gel electrophoresis for the separation of proteins in the range from 1 to 100 kDa. *Anal Biochem.*, 166: 368–379.

[97] Bicker KL, Subramanian V, Chumanevich AA, Hofseth LJ, Thompson PR, 2012. Seeing citrulline: development of a phenylglyoxal-based probe to visualize protein citrullination. *J Am Chem Soc.*, 134(41):17015-17018.

[98] Livak KJ, Schmittgen TD, 2001. Analysis of relative gene expression data using real-time quantitative PCR and the 2(-Delta Delta C(T)) method. *Methods*, 25(4):402-408.

[99] Chamilos G, Gregorio J, Meller S, Lande R, Kontoyiannis DP, Modlin RL, Gilliet M, 2012. Cytosolic sensing of extracellular self-DNA transported into monocytes by the antimicrobial peptide LL-37. *Blood*, 120(18):3699-3707.

[100] Zhou Y, Chen B, Mittereder N, Chaerkady R, Strain M, An LL, Rahman S, Ma W, Low CP, Chan D, Neal F, Bingham CO, Sampson K, Darrah E, Siegel RM, Hasni S, Andrade F, Vousden KA, Mustelin T, Sims GP, 2017. Spontaneous secretion of the citrullination enzyme PAD2 and cell surface exposure of PAD4 by neutrophils. *Front Immunol.*, 8:1200.
[101] Hellman LM, Fried MG, 2007. Electrophoretic mobility shift assay (EMSA) for detecting protein-nucleic acid interactions. *Nat Protoc.*, 2(8):1849-1861.
[102] Wang Y, Johansson J, Agerberth B, Jörnvall H, Griffiths WJ, 2004. The antimicrobial peptide LL-37 binds to the human plasma protein apolipoprotein A-I. *Rapid Commun Mass Spectrom.*,18(5):588-589.
[103] Pruijin GJM, 2015. Citrullination and Carbamylation in the pathophysiology of rheumatoid arthritis. *Front Immunol*, 6:192.
[104] Barton GM, Kagan JC, Medzhitov R, 2006. Intracellular localization of Toll-like receptor 9 prevents recognition of self DNA but facilitates access to viral DNA. *Nat. Immunol.*, 7: 49–56.
[105] Krieg AM, 2003. CpG motifs:the active ingredient in bacterial extracts? *Nat Med.*, 9:831-835.
[106] Ahmad-Nejad P, Häcker H, Rutz M, Bauer S, Vabulas RM, Wagner H, 2002. Bacterial CpG-DNA and lipopolysaccharides activate toll-like receptors at distinct cellular compartments. *Eur J Immunol.*, 32(7):1958-1968.
[107] Parameswaran N, Patial S, 2010. Tumor necrosis factor -a signalling in macrophages. *Crit Rev Eukaryot Gene Expr*, 20:87-103.
[108] Kerkmann M, Rothenfusser S, Hornung V, Towarowski A, Wagner M, Sarris A, Giese T, Endres S, Hartmann G, 2003. Activation with CpG-A and CpG-B oligonucleotides reveals two distinct regulatory pathways of type I IFN synthesis in human plasmacytoid dendritic cells. *J Immunol*, 170(9):4465-4474.
[109] Neumann A, Berends ET, Nerlich A, Molhoek EM, Gallo RL, Meerloo T, Nizet V, Naim HY, von Köckritz-Blickwede M, 2014. The antimicrobial peptide LL-37 facilitates the formation of neutrophil extracellular traps. *Biochem J.*, 464(1):3-11.
[110] Xhindoli D, Pacor S, Benincasa M, Scocchi M, Gennaro R, Tossi A, 2016. The human cathelicidin LL-37 – A pore-forming antibacterial peptide and host cell-modulator. *Biochim Biophysic Acta*, 1858:546-566.
[111] Liu S, Cai X, Wu J, Cong Q, Chen X, Li T, Du F, Ren J, Wu YT, Grishin NV, Chen ZJ, 2015. Phosphorylation of innate immune adaptor proteins MAVS, STING and TRIF induces IFR3 activation. *Science*, 347(6227):aaa2630.
[112] Liu J, Qian C, Cao X, 2016. Post-translational modification control of innate immunity. *Immunity*, 45(1):15-30.
[113] Zhang YQ, Sarge KD, 2008. Sumoylation regulates lamin A function and is lost in lamin A mutants associated with familial cardiomyopathies. *J Cell Biol.*, 182(1):35-39.
[114] Dalle-Donne I, Rossi R, Giustarini D, Milzani A, Colombo R, 2003. Protein carbonyl groups as biomarkers of oxidative stress. *Clinica Chimica Acta*, 329(1-2):23-38.
[115] Darrah E, Rosen A, Giles JT, Andrade F, 2012. Peptidylarginine deiminase 2,3 and 4 have distinct specificities against cellular substrates: novel insights into autoantigen selection in rheumatoid arthritis. *Ann Rheum Dis.*, 71(1):92-98.
[116] Stensland ME, Pollmann S, Molberg Ø, Sollid LM, Fleckenstein B, 2009. Primary sequence, together with other factors, influence peptide deimination by peptidylarginine deiminase-4. *Biol Chem.*, 390(2):99-107.
[117] Moscarello MA, Mastronardi FG, Wood DD, 2007. The role of citrullinated proteins suggests a novel mechanism in the pathogenesis of multiple sclerosis. *Neurochem Res.*, 32(2):251-256.

[118] Loos T, Mortier A, Gouwy M, Ronsse I, Put W, Lenaerts JP, Van Damme J, Proost P, 2008. Citrullination of CXCL10 and CXCL11 by peptidylarginine deiminase: a naturally occurring posttranslational modification of chemokines and new dimension of immunoregulation. *Blood*, 112(7):2648-2656.
[119] Frank M, 2016. Circulating cell-free DNA differentiates severity of inflammation. *Biol Res Nurs*, 18(5):477-488.
[120] Kim S, Kaiser V, Beier E, Bechheim M, Guenthner-Biller M, Ablasser A, Berger M, Endres S, Hartmann G, Hornung V, 2014. Self-priming determines high type I IFN production by plasmacytoid dendritic cells. *Eur J Immunol.*, 44(3):807-818.
[121] Balakrishnan S, Scheuermann MJ, Zondlo NJ, 2012. Arginine mimetics using α-guanidino acids: introduction of functional groups and stereochemistry adjacent to recognition guanidiniums in peptides. *Chembiochem*, 13(2):259-270.
[122] Schmidt N, Mishra A, Lai GH, Wong GC, 2010. Arginine-rich cell-penetrating peptides. *FEBS Letter*, 584(9):1806-1813.
[123] Tang X, Basavarajappa D, Haeggström JZ, Wan M, 2015. P2X7 receptor regulates internalization of antimicrobial peptide LL-37 by human macrophages that promotes intracellular pathogen clearance. *J Immunol.*, 195(3):1191-1201.
[124] Tokarev AA, Alfonso A, Segev N, 2009. Overview of intracellular compartments and trafficking pathways. *Landes Bioscience*, 2000-2013.
[125] Schroder K, Spille M, Pilz A, Lattin J, Bode KA, Irvine KM, Burrows AD, Ravasi T, Weighardt H, Stacey KJ, Decker T, Hume DA, Dalpke AH, Sweet MJ, 2007. Differential effects of CpG DNA on IFN-beta induction and STAT1 activation in murine macrophages versus dendritic cells: alternatively activated STAT1 negatively regulates TLR signalling in macrophages. *J Immunol.*, 179(6):3495-3503.
[126] Kawai T and Akira S, 2007. Signaling to NF-κB by toll-like receptors. *Trends Mol Med.*, 13(11):460-469.
[127] Marié I, Durbin JE, Levy DE, 1998. Differential viral induction of distinct interferon-alpha genes by positive feedback through interferon regulatory factor-7. *EMBO J,* 17(22):6660-6669.
[128] Decker T, Müller M, Stockinger S, 2005. The yin and yang of type I interferon activity in bacterial infection. *Nat Rev Immunol.*, 5(9):675-687.
[129] Guiducci C, Ott G, Chan JH, Damon E, Calacsan C, Matray T, Lee KD, Coffman RL, Barrat FJ, 2006. Properties regulating the nature of the plasmacytoid dendritic cell response to Toll-like receptor 9 activation. *J Exp Med.*, 203(8):1999-2008.
[130] Biron BM, Chung CS, O'Brien XM, Chen Y, Reichner JS, Ayala A, 2017. Cl-Amidine prevents Histone 3 citrullination and neutrophil extracellular trap formation, and improves survival in a murine sepsis model. *J Innate Immun.*, 9(1):22-32.
[131] Spengler J, Lugonja B, Ytterberg AJ, Zubarev RA, Creese AJ, Pearson MJ, Grant MM, Milward M, Lundberg K, Buckley CD, Filer A, Raza K, Cooper PR, Chapple IL, Scheel-Toellner D, 2015. Release of active peptidyl arginine deiminases by neutrophils can explain production of extracellular citrullinated autoantigens in rheumatoid arthritis synovial fluid. *Arthritis Rheumatol.*, 67(12):3135-3145.
[132] O'Donoghue AJ, Jin Y, Knudsen GM, Perera NC, Jenne DE, Murphy JE, Craik CS, Hermiston TW, 2013. Global substrate profiling of proteases in human neutrophil extracellular traps reveals consensus motif predominantly contributed by elastase. *PLoS One*, 8(9):e75141.
[133] Hahn J, Schauer C, Czegley C, Kling L, Petru L, Schmid B, Weidner D, Reinwald C, Biermann MHC, Blunder S, Ernst J, Lesner A, Bäuerle T, Palmisano R, Christiansen S, Herrmann M, Bozec A, Gruber R, Schett G, Hoffmann MH, 2018. Aggregated neutrophil extracellular traps resolve inflammation by proteolysis of

cytokines and chemokines and protection from antiproteases. *FASEB J*, 21:fj201800752R.

[134] Kienhöfer D, Hahn J, Stoof J, Csepregi JZ, Reinwald C, Urbonaviciute V, Johnsson C, Maueröder C, Podolska MJ, Biermann MH, Leppkes M, Harrer T, Hultqvist M, Olofsson P, Munoz LE, Mocsai A, Herrmann M, Schett G, Holmdahl R, Hoffmann MH., 2017. Experimental lupus is aggravated in mouse strains with impaired induction of neutrophil extracellular traps. *JCI Insight*, 18:2(10).

[135] Schauer C, Janko C, Munoz LE, Zhao Y, Kienhöfer D, Frey B, Lell M, Manger B, Rech J, Naschberger E, Holmdahl R, Krenn V, Harrer T, Jeremic I, Bilyy R, Schett G, Hoffmann M, Herrmann M, 2014. Aggregated neutrophil extracellular traps limit inflammation by degrading cytokines and chemokines. *Nat Med.*, 20(5):511–517.

[136] Sur Chowdhury C, Giaglis S, Walker UA, Buser A, Hahn S, Hasler P, 2014. Enhanced neutrophil extracellular trap generation in rheumatoid arthritis:analysis of underlying signal transduction pathways and potential diagnostic utility. *Arthritis Res Ther.*, 16(3):R122.

[137] Laugisch O, Wong A, Sroka A, Kantyka T, Koziel J, Neuhaus K, Sculean A, Venables PJ, Potempa J, Möller B, Eick S, 2016. Citrullination in the periodontium-a possible link between periodontitis and rheumatoid arthritis. *Clin Oral Investig.*, 20(4):675-683.

[138] Kienhöfer D, Hahn J, Schubert I, Reinwald C, Ipseiz N, Lang SC, Borràs ÈB, Amann K, Sjöwall C, Barron AE, Hueber AJ, Agerberth B, Schett G, Hoffmann MH., 2014. No evidence of pathogenic involvement of cathelicidins in patient cohorts and mouse models of lupus and arthritis. *PLos One*, 9(12):e115474.

[139] Goulas T, Mizgalska D, Garcia-Ferrer I, Kantyka T, Guevara T, Szmigielski B, Sroka A, Millán C, Usón I, Veillard F, Potempa B, Mydel P, Solà M, Potempa J, Gomis-Rüth FX, 2015. Strcuture and mechanism of a bacterial host-protein citrullinating virulence factor, Porphyromonas gingivalis peptidylarginine deiminase. *Sci Rep.*, 5:11969.

[140] Bielecka E, Scavenius C, Kantyka T, Jusko M, Mizgalska D, Szmigielski B, Potempa B, Enghild JJ, Prossnitz ER, Blom AM, Potempa J, 2014. Peptidyl arginine deiminase from Porphyromonas gingivalis abolishes anaphylatoxin C5a activity. *J Biol Chem.,* 289(47):32481-32487.

[141] Moelants EA, Loozen G, Mortier A, Martens E, Opdenakker G, Mizgalska D, Szmigielski B, Potempa J, Van Damme J, Teughels W, Proost P, 2014. Citrullination and proteolytic processing of chemokines by porphyromonas gingivalis. *Infect Immun.*, 82(6):2511-2519.

[142] Vitkov L, Klappacher M, Hannig M, Krautgartner WD. Neutrophil fate in gingival crevicular fluid. *Ultrastruct Pathol.,* 2010;34:25–30.

[143] Schuster S, Hurrell B, Tacchini-Cottier F, 2013. Crosstalk between neutrophils and dendritic cells: a context-dependent process. *J Leukoc Biol.*, 94(4):671-675.

[144] Makrygiannakis D, Klint E, Lundberg IE, Löfberg R, Ulfgren AK, Klareskog L, Catrina AI., 2006. Citrullination is an inflammation-dependent process. *Ann Rheum Dis.,* 65(9):1219-1222.

[145] He Y, Yang FY, Sun EW, 2018. Neutrophil extracellular traps in autoimmune diseases. *Chin Med J(Engl).*, 131(13):1513-1519.